XBeach Technical Reference: Kingsday Release

Model description and reference guide to functionalities

Keywords

Hydrodynamics, infragravity waves, run-up, overtopping, hydrostatic, surfbeat, non-hydrostatic, morphodynamics, dune erosion, overwash, breaching, coral reefs, vegetation, ships

Organizations

Deltares, UNESCO-IHE Institute of Water Education and Delft University of Technology

Authors

Dano Roelvink, Ap van Dongeren, Robert McCall, Bas Hoonhout, Arnold van Rooijen, Pieter van Geer, Lodewijk de Vet, Kees Nederhoff, Ellen Quataert

Summary

XBeach is an open-source numerical model which originally was developed to simulate hydrodynamic and morphodynamic processes and impacts on sandy coasts with a domain size of kilometers and on the time scale of storms. Since then, the model has been applied to other types of coasts and purposes. This reference guide provides an overview of the model formulations and many functionalities, options and parameters in the model. This technical reference applies to XBeach version 1.22 (revision 4567) also known as the 'Kingsday' release.

Version	Date	Author	Initials	Review	Initials	Approval	Initials
4	Jun 2015	Kees Nederhoff					
5	Oct 2015	Ellen Quataert					

State
final

Contents

Appendices

Deltares

1 Introduction

1.1 Description of the development of XBeach

XBeach is an open-source numerical model which originally was developed to simulate hydrodynamic and morphodynamic processes and impacts on sandy coasts with a domain size of kilometers and on the time scale of storms. Since then, the model has been applied to other types of coasts and purposes.

The model includes the hydrodynamic processes of short wave transformation (refraction, shoaling and breaking), long wave (infragravity wave) transformation (generation, propagation and dissipation), wave-induced setup and unsteady currents, as well as overwash and inundation. The morphodynamic processes include bed load and suspended sediment transport, dune face avalanching, bed update and breaching. Effects of vegetation and of hard structures have been included. The model has been validated with a series of analytical, laboratory and field test cases using a standard set of parameter settings.

XBeach has two modes: a hydrostatic and a non-hydrostatic mode. In the hydrostatic mode, the short wave amplitude variation is solved separately from the long waves, currents and morphological change. This saves considerable computational time, with the expense that the phase of the short waves is not simulated. A more complete model is the non-hydrostatic model which solves all processes including short wave motions, but with more computational demand.

The original application (surfbeat mode), funded by the U.S. Corps of Engineers in the framework of the Morphos project and the U.S. Geological Survey, was to be able to assess hurricane impacts on sandy beaches. Since then with funding from the Rijkswaterstaat, part of The Netherlands Ministry of Infrastructure and the Environment, the model has been extended, applied and validated for storm impacts on dune and urbanized coasts for the purpose of dune safety assessments. With support from the European Commission XBeach has been validated on a number of dissipative and reflective beaches bordering all regional seas in the EU.

Beyond sandy coasts, the model has been applied to coral fringing and atoll reefs, in cooperation with and with funding by the University of Western Australia, the USGS and the Asian Development Bank. The model now also includes vegetative damping effects, with support of the U.S. Office of Naval Research.

The non-hydrostatic model has been developed initially by the TU Delft (as a prototype version of the SWASH (Zijlema et al. 2011) model). For the purpose of simulating the morphodynamic processes on gravel beaches, the model was extended and validated with support from the University of Plymouth. In this mode, ship-induced waves can be simulated as well, demonstrating the flight that the model has taken since its first inception.

This development of XBeach could not have been possible without all of the above mentioned funding agencies and partners. It would also not have been possible without the enthusiastic, critical and constructive approach of all consultants, researchers, M.Sc. and Ph.D. students who have taken up XBeach, and made it into the tool that it is today.

This manual serves as an introduction to the model and a reference guide to its many functionalities, options and parameters. We sincerely hope that this document will help existing and new researchers apply the model for their purposes and advance our knowledge of coastal hydro- and morphodynamics.

1.2 Scope

This is a technical reference guide which provides a description of the physics behind the many functionalities of the model, the different model settings and the numerical implementation. For the latest news on XBeach courses and releases, or if you have questions, visit our website: www.xbeach.org.

1.3 Readers guide

To make this guide more accessible we briefly describe the contents of each chapter and the appendix. If this is your first time to start working with XBeach we suggest you to read Section 4.1 which gives an overview which settings are needed to run an XBeach simulation and to practice with the hands-on exercises in Appendix A.

Chapter 2: **Processes and model formulations**. This Chapter describes the theoretical physics modeled in XBeach. This includes short wave propagation, flow, sediment transport and bed level change.

Chapter 3: **Boundary Conditions**. Several possibilities to impose information at the offshore and lateral boundary are implemented in XBeach (eg. wave energy, water levels).

Chapter 4: **Input description.** XBeach works by reading a configuration file called *params.txt*. In this Chapter all the standard keywords for this configuration file are treated. This includes keyword to switch on and off specific processes.

Chapter 5: **References**. Provides a list of publications and related material of XBeach.

Appendix A: **Hands-on exercises.** Several exercises for XBeach to get familiar with the numerical program based on basic course given during the Delft Software Days 2014.

Appendix B: **Advanced model coefficients**. In Chapter 4 the main input parameters and files required by XBeach to start a simulation are explained. In this chapter many more parameters to fine-tune the simulation of different processes are elaborated.

Appendix C: **Numerical implementation**. Discusses the numerical implementation of the processes and model formulation of Chapter 2.

1.4 Technical reference version and revisions

This manual applies to XBeach version 1.22 (revision 4567) also known as the 'King's 'day release. The changes with respect to the previous XBeach release; the v1.21.3657 Groundhog Day version (February 7th, 2014):

Modifications physical formulations
- Groundwater model
- Setbathy
- Bed slope terms
- Single_dir

New physical formulations
- Ship waves
- Spatially varying bed roughness
- Bed roughess formulations (C, Cf not supported anymore)

         XBeach Technical Reference

- Vegetation effects
- Hindered erosion (dilatancy effects)
- Wave dissipation Janssen-Battjes
- Non-hydrostatic wave breaking
- Skewness and asymmetry

Boundary conditions
- Spatially varying wave boundary conditions
- Wave flume boundary
- Cyclic boundaries
- Spectral boundary conditions for non-hydrostatic model
- Time- and space varying short wave time series

Numerical modifications
- Double row/column internal boundaries for parallel implementation
- Separate process for output in MPI
- Output is single precision
- Default outputformat NetCDF

Bug fixes
- Improved interpolation of directional wave spectra
- Wind shear stress with correct magnitude and direction

2 Processes and model formulation

2.1 Domain and definitions

2.1.1 Coordinate system

XBeach uses a coordinate system where the computational x-axis is always oriented towards the coast, approximately perpendicular to the coastline, and the y-axis is alongshore, see Figure 2.1 and Figure 2.2. This coordinate system is defined in world coordinates (x and y in Figure 2.1). The grid size in x- and y-direction (x' and y' in Figure 2.1) may be variable but the grid must be curvilinear. Alternatively, in case of a rectangular grid (a special case of a curvilinear grid) the user can provide coordinates in a local coordinate system that is oriented with respect to world coordinates (x, y) through an origin (xori, yori) and an orientation (alfa) as depicted in Figure 2.1. The orientation is defined counter-clockwise w.r.t. the x-axis (East).

$$x = xori + x'\cos(alfa) - y'\sin(alfa)$$
$$y = yori + x'\sin(alfa) + y'\cos(alfa)$$
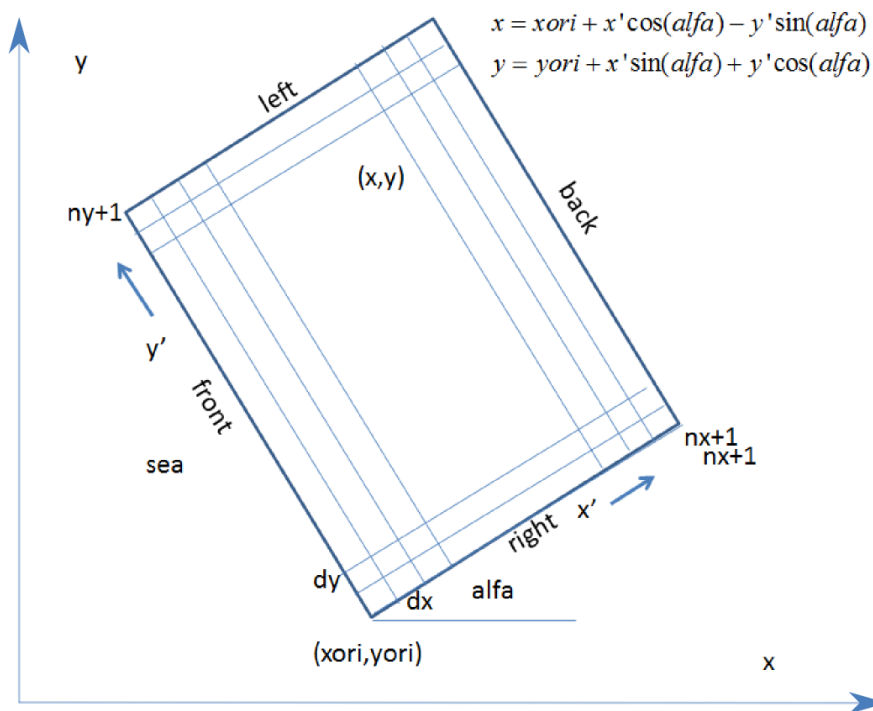
Figure 2.1   Rectangular coordinate system of XBeach, with world coordinates (x, y) and model coordinates (x', y').

2.1.2 Grid set-up

The grid applied is a staggered grid, where the bed levels, water levels, water depths and concentrations are defined in cell centers, and velocities and sediment transports are defined in u- and v-points, viz. at the cell interfaces. In the wave energy balance, the energy, roller energy and radiation stress are defined at the cell centers, whereas the radiation stress gradients are defined at u- and v-points.

Velocities at the u- and v-points are denoted by the output variables uu and vv respectively; velocities u and v at the cell centers are obtained by interpolation and are for output purpose only. The water level, zs, and the bed level, zb, are both defined positive upward. uv and vu are the u-velocity at the v-grid point and the v-velocity at the u-grid point respectively. These are obtained by interpolation of the values of the velocities at the four surrounding grid points.

The model solves coupled 2D horizontal equations for wave propagation, flow, sediment transport and bottom changes, for varying (spectral) wave and flow boundary conditions.
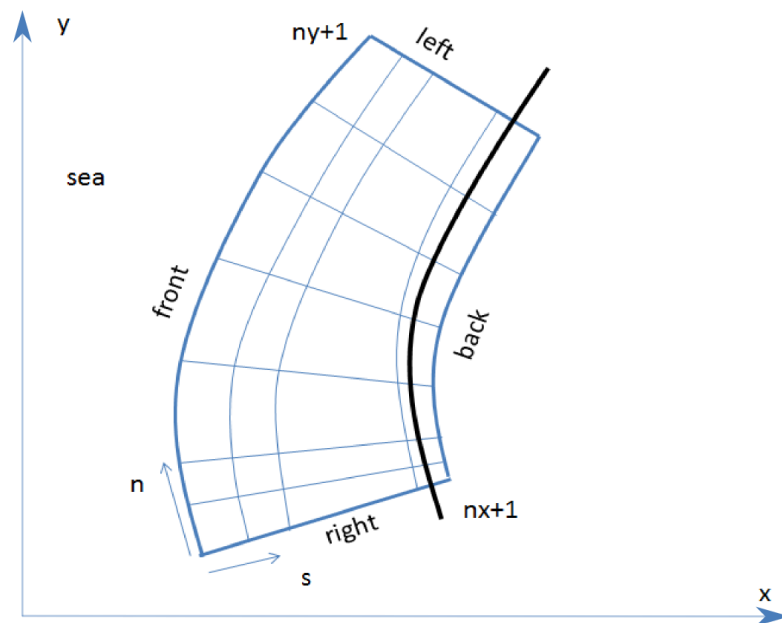
Figure 2.2   Curvilinear coordinate system of XBeach

In XBeach several options are available, depending on the circumstances:
- **1D cross-shore;** in this case the longshore gradients are ignored and the domain reduces to a single gridline (keyword: *ny = 0).* Within this mode the following options are available:
  - Retaining directional spreading (keyword: *dtheta < thetamax – thetamin*); this has a limited effect on the wave heights because of refraction, but can also allow obliquely incident waves and the resulting longshore currents;
  - Using a single directional bin (keyword: *dtheta = thetamax – thetamin*); this leads to perpendicular waves always and ignores refraction. If the keyword *snells = 1* is applied, the mean wave direction is determined based on Snell's law. In this case also longshore currents are generated.

- **2DH area;** the model is solved on a curvilinear staggered grid (rectilinear is a special case). The incoming short wave energy will vary along the seaward boundary and in time, depending on the wave boundary conditions. This variation is propagated into the model domain. Within this mode the following options are available:
  - Resolving the wave refraction 'on the fly' using the propagation in wave directional space. For large directional spreading or long distances this can lead to some smoothing of groupiness since the waves from different directions do not interfere but their energy is summed up. This option is possible for arbitrary bathymetry and any wave direction. The user must specify the width of the directional bins for the surfbeat mode (keyword: *dtheta*)
  - Solving the wave direction at regular intervals using the stationary solver, and then propagating the wave energy along the mean wave direction. This

preserves the groupiness of the waves therefore leads to more forcing of the infragravity waves (keyword: *single_dir = 1*). The user must now specify a single directional bin for the instationary mode (*dtheta = thetamax - thetaminn*) and a smaller bin size for the stationary solver (keyword: *dtheta_s).*For schematic, longshore uniform cases the mean wave direction can also be computed using Snell's law (keyword: *snells = 1*). This will then give comparable results to the *single_dir* option.

2.2 Hydrodynamics options

XBeach was originally developed as a short-wave averaged but wave-group resolving model, allowing resolving the short wave variations on the wave group scale and the long waves associated with them (Figure 2.3). Since the original paper by Roelvink et al. (2009) a number of additional model options have been implemented, thereby allowing users to choose which time-scales to resolve:

- Stationary wave model, .efficiently solving wave-averaged equations but neglecting infragravity waves;
- Surfbeat mode (instationary) ., where the short wave variations on the wave group scale (short wave envelope) and the long waves associated with them are resolved;
- Non-hydrostatic mode (wave-resolving)., where a combination of the non-linear shallow water equations with a pressure correction term is applied, allowing to model the propagation and decay of individual waves.

In the following these options are discussed in more detail.
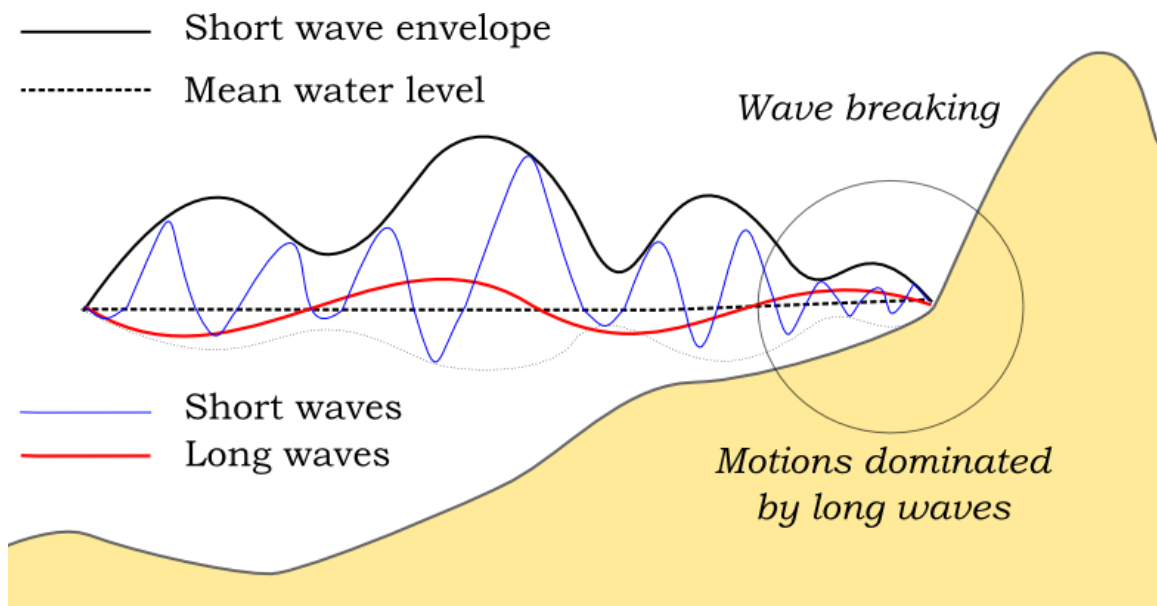
Figure 2.3 Principle sketch of the relevant wave processes

2.2.1 Stationary mode

In stationary mode the wave-group variations and thereby all infragravity motions are neglected. This is useful for conditions where the incident waves are relatively small and/or short, and these motions would be small anyway. The model equations are similar to HISWA (Holthuijsen et al., 1989) but do not include wave growth or wave period variations. Processes that are resolved are wave propagation, directional spreading, shoaling, refraction, bottom dissipation and wave breaking, and a roller model (Svendsen, 1984; Nairn et al., 1990; Stive and de Vriend, 1994) is included; these processes are usually dominant in

nearshore areas of limited extent. For the breaking dissipation we use the Baldock et al. (1998) model, which is valid for wave-averaged modeling. The radiation stress gradients from the wave and roller model force the shallow water equations, drive currents and lead to wave setdown and setup. Additionally, wind and tidal forcing can be applied.

The mean return flow due to mass flux and roller is included in the model and affects the sediment transport, leading to an offshore sediment flux. Effects of wave asymmetry and skewness are included as well. Bed slope effects can further modify the cross-shore behavior. A limited number of model coefficients allow the user to calibrate the profile shape resulting from these interactions.

A typical application would be to model morphological changes during moderate wave conditions, often in combination with tides. The wave boundary conditions can be specified as constant (keyword: *wbctype = stat*) or as a time-series of wave conditions (keyword: *wbctype = stat_table)*. Typical examples of such model applications are given in Figure 2.4 for tombolo formation behind an offshore breakwater (left panel) and development of an ebb delta at a tidal inlet (right panel). A big advantage of the stationary XBeach wave model over other models is that the lateral boundaries are entirely without disturbance if the coast is longshore uniform near these boundaries.
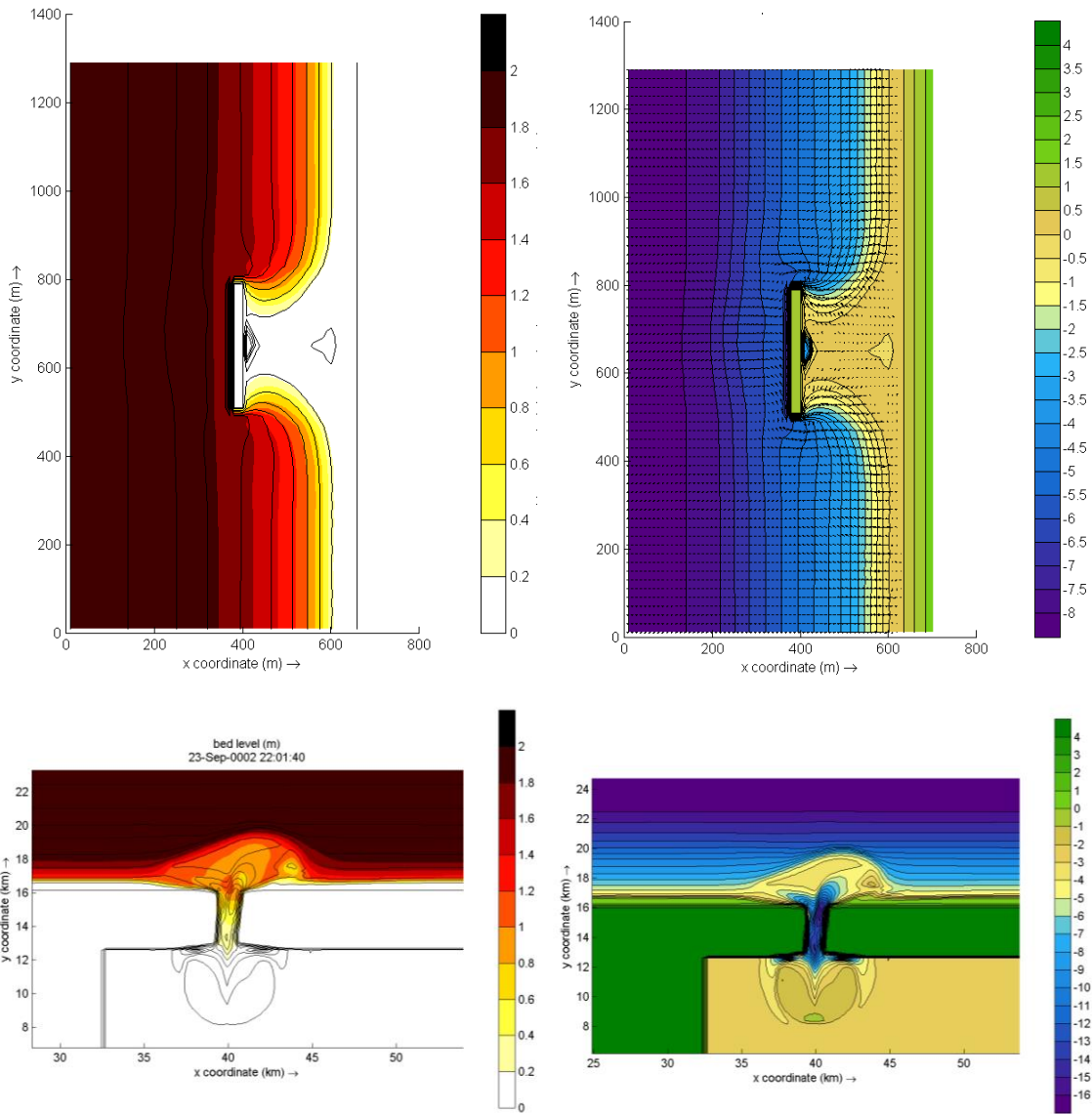
Figure 2.4 Model applications in stationary mode. Root-mean square wave height (left panels) and final bathymetry (right panels) for an offshore breakwater case (upper panels) and a tidal inlet with waves from 330 degrees (lower panels).

2.2.2 Surfbeat mode (instationary)

The short-wave motion is solved using the wave action equation which is a time-dependent forcing of the HISWA equations (Holthuijsen et al., 1989). These equations solve the variation of short-waves envelope (wave height) on the scale of wave groups. It employs a dissipation model for use with wave groups (Roelvink, 1993a; Daly et al., 2012) and a roller model (Svendsen, 1984; Nairn et al., 1990; Stive and de Vriend, 1994) to represent momentum stored at the surface after breaking. These variations, through radiation stress gradients (Longuet-Higgins and Stewart, 1962, 1964) exert a force on the water column and drive longer period waves (infragravity waves) and unsteady currents, which are solved by the nonlinear shallow water equations (e.g. Phillips, 1977). Thus, wave-driven currents (longshore current, rip currents and undertow), and wind-driven currents (stationary and uniform) for local wind set-up, long (infragravity) waves, and runup and rundown of long waves (swash) are included.

Using the surfbeat mode it is necessary when the focus is on swash zone processes rather than time-averaged currents and setup. This assumption is valid on dissipative beaches, where the short waves are mostly dissipated by depth-induced wave breaking. On intermediate beaches and during extreme events the swash motions are still predominantly in the infragravity band and so is the wave runup.

o

In Figure 2.5 and Figure 2.6some typical applications of 1D and 2D models are shown; a reproduction of a large-scale flume test, showing the ability of XBeach to model both short-wave (HF) and long-wave (LF) wave heights and velocities; and a recent 2DH simulation (Nederhoff et al., 2015) of the impact of hurricane Sandy on Camp Osborne, Brick, NJ.
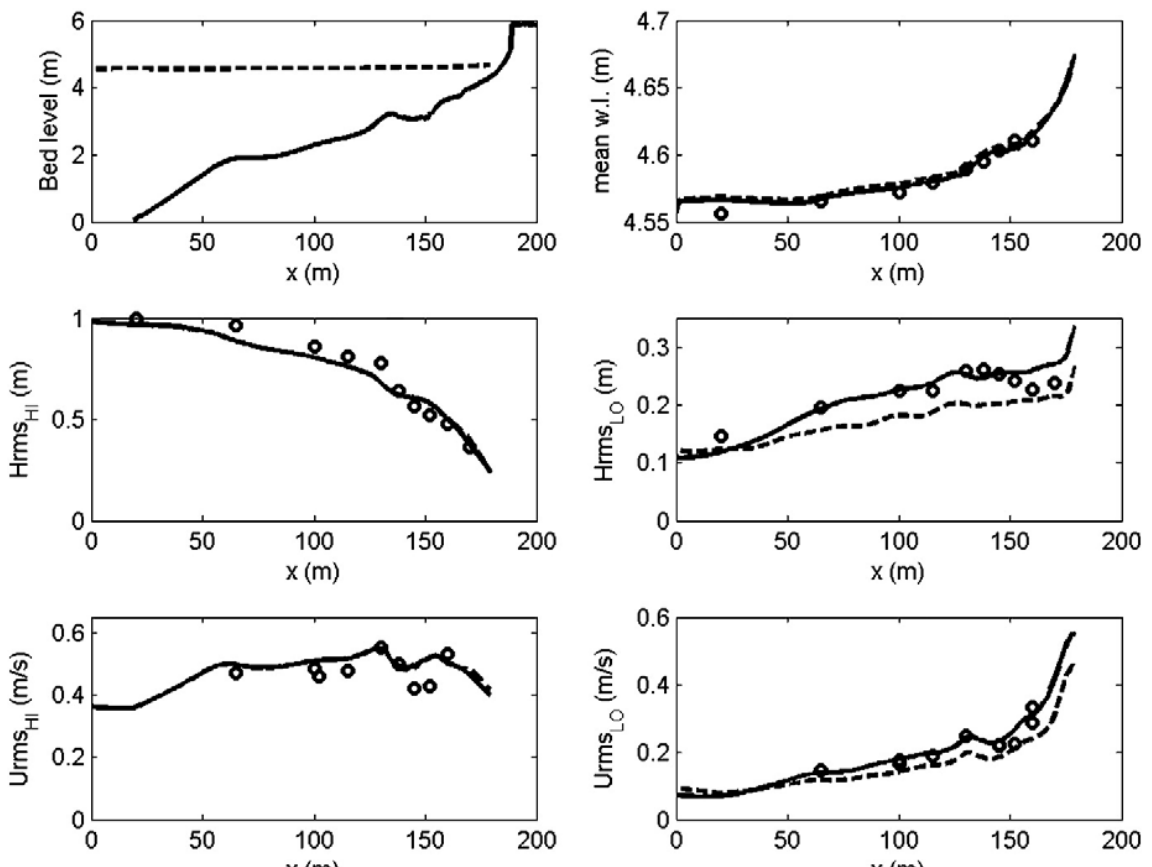
Figure 2.5 Computed and observed hydrodynamic parameters for test 2E of the LIP11D experiment (2E). Top left: bed level and mean water level. From top to bottom: measured (dots) and computed mean water levels, wave heights for the low en high frequency bands (H_{rms}) and velocities for the high and low frequency bands (u_{rms}).
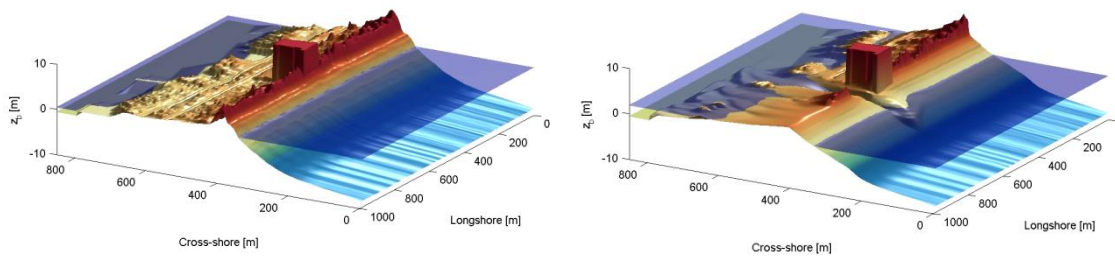
Figure 2.6 Pre (left) and post-Sandy (right) in a three dimensional plot with both bed and water levels as simulated by XBeach (Nederhoff et al. 2015)

2.2.3 Non-hydrostatic mode (wave resolving)

For non-hydrostatic XBeach calculations . depth-averaged flow due to waves and currents are computed using the non-linear shallow water equations, including a non-hydrostatic pressure. The depth-averaged dynamic pressure (q) is derived in a method similar to a one-layer version of the SWASH model (Zijlema et al. 2011). The depth averaged dynamic pressure is computed from the mean of the dynamic pressure at the surface and at the bed by assuming the dynamic pressure at the surface to be zero and a linear change over depth.

Under these formulations dispersive behavior is added to the long wave equations and the model can be used as a short-wave resolving model. Wave breaking is implemented by disabling the non-hydrostatic pressure term when waves exceed a certain steepness, after which the bore-like breaking implicit in the momentum-conserving shallow water equations takes over.

In case the non-hydrostatic mode is used, the short wave action balance is no longer required. However, in the wave-resolving mode we need much higher spatial resolution and associated smaller time steps, making this mode much more computationally expensive than the surfbeat mode.

The main advantages of the non-hydrostatic mode are that the incident-band (short wave) runup and overwashing are included, which is especially important on steep slopes such as gravel beaches. Another advantage is that the wave asymmetry and skewness are resolved by the model and no approximate local model or empirical formulation is required for these terms. Finally, in cases where diffraction is a dominant process, wave-resolving modeling is needed as it is neglected in the short wave averaged mode.

An application of the non-hydrostatic mode is XBeach-G, which is a branch of the main XBeach source code but is specifically developed to simulate storm impacts on gravel beaches (McCall et al, 2014), see Figure 2.7. The formulations for gravel beaches are developed for the non-hydrostatic mode and although sandy morphology can be simulated using the wave-resolving mode, it has not been extensively validated and it is likely that changes in the sediment transport formulations will be implemented in the near future.

An interesting recent application that has been validated for a number of cases concerns the modeling of primary waves generated by large ships, see Section 2.9.

Deltares
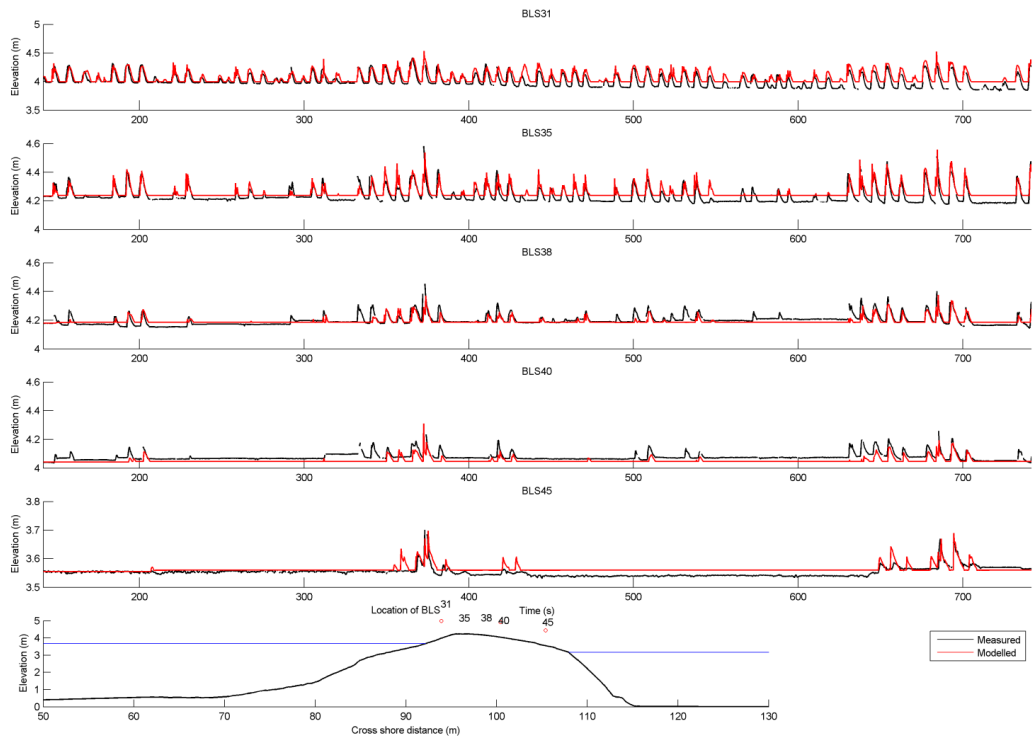
Figure 2.7 Measured (black) and modeled (red) time series of overtopping during BARDEX experiment, from McCall et al, 2014.

2.3 Short wave action

2.3.1 Short wave action balance

The wave forcing in the shallow water momentum equation is obtained from a time dependent version of the wave action balance equation. Similar to Delft University's (stationary) HISWA model (Holthuijsen et al., 1989) the directional distribution of the action density is taken into account, whereas the frequency spectrum is represented by a frequency, best represented by the spectral parameter $f_{m-1,0}$. The wave action balance (keyword: *swave*) is then given by:

$$\frac{\partial A}{\partial t} + \frac{\partial c_{gx} A}{\partial x} + \frac{\partial c_{gy} A}{\partial y} + \frac{\partial c_\theta A}{\partial \theta} = -\frac{D_w + D_f + D_v}{\sigma} \tag{2.1}$$

In which the wave action A is calculated as:

$$A(x,y,t,\theta) = \frac{S_w(x,y,t,\theta)}{\sigma(x,y,t)} \tag{2.2}$$

where θ represents the angle of incidence with respect to the x-axis, S_w represents the wave energy density in each directional bin and σ the intrinsic wave frequency. The intrinsic frequency σ and group velocity c_g is obtained from the linear dispersion relation. D_w, D_f and D_v are dissipation terms for respectively waves, bottom friction and vegetation. The intrinsic frequency is for example obtained with:

$$\sigma = \sqrt{gk \tanh kh} \tag{2.3}$$

The wave action propagation speeds in *x, y* and directional space are given by:

$$c_{gx}(x,y,t,\theta) = c_g \cos(\theta)$$
$$c_{gy}(x,y,t,\theta) = c_g \sin(\theta) \tag{2.4}$$
$$c_\theta(x,y,t,\theta) = \frac{\sigma}{\sinh 2kh} \left(\frac{\partial h}{\partial x} \sin\theta - \frac{\partial h}{\partial y} \cos\theta \right)$$

where h represents the local water depth and k the wave number. The intrinsic wave frequency σ is determined without wave current interaction (keyword: wci=1, see Section 2.3.1.1), which means it is equal to the absolute radial frequency ω.

2.3.1.1 *Wave current interaction (wci)*

Wave-current interaction is the interaction between waves and the mean flow. The interaction implies an exchange of energy, so after the start of the interaction both the waves and the mean flow are affected by each other. This feature is especially of importance in gullies and rip-currents (Reniers et al., 2007).

In XBeach this is taken into account by correcting the wave number k with the use of Eikonal equations, which will have impact on the group and wave propagation speed (x, y, and directional space). The cross-shore and alongshore wave numbers, k_x and k_y, are defined according to (2.5). In these formulations the subscripts refer to the direction of the wave vector components.

$$k_x = k_x^{n-1} + k_x^{\sim}$$
$$k_y = k_y^{n-1} + k_y^{\sim}$$

$$(2.5)$$

Where subscript *n-1* refers the wave number of the previous time step, $k_x^{\sim}$ and $k_y^{\sim}$ are the wave number corrections and k_x and k_y are the corrected wave numbers that take into account the presence of a current. The correction terms are determined with a second set of equations, the Eikonal equations:

$$\frac{\partial k_x}{\partial t} + \frac{\partial \omega}{\partial x} = 0$$
$$\frac{\partial k_y}{\partial t} + \frac{\partial \omega}{\partial y} = 0$$

$$(2.6)$$

The wave number is then given by:

$$k = \sqrt{k_x^2 + k_y^2}$$

$$(2.7)$$

The absolute radial frequency *ω* is calculated with:

$$\omega = \sigma + k_x u^L + k_y v^L$$

$$(2.8)$$

where u^L and v^L are the cross-shore and alongshore depth-averaged Lagrangian velocities respectively. The wave action propagation speed (in x and y direction) is given by:

$$c_x(x, y, t, \theta) = c_g \cos(\theta) + u^L$$
$$c_y(x, y, t, \theta) = c_g \sin(\theta) + v^L$$

$$(2.9)$$

The propagation speed in directional (*θ)* space, where bottom refraction (first term) and current refraction (last two terms) are taken into account, is obtained from:

$$c_\theta(x, y, t, \theta) = \frac{\sigma}{\sinh 2kh}\left(\frac{\partial h}{\partial x}\sin\theta - \frac{\partial h}{\partial y}\cos\theta \right) + \cos\theta\left(\sin\theta\frac{\partial u}{\partial x} - \cos\theta\frac{\partial u}{\partial y} \right)$$
$$+ \sin\theta\left(\sin\theta\frac{\partial v}{\partial x} - \cos\theta\frac{\partial v}{\partial y} \right)$$

$$(2.10)$$

2.3.2 Dissipation

In XBeach there are three short wave dissipation processes that can be accounted for: wave breaking (D_w), bottom friction (D_f) and vegetation (D_v). The three processes are explained in more detail in the following subsections.

2.3.2.1 Wave breaking

Five different wave breaking formulations are implemented in XBeach. The formulations can be selected using the keyword *break* (Table 2.1).

Table 2.1   Different wave breaking formulations implemented

Wave breaking formula	Type of waves	keyword
Roelvink (1993a)	Instationary	roelvink1
Roelvink (1993a) extended	Instationary	roelvink2
Daly et al. (2010)	Instationary	roelvink_daly
Baldock et al. (1998)	Stationary	baldock
Janssen & Battjes (2007)	Stationary	janssen

For the surf beat approach the total wave energy dissipation, i.e. directionally integrated, due to wave breaking can be modeled according to Roelvink (1993a, keyword: *break=roelvink1*). In the formulation of the dissipation due to wave breaking the idea is to calculate the dissipation with a fraction of breaking waves (Q_b) multiplied by the dissipation per breaking event. In this formulation α is applied as wave dissipation coefficient of O(1) (keyword: *alpha*), T_{rep} is the representative wave period and E_w is the energy of the wave. T_{rep} is equal to T_{m01} by default using keyword *Tm01switch=1*, and becomes $T_{m-1,0}$ for *Tm01switch=0*. The fraction of wave breaking is determined with the root-mean-square wave height (H_{rms}) and the maximum wave height (H_{max}). The maximum wave height is calculated as ratio of the water depth (h) plus a fraction of the wave height *(δH_{rms}, keyword: delta)* using a breaker index γ (keyword: *gamma*). In the formulation for H_{rms} the ρ represents the water density and g the gravitational constant. The total wave energy E_w is calculated by integrating over the wave directional bins.

$$\bar{D}_w = 2\frac{\alpha}{T_{rep}} Q_b E_w$$

$$Q_b = 1 - \exp\left(-\left(\frac{H_{rms}}{H_{max}}\right)^n\right), \quad H_{rms} = \sqrt{\frac{8E_w}{\rho g}}, \quad H_{max} = \gamma \cdot (h + \delta H_{rms}) \qquad (2.11)$$

$$E_w(x, y, t) = \int_0^{2\pi} S_w(x, y, t, \theta) d\theta$$

In variation of (2.11), one could also use another wave breaking formulation, presented in (2.12). This formulation is somewhat different than the formulation of Roelvink (1993a) and selected using keyword *break=roelvink2*. The main difference with the original formulation is that wave dissipation with *break=roelvink2* is proportional to H^3/h instead of H^2.

$$\bar{D}_w = 2\frac{\alpha}{T_{rep}} Q_b E_w \frac{H_{rms}}{h} \qquad (2.12)$$

Alternatively the formulation of Daly et al. (2010) states that waves are fully breaking if the wave height exceeds a threshold (γ) and stop breaking if the wave height fall below another threshold (γ_2). This formulation is selected by *break=roelvink_daly* and the second threshold, γ_2, can be set using keyword: *gamma2*.

$$\begin{cases} Q_b = 1 & if \quad H_{rms} > \gamma h \\ Q_b = 0 & if \quad H_{rms} < \gamma_2 h \end{cases} \qquad (2.13)$$

In case of stationary waves Baldock et al. (1998) is applied (keyword: *break=baldock*), which is presented in (2.14). In this breaking formulation the fraction breaking waves Q_b and breaking wave height H_b are calculated differently compared to the breaking formulations used for the non-stationary situation. In (2.14) α is applied as wave dissipation coefficient, f_{rep} represents a representative intrinsic frequency and y is a calibration factor.

$$\bar{D}_w = \frac{1}{4}\alpha Q_b \rho g f_{rep}\left(H_b^2 + H_{rms}^2\right)$$

$$Q_b = \exp\left[-\left(\frac{H_b^2}{H_{rms}^2}\right)\right] \ , \ H_b = \frac{0.88}{k}\tanh\left[\frac{\gamma kh}{0.88}\right] \tag{2.14}$$

Finally, it is possible to use the Janssen & Battjes (2007) formulation for wave breaking of stationary waves (keyword: *break=janssen*). This formulation is a revision of Baldock's formulation.

$$\bar{D}_w = \frac{3\sqrt{\pi}\,\alpha f_{rep}\rho g H_{rms}^3}{16h}Q_b$$

$$Q_b = 1 + \frac{4}{3\sqrt{\pi}}\left(R^3 + \frac{3}{2}R\right)\exp\left(-R^2\right) - erf\left(R\right) \tag{2.15}$$

$$R = \frac{H_b}{H_{rms}}$$

In both the instationary or stationary case the total wave dissipation is distributed proportionally over the wave directions with the formulation in (2.16).

$$D_w(x,y,t,\theta) = \frac{S_w(x,y,t,\theta)}{E_w(x,y,t)}\bar{D}_w(x,y,t) \tag{2.16}$$

2.3.2.2 *Bottom friction*
The momentum equations used to compute the mean currents, orbital velocities and surface elevations contain a friction term following (Ruessink et al, 2001; see Section 2.4.2) and are thus considered separately from the bottom friction that has an impact on the wave action balance. The short wave dissipation by bottom friction is especially of importance for coral reeds (eg. Van Dongeren et al, 2012, Quataert et al, 2015) and is modeled as

$$D_f = \frac{2}{3\pi}\rho f_w\left(\frac{\pi H_{rms}}{T_{m01}\sinh kh}\right)^3 \tag{2.17}$$

In (2.17) the f_w (keyword: *fw*) is the short-wave friction coefficient and T_{m01} is the mean period defined by the first and zeroth moments of the wave spectrum. This value only affects the wave action equation and is unrelated to bed friction in the flow equation. Studies conducted on reefs (e.g. Lowe et al., 2007) indicate that f_w should be an order of magnitude (or more) larger than the friction coefficient for flow (c_f) due to the dependency of wave frictional dissipation rates on the frequency of the motion.

The derivation of the short wave dissipation term is based time-averaged instantaneous bottom dissipation using the Johnson friction factor f_w of the bed shear stress:

$$\tilde{D}_f = |\tau u| = \frac{1}{2}\rho f_w |\tilde{u}|^3 \tag{2.18}$$

The evaluation of the term $\left\langle |\tilde{u}|^3 \right\rangle$, the so-called third even velocity moment, depends on the situation. First we need expressions for the orbital velocity amplitude, which is expressed as:

$$u_{orb} = \frac{\pi H_{rms}}{T_p \sinh(kh)} \tag{2.19}$$

In this formulation T_p is the peak wave period, H_{rms} is the root-mean-square wave height, k is the wave number and h is the local water depth.

If we consider the slowly-varying dissipation in wave groups, we need only to average over a single wave period and we can use a monochromatic (regular wave) expression. If we want to have the time-average dissipation over a full spectrum we get the best approximation from considering a linear Gaussian distribution. Guza and Thornton (1985) give pragmatic expressions for both cases.

For the monochromatic case:

$$\left\langle |\tilde{u}|^3 \right\rangle = 1.20 \left\langle |\tilde{u}|^2 \right\rangle^{3/2} = 1.20 \left(\frac{1}{2}u_{orb}^2 \right)^{3/2} = 0.42 u_{orb}^3 \tag{2.20}$$

For the linear Gaussian approximation:

$$\left\langle |\tilde{u}|^3 \right\rangle = 1.60 \left\langle |\tilde{u}|^2 \right\rangle^{3/2} = 1.60 \left(\frac{1}{2}u_{orb}^2 \right)^{3/2} = 0.57 u_{orb}^3 \tag{2.21}$$

Combining (2.18) and (2.12) we get:

$$\left\langle \tilde{D}_f \right\rangle = 0.21 \rho f_w u_{orb}^3 \tag{2.22}$$

In XBeach the orbital velocity amplitude is computed as in (2.19) and the dissipation according to (2.22) which is correct for the case of instationary simulations on wave-group scale.

For the stationary case formulations (2.19) and (2.21) are similarly combined into:

$$\left\langle \tilde{D}_f \right\rangle = 0.28 \rho f_w u_{orb}^3 \tag{2.23}$$

2.3.2.3 *Vegetation*

The presence of aquatic vegetation (keyword: *vegetation*) within the area of wave propagation or wave breaking results in an additional dissipation mechanism for short waves.

This is modeled using the approach of Mendez & Losada (2004), which was adjusted by Suzuki et al., (2011) to take into account vertically heterogeneous vegetation, see Van Rooijen et al. (2015). The short wave dissipation due to vegetation is calculated as function of the local wave height and several vegetation parameters (keyword: *veggiefile*) at a specific number of locations (keyword: *veggiemapfile*). The vegetation can be schematized in a number of vertical elements with each specific property. In this way the wave damping effect of vegetation such as mangrove trees, with a relatively dense root system but sparse stem area, can be modeled. The dissipation term is then computed as the sum of the dissipation per vegetation layer (Suzuki et al, 2011):

$$D_v = \sum_{i=1}^{n_v} D_{v,i} \tag{2.24}$$

where $D_{v,i}$ is the dissipation by vegetation in vegetation layer i and n_v is the number of vegetation layers. The dissipation per layer is given by:

$$D_{v,i} = A_v \cdot \frac{\rho C_{D,i} b_{v,i} N_{v,i}}{2\sqrt{\pi}} \left(\frac{gk}{2\sigma}\right)^3 H_{rms}^{\ 3}, \text{ with}$$

$$A_v = \frac{\left(\sinh^3 k\alpha_i h - \sinh^3 k\alpha_{i-1}h\right) + 3\left(\sinh k\alpha_i h - \sinh k\alpha_{i-1}h\right)}{3k\cosh^3 kh} \tag{2.25}$$

where $C_{D,i}$ is a (bulk) drag coefficient, $b_{v,i}$ is the vegetation stem diameter, $N_{v,i}$ is the vegetation density, and α_i is the relative vegetation height (= h_v / h) for layer i. In case only one vegetation layer is specified, the plants are assumed to be vertically uniform, which would for example typically apply in case of modeling sea grass.

2.3.3 Radiation stresses

Given the spatial distribution of the wave action (and therefore wave energy) the radiation stresses can be evaluated by using linear wave theory as described by:

$$S_{xx,w}(x,y,t) = \int \left(\frac{c_g}{c}\left(1+\cos^2\theta\right) - \frac{1}{2}\right) S_w d\theta$$

$$S_{xy,w}(x,y,t) = S_{yx,w}(x,y,t) = \int \sin\theta\cos\theta \frac{c_g}{c} S_w d\theta \tag{2.26}$$

$$S_{yy,w}(x,y,t) = \int \left(\frac{c_g}{c}\left(1+\sin^2\theta\right) - \frac{1}{2}\right) S_w d\theta$$

2.3.4 Wave shape

The model considered is (short) wave averaged and resolves hydrodynamics associated with the wave group time scale. As a result the short wave shape is not solved for. However, as waves propagate from deep water onto beaches, their surface form and orbital water motion become increasingly non-linear because of the amplification of the higher harmonics.

There are two wave forms implemented to take this non-linearity into account:
1. A formulation of Ruessink et al. (2012) based on a parameterization with the Ursell number. (keyword: *waveform = ruessink_vanrijn*)

2. A formulation of Van Thiel de Vries (2009) based on the parameterized wave shape model of Rienecker and Fenton (1981) (keyword: *waveform = vanthiel*)

The formulation of Ruessink et al. (2012) relies on parameterizations for the non-linearity parameter r and phase Φ. The parameterizations are based on a data set of 30.000+ field observations of the orbital skewness S_k and asymmetry A_s, collected under non-breaking and breaking wave conditions. The only variable parameter is the Ursell number, since according to Ruessink et al. (2012) the Ursell that includes H_s, T and h, describes the variability in S_k and A_s well. The Ursell number is calculated with the equation below.

$$ \tag{2.27} $$

The value for the skewness and asymmetry is calculated with the use of a Boltzmann sigmoid. The skewness and asymmetry are a function of Ψ. In the formulation of Ruessink et al. (2012) the $p_{1:6}$ are used as parameterized factors on the data set of field observations.

$$ B = p_1 + \frac{p_2 - p_1}{1 + \exp \dfrac{p_3 - \log Ur}{p_4}} $$

$$ \psi = -90 + 90 \tanh(p_5 / Ur^{p_6}) \tag{2.28} $$

$$ S_k = B \cos \psi \quad \text{and} \quad A_s = B \sin \psi $$

Alternatively, Van Thiel de Vries (2009) utilized and extended the wave shape model of Rienecker and Fenton (1981). In this model the short wave shape is described by the weighted sum of eight sine and cosine functions

$$ u_{bed} = \sum_{i=1}^{i=8} w A_i \cos(i\omega t) + (1-w) A_i \sin(i\omega t) \tag{2.29} $$

where u_{bed} is the near-bed short wave flow velocity, i refers to the ith harmonic, ω is the angular wave frequency, A_i is the amplitude of a specific harmonic and w is a weighting function affecting the wave shape. The amplitudes $A_{1:8}$ are computed from stream function theory and vary with the dimensionless wave height and dimensionless wave period.

The wave skewness of near bed flow velocities is computed according to (2.30). The wave asymmetries (A_s) can be computed with the same expression replacing u_{bed} by its Hilbert transform.

$$ S_k = \frac{\overline{u_{bed}^3}}{\sigma_{u_{bed}}^3} \tag{2.30} $$

For w equals one a skewed (Stokes) wave is obtained with high peaks and flat troughs whereas w equals zero results in an asymmetric (saw tooth) wave with steep wave fronts. It is hypothesized that the weighting w can be expressed as a function of wave skewness and asymmetry. The relation between the phase and the weighting is studied in more detail by Van Thiel de Vries (2009) by varying w between zero and one in small steps and computing

the amplitudes $A_{1:8}$ with Rienecker and Fenton for a range of wave heights, wave periods and water depths. It is found that a unique relation between w and Φ exists for any combination of wave height, wave period and water depth that is described by:

$$w = 0.2719 \ln \left(\left| \frac{\phi - 1.8642}{0.2933 - \phi} \right| \right) + 0.5 \tag{2.31}$$

As explained in the next section, short-wave turbulence can be computed averaged over the bore interval (T_{bore}). The bore interval is directly related to the wave shape and hence requires the weighting function w is determined. For the formulation of Ruessink et al. (2012) no exact wave shape is determined and therefore no bore interval can be calculated. Therefore this approach cannot be combined with bore averaged short-wave turbulence.

2.3.5 Turbulence

Wave breaking induced turbulence at the water surface has to be transported towards the bed in order to affect the up-stirring of sediment. Roelvink and Stive (1989) used an exponential decay model with the mixing length proportional to H_{rms} to estimate the time averaged turbulence energy at the bed from turbulence at the water surface:

$$k_b = \frac{k}{\exp(h / H_{rms}) - 1} \tag{2.32}$$

where k_b is turbulence variance at the bed and k is the time averaged turbulence variance at the water surface.

There are three possibilities for the turbulence variance at the bed (k_b) implemented into XBeach:

1   Wave averaged near-bed turbulence energy (keyword: *turb = wave_averaged*):

$$k_b = \frac{\overline{k_s}}{\exp(h / L_{mix}) - 1} \tag{2.33}$$

2   Bore-averaged near-bed turbulence energy[1] (keyword: *turb = bore_averaged*)

$$k_b = \frac{\overline{k_s} \cdot T_{rep} / T_{bore}}{\exp(h / L_{mix}) - 1} \tag{2.34}$$

3   Not taking into account the turbulence variance at the bed (keyword: *turb = none*)

Both formulations make use of the wave-averaged turbulence energy (k_s) and a mixing length (L_{mix}). The wave averaged turbulence energy at the surface is computed from the roller energy dissipation and following Battjes (1975) in which D_r is roller dissipation:

$$\overline{k_s} = \left(D_r / \rho_w \right)^{2/3} \tag{2.35}$$

---

[1] *Currently, this formulation is only possible when the wave shape formulation of Van Thiel de Vries (2009) is applied, see Section 2.3.4.*

The mixing length (L_{mix}) is expressed as thickness of the surface roller near the water surface and depends on the roller volume A_r (Svendsen, 1984):

$$L_{mix} = \sqrt{A_r} = \sqrt{\frac{2E_r T_{rep}}{\rho c}} \tag{2.36}$$

2.3.6 Roller energy balance

While the short wave action balance adequately describes the propagation and decay of organized wave energy, it has often been found that there is a delay between the point where the waves start to break (which is where you would expect the strongest radiation stress gradients to occur) and the point where the wave set-up and longshore current start to build. This transition zone effect is generally attributed to the temporary storage of shoreward momentum in the surface rollers. Several authors have analyzed the typical dimensions of such rollers and their effect on the radiation stress (e.g. Longuet-Higgins and Turner, 1974, Svendsen, 1984, Roelvink and Stive, 1989, Nairn et al., 1990, Deigaard 1993, Stive and De Vriend, 1994).

In XBeach, The roller energy balance is coupled to the wave-action/energy balance where dissipation of wave energy serves as a source term for the roller energy balance. Similar to the wave action the directional distribution of the roller energy is taken into account whereas the frequency spectrum is represented by a single mean frequency. The roller energy balance is then given by:

$$\frac{\partial E_r}{\partial t} + \frac{\partial E_r c \cos\theta}{\partial x} + \frac{\partial E_r c \sin\theta}{\partial y} = D_w - D_r \tag{2.37}$$

$$\tag{2.38}$$

where D_w is the loss of organized wave motion due to breaking and D_r is the dissipation due to the roller, where

$$D_r = \frac{2g\beta_r E_r}{c} \tag{2.39}$$

The roller contribution to the radiation stress is:

$$S_{xx,r}(x,y,t) = \int \cos^2\theta S_r d\theta$$

$$S_{xy,r}(x,y,t) = S_{yx,r}(x,y,t) = \int \sin\theta\cos\theta S_r d\theta \tag{2.40}$$

$$S_{yy,r}(x,y,t) = \int \sin^2\theta S_r d\theta$$

$$\tag{2.41}$$

$$\tag{2.42}$$

2.4 Shallow water equations

For the low-frequency waves and mean flows we use the shallow water equations. To account for the wave induced mass-flux and the subsequent (return) flow these are cast into

a depth-averaged Generalized Lagrangian Mean (GLM) formulation (Andrews and McIntyre, 1978, Walstra et al, 2000). In such a framework, the momentum and continuity equations are formulated in terms of the Lagrangian velocity u^L which is defined as the distance a water particle travels in one wave period, divided by that period. This velocity is related to the Eulerian velocity u^E and v^E (the short-wave-averaged velocity observed at a fixed point) by:

$$u^L = u^E + u^S \quad and \quad v^L = v^E + v^S \tag{2.43}$$

where u^S and v^S represent the Stokes drift in *x*- and *y*-direction respectively (Phillips, 1977). The Strokes drift is calculated with (2.44) in which the wave-group varying short wave energy E_w and direction are obtained from the wave-action balance.

$$u^S = \frac{E_w \cos\theta}{\rho h c} \quad and \quad v^S = \frac{E_w \sin\theta}{\rho h c} \tag{2.44}$$

The resulting GLM-momentum equations are given by:

$$\frac{\partial u^L}{\partial t} + u^L \frac{\partial u^L}{\partial x} + v^L \frac{\partial u^L}{\partial y} - f\, v^L - v_h \left(\frac{\partial^2 u^L}{\partial x^2} + \frac{\partial^2 u^L}{\partial y^2} \right) = \frac{\tau_{sx}}{\rho h} - \frac{\tau_{bx}^E}{\rho h} - g \frac{\partial \eta}{\partial x} + \frac{F_x}{\rho h} - \frac{F_{v,x}}{\rho h}$$

$$\frac{\partial v^L}{\partial t} + u^L \frac{\partial v^L}{\partial x} + v^L \frac{\partial v^L}{\partial y} + f\, u^L - v_h \left(\frac{\partial^2 v^L}{\partial x^2} + \frac{\partial^2 v^L}{\partial y^2} \right) = \frac{\tau_{sy}}{\rho h} - \frac{\tau_{by}^E}{\rho h} - g \frac{\partial \eta}{\partial y} + \frac{F_y}{\rho h} - \frac{F_{v,y}}{\rho h} \tag{2.45}$$

$$\frac{\partial \eta}{\partial t} + \frac{\partial h u^L}{\partial x} + \frac{\partial h v^L}{\partial y} = 0$$

where τ_{sx} and τ_{sy} are the wind shear stresses, τ_{bx} and τ_{by} are the bed shear stresses, η is the water level, F_x and F_y are the wave-induced stresses, $F_{v,x}$ and $F_{v,y}$ are the stresses induced by vegetation, v_h is the horizontal viscosity and *f* is the Coriolis coefficient. Note that the shear stress terms are calculated with the Eulerian velocities as experienced by the bed and not with the GLM velocities, as can be seen in (2.45).

2.4.1 Horizontal viscosity

The horizontal viscosity (v_h) is by default computed using the Smagorinsky (1963) model to account for the exchange of horizontal momentum at spatial scales smaller than the computational grid size, which is given as:

$$v_h = c_S{}^2 2^{\frac{1}{2}} \sqrt{ \left(\frac{\delta u}{\delta x} \right)^2 + \left(\frac{\delta v}{\delta y} \right)^2 + \frac{1}{2} \left(\frac{\delta u}{\delta x} + \frac{\delta v}{\delta y} \right)^2 } \Delta x \Delta y \tag{2.46}$$

In (2.46) c_S is the Smagorinsky constant (keyword: *nuh*), set at 0.1 in all model simulations. It is also possible to use a user-defined value for the horizontal viscosity by turning off the Smagorinsky model (keyword: *smag = 0*) and specifying the value directly (also keyword: *nuh*).

2.4.2 Bed shear stress

The bed friction associated with mean currents and long waves is included via the formulation of the bed shear stress (τ_b). Using the approach of Ruessink et al. (2001) the bed shear stress is calculated with:

$$\tau_{bx}^{E} = c_f \rho u_E \sqrt{\left(1.16 u_{rms}\right)^2 + \left(u_E + v_E\right)^2}$$

$$\tau_{by}^{E} = c_f \rho v_E \sqrt{\left(1.16 u_{rms}\right)^2 + \left(u_E + v_E\right)^2}$$

$$(2.47)$$

There are five different formulations in order to determine the dimensionless bed friction coefficient c_f (keyword: *bedfriction*) implemented in XBeach (Table 2.2).

Table 2.2   Different bed friction formulations implemented

Bed friction formulation	Relevant coefficient	keyword	Default value
Dimensionless friction coefficient	c_f	cf	0.003
Chézy	C	Chezy	55 m$^{1/2}$/s
Manning	n	manning	0.02
White-Colebrook	k_s	white-colebrook	0.01
White-Colebrook grain size	D_{90}	white-colebrook-grainsize	0.0003 m

The dimensionless friction coefficient can be calculated from the Chézy value with (2.48). A typical Chézy value for sandy coasts is in the order of 55 m$^{1/2}$/s.

$$c_f = \frac{g}{C^2}$$

$$(2.48)$$

In the Manning formulation the Manning coefficient (n) must be specified. The dimensionless friction coefficient is calculated from (2.49). Manning can be seen as a depth-dependent Chézy value and a typical Manning value for sandy coasts would be in the order of 0.02 s/m$^{1/3}$.

$$c_f = \frac{g n^2}{h^{1/3}}$$

$$(2.49)$$

In the White-Colebrook formulation the geometrical roughness of Nikuradse (k_s) must be specified. The dimensionless friction coefficient is calculated from (2.50) The White-Colebrook formulation has al log relation with the water depth and a typical k_s value for sandy coasts would be in the order of 0.01 - 0.15 m.

$$c_f = \frac{g}{\left(18 \log\left(\frac{12h}{k_s}\right)\right)^2}$$

$$(2.50)$$

The option of White-Colebrook based on the grain size is somewhat different than the other four formulations. This formulation is based on the relation between the D_{90} of the top bed layer and the geometrical roughness of Nikuradse according to (2.51).The user doesn't have to specify a value for the bed friction coefficient, but a value for the D_{90}.

$$c_f = \frac{g}{\left(18\log\left(\frac{12h}{3D_{90}}\right)\right)^2}$$

(2.51)

Values of the drag coefficient for different seabed sediment grain sizes (flat beds) and similarly for bed form scenarios have been empirically derived from field and laboratory data in previous studies for different bed friction coefficients. The value of the friction coefficient (C, c_f, n or k_s) can be defined with one single value (keyword: *bedfriccoef*) or for a separate value per grid cell (keyword: *bedfricfile*)

2.4.3   Damping by vegetation
The presence of aquatic vegetation within the area of wave propagation or wave breaking may not only result in short wave dissipation (Section 2.3.2.3), but also in damping of infragravity waves and/or mean flow. Since both long waves and mean flow are fully resolved with the nonlinear shallow water equations, the effect of vegetation can be modeled using a drag force (e.g. Dalrymple et al., 1984), which can be directly added to the momentum equations (Van Rooijen et al., 2015 or see (2.45)):

$$F_v = F_D = \int_{-h}^{-h+h_{veg}} \frac{1}{2}\rho C_D b_v N u |u| dz$$

(2.52)

Where C_D is a drag coefficient, b_v is the vegetation stem diameter, N is the vegetation density and u is the wave or current related velocity. To take into account the velocity due to mean flow and infragravity waves, we use the Lagrangian velocity (u^L) here. The vegetation-induced time varying drag force is then calculated as the sum of the vegetation-induced drag force per vegetation layer:

$$F_v(t) = \sum_{i=1}^{n_v} F_{v,i}(t)$$

$$F_{v,i}(t) = \frac{1}{2}\rho C_{D,i} b_{v,i} N_{v,i} h_{v,i} u^L(t)\left|u^L(t)\right|$$

(2.53)

where $C_{D,i}$ is a (bulk) drag coefficient, $b_{v,i}$ is the vegetation stem diameter, $N_{v,i}$ is the vegetation density, and $h_{v,i}$ is the vegetation height for layer *i*.

2.4.4   Wind
The first term on the right hand side of the momentum equations [(2.45)] represents the forcing due to the wind stress. These forcing terms due to the wind are formulated as:

$$\tau_{sx} = \rho_a C_d W |W_x|$$

$$\tau_{sy} = \rho_a C_d W |W_y|$$

(2.54)

where τ_w is wind stress, ρ_a is density of air, C_d is the wind drag the coefficient, W is the wind velocity. The wind stress is turned off by default, and can be turned on specifying a constant wind velocity (keyword: windv = *value*) or by specifying a time varying wind file.

2.5 Non-hydrostatic pressure correction

For non-hydrostatic XBeach calculations (keyword: *waveform = nonh*) depth-averaged flow due to waves and currents are computed using the non-linear shallow water equations, including a non-hydrostatic pressure. The non-hydrostatic model accounts for all wave motions (including short waves) within the shallow water equations, so the wave action balance should be turned off (keyword: *swave = 0*). The depth-averaged normalized dynamic pressure (q) is derived in a method similar to a one-layer version of the SWASH model (Zijlema et al. 2011). The depth averaged dynamic pressure is computed from the mean of the dynamic pressure at the surface and at the bed by assuming the dynamic pressure at the surface to be zero and a linear change over depth. In order to compute the normalized dynamic pressure at the bed, the contributions of advective and diffusive terms to the vertical momentum balance are assumed to be negligible.

$$\frac{\delta w}{\delta t} + \frac{\delta q}{\delta z} = 0 \qquad (2.55)$$

In (2.55) w is the vertical velocity and z is the vertical coordinate. The vertical velocity at the bed is set by the kinematic boundary condition:

$$w_b = u \frac{\delta(\eta - h)}{\delta x} \qquad (2.56)$$

Combining the Keller-box method (Lam and Simpson 1976), as applied by Stelling and Zijlema (2003) for the description of the pressure gradient in the vertical, the dynamic pressure at the bed can be described by:

$$q_b = -\frac{h}{2}\left(\frac{\delta q}{\delta z}\bigg|_s + \frac{\delta q}{\delta z}\bigg|_b \right) \qquad (2.57)$$

Substituting (2.56) in (2.55) allows the vertical momentum balance at the surface to be described by:

$$\frac{\delta w_s}{\delta t} = 2\frac{q_b}{h} - \frac{\delta w_b}{\delta t} \qquad (2.58)$$

In (2.58) the subscript *s* refers to the location at the surface. The dynamic pressure at the bed is subsequently solved by combining (2.57) and the local continuity equation:

$$\frac{\delta u}{\delta x} + \frac{w_s - w_b}{h} = 0 \qquad (2.59)$$

In order to improve the computed location and magnitude of wave breaking, the hydrostatic front approximation (HFA) of Smit et al. (2010) is applied, in which the pressure distribution under breaking bores is assumed to be hydrostatic. Following the recommendations of Smit et al. (2010), we consider hydrostatic bores if $\frac{\delta \eta}{\delta t} > 0.6$ and reform if $\frac{\delta \eta}{\delta t} < 0.3$. The values can respectively be changed with the keywords *maxbrsteep* and *secbrsteep*.
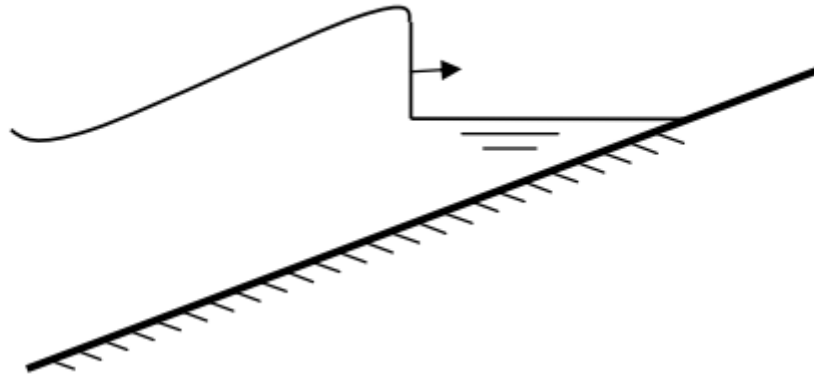
Figure 2.8   During wave breaking and wave runup the wave is modelled as a bore (Smit et al, 2010)

Although this method greatly oversimplifies the complex hydrodynamics of plunging waves, McCall et al. (2014) shows that the application of this method provides sufficient skill to describe dominant characteristics of the flow, without requiring computationally expensive high-resolution discretization of the vertical and surface tracking of overturning waves.

2.6   Groundwater flow

The groundwater module (keyword: *gwflow = 1*) in XBeach utilizes the principle of Darcy flow for laminar flow conditions and a parameterization of the Forchheimer equations for turbulent groundwater flow. The module includes a vertical interaction flow between the surface water and groundwater. This flow is assumed to be a magnitude smaller than the horizontal flow and is not incorporated in the momentum balance.

2.6.1   Continuity

In order to solve mass continuity in the groundwater model, the groundwater is assumed to be incompressible. Continuity is achieved by imposing a non-divergent flow field:

$$\nabla U = 0 \tag{2.60}$$

where U is the total specific discharge velocity vector, with components in the horizontal (u_{gw}, v_{gw}) and vertical (w_{gw}) direction:

$$U = \begin{bmatrix} u_{gw} \\ v_{gw} \\ w_{gw} \end{bmatrix} \tag{2.61}$$

2.6.2   Equation of motions

Laminar flow of an incompressible fluid through a homogeneous medium can be described using the well-known Law of Darcy (1856), valid for laminar flow conditions (keyword: *gwscheme = laminar*)

$$u_{gw} = -K \frac{\partial H}{\partial x}$$

$$v_{gw} = -K \frac{\partial H}{\partial y} \qquad (2.62)$$

$$w_{gw} = -K \frac{\partial H}{\partial z}$$

in which *K* is the hydraulic conductivity of the medium (keyword: *kx, ky, kz*, for each horizontal and vertical direction) and *H* is the hydraulic head.

In situations in which flow is not laminar, turbulent and inertial terms may become important. In these cases the user can specify XBeach to use a method (keyword: *gwscheme =
turbulent*) that is comparable with the USGS MODFLOW-2005 groundwater model (Harbaugh 2005), in which the turbulent hydraulic conductivity is estimated based on the laminar hydraulic conductivity (K_{lam}) and the Reynolds number at the start of turbulence (Re_{crit}) (Halford 2000):

$$u_{gw} = -K\left(\text{Re}\right)\frac{\partial H}{\partial x} \quad \text{in which} \ \ \text{Re} = \frac{|U| D_{50}}{n_p v}$$

$$K\left(\text{Re}\right) = \begin{cases} K_{lam}\sqrt{\dfrac{\text{Re}_{crit}}{\text{Re}}} & \text{if} \ \ \text{Re} > \text{Re}_{crit} \\ K_{lam} & \text{if} \ \ \text{Re} \leq \text{Re}_{crit} \end{cases} \qquad (2.63)$$

In (2.63) the Reynolds number (*Re*) is calculated using the median grain size (D_{50}), the kinematic viscosity of water (*v*) and the groundwater velocity in the pores (U/n_p), where n_p is the porosity. Similar expressions exist for the other two components of the groundwater flow.

The critical Reynolds number for the start of turbulence (Re_{crit}) is specified by the user, based on in-situ or laboratory measurements, or expert judgment (keyword: *gwReturb*). Since the hydraulic conductivity in the turbulent regime is dependent on the local velocity, an iterative approach is taken to find the correct hydraulic conductivity and velocity.

2.6.2.1 Determination of the groundwater head
The XBeach groundwater model allows two methods to determine the groundwater head: a hydrostatic approach (keyword: *gwnonh = 0*) and a non-hydrostatic approach (keyword: *gwnonh = 1*).

Hydrostatic approach
In the hydrostatic approach, the groundwater head is computed as follows:

1   In cells where there is no surface water the groundwater head is set equal to the groundwater surface level $\eta_{gw.}$
2   In cells where there is surface water, but the groundwater surface level η_{gw} is more than $d_{wetlayer}$ (keyword: *dwetlayer*) below the surface of the bed, the groundwater head is set equal to the groundwater surface level.
3   In cells where there is surface water and the groundwater surface level η_{gw} is equal to the surface of the bed, the groundwater head is set equal to the surface water level.

4   In cells where there is surface water and the groundwater surface level η_{gw} is equal to or less than $d_{wetlayer}$ below the surface of the bed, the groundwater head is linearly weighted between that of the surface water level and the groundwater level, according to the distance from the groundwater surface to the surface of the bed.

It should be noted that the numerical parameter $d_{wetlayer}$ is required to ensure numerical stability of the hydrostatic groundwater model. Larger values of $d_{wetlayer}$ will increase numerical stability, at the expense of numerical accuracy.

Non-hydrostatic approach
Groundwater flow in the swash and surf zone has been shown to be non-hydrostatic (e.g., Li and Barry 2000; Lee et al. 2007). In order to capture this, it may be necessary in certain cases to reject the Dupuit–Forchheimer assumption of hydrostatic groundwater pressure.

In the non-hydrostatic approach, the groundwater head is not assumed to be constant in the vertical. Since XBeach is depth-averaged, the model cannot compute true vertical profiles of the groundwater head and velocity. In order to estimate of the groundwater head variation over the vertical, a quasi-3D modeling approach is applied, which is set by two boundary conditions and one non-hydrostatic shape assumption:

1   There is no exchange of groundwater between the aquifer and the impermeable layer below the aquifer.
2   The groundwater head at the upper surface of the groundwater is continuous with the head applied at the groundwater surface.
3   The shape of the non-hydrostatic head profile is parabolic (keyword: *gwheadmodel = parabolic*), implying that the vertical velocity increases or decreases linearly from the bottom of the aquifer to the upper surface of the groundwater, or the non-hydrostatic head profile is hyperbolic (keyword: *gwheadmodel = exponential*), cf., Raubenheimer et al. (1998).

The vertical groundwater head approximation can be solved for the three imposed conditions by a vertical head function, shown here for the parabolic head assumption. The depth-average value of the groundwater head is used to calculate the horizontal groundwater flux and is found by integrating the groundwater head approximation over the vertical:

$$\overline{H} = \frac{1}{h_{gw}} \int_{0}^{h_{gw}} H(\sigma) d\sigma = H_{bc} - \frac{2}{3} \beta h_{gw}^{1} \tag{2.64}$$

In (2.64) the mean vertical ground water head (*H*) is calculated using the groundwater head imposed at the groundwater surface (H_{bc}), the groundwater head parabolic curvature coefficient (*β*) and the height of the groundwater level above the bottom of the aquifer (h_{gw}).

The unknown curvature coefficient (*β*) in the vertical groundwater head approximation (2.64) is solved using the coupled equations for continuity and motion [Equations (2.60) and (2.62)], thereby producing the depth-average horizontal groundwater head gradients and vertical head gradients at the groundwater surface.

Although the requirement for non-hydrostatic pressure has the benefit of being a more accurate representation of reality, and does not require the numerical smoothing parameter

$d_{wetlayer}$, resolving the non-hydrostatic pressure field can be computationally expensive, particularly in 2DH applications.

2.6.2.2 Exchange with surface water

In the groundwater model there are three mechanisms for the vertical exchange of groundwater and surface water: 1) submarine exchange, 2) infiltration and 3) exfiltration. The rate of exchange between the groundwater and surface water (S) is given in terms of surface water volume, and is defined positive when water is exchanged from the surface water to the groundwater.

Infiltration and exfiltration can only occur in locations where the groundwater and surface water are not connected. Infiltration takes place when surface water covers an area in which the groundwater level is lower than the bed level. The flux of surface water into the bed is related to the pressure gradient across the wetting front.

$$S_{inf} = K\left(\frac{1}{\rho g} \frac{p\big|^{z=\xi}}{d_{infill}} + 1 \right)$$

$$\text{in which } d_{infill}(t) = \int \frac{S}{n_p} dt$$

(2.65)

In (2.65) the surface water-groundwater exchange flow of infiltration (S_{inf}) is calculated using the effective hydraulic conductivity (K), the surface water pressure at the bed ($p\big|^{z=\xi}$) and the thickness of the wetting front (d_{infill}).

Since the groundwater model is depth-averaged and cannot track multiple layers of groundwater infiltrating into the bed, the wetting front thickness is reset to zero when there is no available surface water, the groundwater exceeds the surface of the bed, or the groundwater and the surface water become connected. In addition, all infiltrating surface water is instantaneously added to the groundwater volume, independent of the distance from the bed to the groundwater table. Since the groundwater model neglects the time lag between infiltration at the beach surface and connection with the groundwater table a phase error may occur in the groundwater response to swash dynamics

Exfiltration (S_{exf}) occurs where the groundwater and surface water are not connected and the groundwater level (η_{gw}) exceeds the bed level (z_b). The rate of exfiltration is related to the rate of the groundwater level exceeding the bed level.

$$S_{exf} = n_p \frac{\delta(z_b - \eta_{gw})}{\delta t}$$

(2.66)

Submarine exchange (S_{sub}) represents the high and low frequency infiltration and exfiltration through the bed due pressure gradients across the saturated bed. This process only takes place where the groundwater and surface water are connected. In the case of the non-hydrostatic groundwater model, the rate of submarine exchange is determined by the vertical specific discharge velocity at the interface between the groundwater and surface water. The value of this velocity can be found using the vertical derivative of the approximated groundwater head at the groundwater-surface water interface (shown for the parabolic head approximation).

$$S_{sub} = 2\beta h_{gw} K \tag{2.67}$$

In the case of the hydrostatic groundwater model, the difference between the surface water head and the groundwater head is used to drive submarine discharge when the groundwater level is less than $d_{wetlayer}$ from the bed surface.

While most beach systems can acceptably described through vertical exchange of surface water and groundwater, in cases of very steep permeable slopes (e.g., porous breakwaters), it is necessary to include the horizontal exchange of groundwater and surface water between neighboring cells (keyword: *gwhorinfil = 1*). In this case the horizontal head gradient between the surface water and groundwater across vertical interface between the cells is used to determine the horizontal exchange flux:

$$S_{hor} = -K \frac{\partial H_s}{\partial s} A \tag{2.68}$$

where δH_s is the head gradient between the surface water and groundwater in neighboring cell, δs is the gradient distance, defined as the numerical grid size, and A is the surface area through which the exchange takes place, defined as the difference in bed level between the neighboring cells.

2.6.2.3 *Calculation of groundwater and surface water levels*
Groundwater levels are updated through the continuity relation:

$$n_p \frac{\delta \eta_{gw}}{\delta t} = -\frac{\partial h_{gw} u_{gw}}{\partial x} - \frac{\partial h_{gw} v_{gw}}{\partial y} + S_{inf} + S_{exf} + S_{sub} + S_{hor} \tag{2.69}$$

In these same areas the surface water level is modified to account for exchange fluxes:

$$\frac{\delta \eta}{\delta t} = -S_{inf} - S_{exf} - S_{sub} - S_{hor} \tag{2.70}$$

2.6.2.4 *Boundary conditions*
Since the groundwater dynamics are described by a parabolic equation, the system of equations requires boundary conditions at all horizontal and vertical boundaries, as well as an initial condition:
- A zero flux condition is imposed at the horizontal boundaries and bottom of the aquifer.
- The initial condition for the solution is specified by the model user in terms of the initial groundwater head (keyword: *gw0*, or *gw0file*).

2.7 Sediment transport

2.7.1 Advection-diffusion equation
Sediment concentrations in the water column are modeled using a depth-averaged advection-diffusion scheme with a source-sink term based on equilibrium sediment concentrations (Galappatti and Vreugdenhil, 1985):

$$\frac{\partial hC}{\partial t} + \frac{\partial hCu^E}{\partial x} + \frac{\partial hCv^E}{\partial y} + \frac{\partial}{\partial x}\left[D_h h \frac{\partial C}{\partial x} \right] + \frac{\partial}{\partial y}\left[D_h h \frac{\partial C}{\partial y} \right] = \frac{hC_{eq} - hC}{T_s} \tag{2.71}$$

In (2.71) C represents the depth-averaged sediment concentration which varies on the wave-group time scale and D_h is the sediment diffusion coefficient. The entrainment of the sediment is represented by an adaptation time T_s, given by a simple approximation based on the local water depth h and sediment fall velocity w_s. A small value of T_s corresponds to nearly instantaneous sediment response (keyword: *Tsmin*). The factor f_{Ts} is a correction and calibration factor to take into account the fact that w_s is determined on depth-averaged data (keyword: *tsfac*).

$$T_s = \max\left(f_{Ts} \frac{h}{w_s}, T_{s,\min} \right)$$

(2.72)

The entrainment or deposition of sediment is determined by the mismatch between the actual sediment concentration C and the equilibrium concentration C_{eq} thus representing the source term in the sediment transport equation.

2.7.2 General parameters

In the sediment transport formulations, the equilibrium sediment concentration C_{eq} (for both the bed load and the suspended load) is related to the velocity magnitude (v_{mg}), the orbital velocity (u_{rms}) and the fall velocity (w_s). This section elaborates how these are calculated. Important to note: XBeach calculates the equilibrium concentration for the bed and suspended load *separately.*

First of all the Eulerian <u>velocity magnitude</u>, if long wave stirring is turned on (keyword: *lws =* *1*), the velocity magnitude v_{mg} is equal to the magnitude of the Eulerian velocity, as can be seen in Equation (2.73).

$$v_{mg} = \sqrt{\left(u^E\right)^2 + \left(v^E\right)^2}$$

(2.73)

If wave stirring is turned off (*keyword: lws = 0*), the velocity magnitude will be determined by two terms: first of all a factor of the velocity magnitude of the previous time step (v_{mg}^{n-1}) and secondly a current-averaged part. Averaging will be carried out based on a certain factor f_{cats} (keyword: *cats*. Default value is 4.0) of the representative wave period T_{rep}.

$$v_{mg} = \left(1 - \frac{dt}{f_{cats}T_{rep}}\right)v_{mg}^{n-1} + \frac{dt}{f_{cats}T_{rep}}\sqrt{\left(u^E\right)^2 + \left(v^E\right)^2}$$

(2.74)

T_{rep} is the representative wave period and E_w is the energy of the wave. T_{rep} is equal to T_{m01} by default using keyword *Tm01switch=1*, and becomes $T_{m-1,0}$ for *Tm01switch=0*.

Secondly, the <u>root-mean-squared velocity</u>, the u_{rms} is obtained from the wave group varying wave energy using linear wave theory. In this formulation T_{rep} is the representative wave period and the H_{rms} is the root-mean-square wave height. In this equation the water depth is enhanced with a certain factor of the wave height (keyword: *delta,* see equation 2.11).

$$u_{rms} = \frac{\pi H_{rms}}{T_{rep}\sqrt{2}\sinh(k(h + \delta H_{rms}))}$$

(2.75)

To account for wave breaking induced turbulence due to short waves, the orbital velocity is adjusted (van Thiel de Vries, 2009). In this formulation k_b is the wave breaking induced turbulence due to short waves. The turbulence is approximated with an empirical formulation in XBeach.

$$u_{rms,2}^2 = u_{rms}^2 + 1.45 k_b \qquad (2.76)$$

Thirdly, the <u>fall velocity</u>, the w_s is calculated using the formulations of (2000) which are derived based on a relationship suggested by Hallermeier (1981):

$$w_s = \alpha_1 \sqrt{\Delta g D_{50}} + \alpha_2 \frac{\Delta g D_{50}^2}{v} \qquad (2.77)$$

$$\alpha_1 = 1.06 \tanh\left(0.016 A^{0.50} \exp\left(-120/A\right)\right) \qquad (2.78)$$

$$\alpha_2 = 0.055 \tanh\left(12 A^{-0.59} \exp\left(-0.0004 A\right)\right) \qquad (2.79)$$

For high sediment concentrations, the fall velocity is reduced (keyword: *fallvelred = 1*) using the expression of Richardson and Zaki (1954):

$$w_{s,reduced} = \left(1 - C\right)^{\alpha} w_s \qquad (2.80)$$

The exponent α is estimated using the equation of Rowe (1987), which depends purely on the Reynolds particle number R:

$$\alpha = 2.35 \frac{2 + 0.175 \mathrm{R}^{3/4}}{1 + 0.175 \mathrm{R}^{3/4}} \qquad (2.81)$$

$$\mathrm{R} = \frac{w_s D_{50}}{v} \qquad (2.82)$$

2.7.3   Transport formulations

In the present version of XBeach, two sediment transport formulations are available. The formulae of the two formulations are presented in the following sections. For both methods the total equilibrium sediment concentration is calculated with (2.83). In this equation the minimum value of the equilibrium sediment concentration (for both bed load en suspended load) compared to the maximum allowed sediment concentration (keyword: *cmax*).

$$C_{eq} = \max\left(\min\left(C_{eq,b}, \tfrac{1}{2} C_{\max}\right) + \min\left(C_{eq,s}, \tfrac{1}{2} C_{\max}\right),\ 0\right) \qquad (2.83)$$

The transport formulations implemented into XBeach distinguishes bed load and suspended load transport. It is possible to in- and exclude these transports components (keywords: *bed* & *sus*, with bed = 1 one will include bed load transport). There is also a possibility to compute the total bulk transport rather than bed and suspended load separately (keyword: *bulk = 1*). The bed load will be calculated if it is suspended transport. On top of that this switch will have impact on how the bed slope effect (see Section 2.7.6) will be calculated

2.7.3.1   Soulsby-Van Rijn

The first possible sediment transport formulation are the Soulsby-Van Rijn equations (keyword: *form = soulsby_vanrijn*) (Soulsby, 1997; van Rijn, 1984). The equilibrium sediment concentrations are calculated according to:

$$C_{eq,b} = \frac{A_{sb}}{h}\left(\sqrt{v_{mg}^{2} + 0.018\frac{u_{rms,2}^{2}}{C_d}} - U_{cr}\right)^{2.4}$$

$$C_{eq,s} = \frac{A_{ss}}{h}\left(\sqrt{v_{mg}^{2} + 0.018\frac{u_{rms,2}^{2}}{C_d}} - U_{cr}\right)^{2.4}$$

(2.84)

For which the bed load and suspended load coefficients are calculated with:

$$A_{sb} = 0.005h\left(\frac{D_{50}}{h\Delta g D_{50}}\right)^{1.2}, \quad A_{ss} = 0.012 D_{50}\frac{D_*^{-0.6}}{(\Delta g D_{50})^{1.2}}$$

(2.85)

In which the dimensionless sediment diameter (D*) can be calculated with the following formulation. The v is the kinematic viscosity based on the expression of Van Rijn and is a function of the water temperature. XBeach assumes a constant temperature of 20 degrees Celsius, this result in a constant kinematic viscosity of 10^{-6} m^2/s. Note that the D_{50} cancels in the A_{sb} formulation (Soulsby, 1992, eq 136b)

$$D_* = \left(\frac{\Delta g}{v^{2}}\right)^{1/3} D_{50}$$

(2.86)

The critical velocity (U_{cr}) defines at which depth averaged velocity sediment motion is initiated:

$$U_{cr} = \begin{cases} 0.19 D_{50}^{0.1}\log 10\left(\frac{4h}{D_{90}}\right) & \text{for } D_{50} \leq 0.0005m \\ 8.5 D_{50}^{0.6}\log 10\left(\frac{4h}{D_{90}}\right) & \text{for } D_{50} > 0.05m \end{cases}$$

(2.87)

Finally the drag coefficient (C_d) is calculated with Equation (2.88). A drag coefficient is used to determine the equilibrium sediment concentrations (equation 2.89). On top of that Souslby (1997) gives a relation between the bed shear stress of the depth-averaged current speed.

$$C_d = \left(\frac{0.40}{\ln\left(\frac{\max(h,10\,z_0)}{z_0}\right) - 1}\right)^{2}$$

(2.88)

In this equation z_0 is used for the bed roughness length and is used as zero flow velocity level in the formulation of the sediment concentration. In XBeach this is a fixed value (keyword:

z0), but Soulsby (1997) argues there is a relation between the Nikuradse and kinematic viscosity.

2.7.3.2 Van Thiel-Van Rijn

The second possible sediment transport formulation are the Van Thiel-Van Rijn transport equations (keyword: *form = vanthiel_vanrijn*) (van Rijn, 2007; van Thiel de Vries, 2009). The major difference between the Soulsby – Van Rijn equations is twofold. First of all, there is no drag coefficient calculated anymore and secondly the critical velocity is determined by calculating separately the critical velocity for currents (U_{crc}) according to Shields (1936) and for waves (U_{crw}) according to Komen and Miller (1975).

The equilibrium sediment concentrations are calculated according to

$$C_{eq,b} = \frac{A_{sb}}{h} \left(\sqrt{v_{mg}^2 + 0.64 u_{rms,2}^2} - U_{cr} \right)^{1.5}$$

$$C_{eq,s} = \frac{A_{ss}}{h} \left(\sqrt{v_{mg}^2 + 0.64 u_{rms,2}^2} - U_{cr} \right)^{2.4}$$

$$(2.89)$$

For which the bed-load and suspended load coefficient are calculated with:

$$A_{sb} = 0.015 h \frac{\left(D_{50}/h \right)^{1.2}}{\left(\Delta g D_{50} \right)^{0.75}}, \; A_{ss} = 0.012 D_{50} \frac{D_*^{-0.6}}{\left(\Delta g D_{50} \right)^{1.2}} \tag{2.90}$$

The critical velocity is computed as weighted summation of the separate contributions by currents and waves (Van Rijn, 2007):

$$U_{cr} = \beta U_{crc} + (1-\beta) U_{crw} \;\; \text{in which} \;\; \beta = \frac{v_{mg}}{v_{mg} + u_{rms}} \tag{2.91}$$

The critical velocity for currents is based on Shields (1936):

$$U_{crc} = \begin{cases} 0.19 D_{50}^{0.1} \log 10 \left(\dfrac{4h}{D_{90}} \right) & \text{for } D_{50} \le 0.0005 m \\[2ex] 8.5 D_{50}^{0.6} \log 10 \left(\dfrac{4h}{D_{90}} \right) & \text{for } D_{50} \le 0.002 m \\[2ex] 1.3 \sqrt{\Delta g D_{50}} \left(\dfrac{h}{D_{50}} \right)^{1/6} & \text{for } D_{50} > 0.0005 m \end{cases} \tag{2.92}$$

The critical velocity for waves is based on Komer and Miller (1975):

$$U_{crw} = \begin{cases} 0.24 (\Delta g)^{2/3} \left(D_{50} T_{rep} \right)^{1/3} & \text{for } D_{50} <= 0.0005 m \\[2ex] 0.95 (\Delta g)^{0.57} \left(D_{50} \right)^{0.43} T_{rep}^{0.14} & \text{for } D_{50} > 0.0005 m \end{cases} \tag{2.93}$$

2.7.4 Effects of wave nonlinearity

Effects of wave skewness and asymmetry are accounted for in the advection-diffusion equation, repeated here:

$$\frac{\partial hC}{\partial t} + \frac{\partial hC(u^E - u_a \sin\theta)}{\partial x} + \frac{\partial hC(v^E - u_a \cos\theta)}{\partial y}$$
$$+ \frac{\partial}{\partial x}\left[D_h h \frac{\partial C}{\partial x}\right] + \frac{\partial}{\partial y}\left[D_h h \frac{\partial C}{\partial y}\right] = \frac{hC_{eq} - hC}{T_s}$$

(2.94)

XBeach considers the wave energy of short waves as averaged over their length, and hence does not simulate the wave shape. A discretization of the wave skewness and asymmetry was introduced by Van Thiel de Vries (2009), to affect the sediment advection velocity. In this equation u_a is calculated as function of wave skewness (S_k), wave asymmetry parameter (A_s), root-mean square velocity u_{rms} and two calibration factor f_{Sk} and f_{As} (keyword: *facSk & facAs*), see (2.95). To set both values one can use the keyword: *facua*. The method to determine the skewness and asymmetry is described in Section 2.3.4. A higher value for u_a will simulate a stronger onshore sediment transport component.

$$u_a = (f_{Sk}S_k - f_{As}A_s)u_{rms}$$

(2.95)

2.7.5 Hindered erosion by dilatancy

Under overwash and breaching conditions (high flow velocities and large bed level variations in time), dilatancy might hinder the erosion rates (De Vet, 2014). To account for this effect, the theory of Van Rhee (2010) could be applied (keyword: *dilatancy = 1*), reducing the critical Shields parameter θ_{cr} at high flow velocities:

$$\theta_{cr}^{adjusted} = \theta_{cr}\left(1 + \frac{v_e}{k_l}\frac{n_l - n_0}{1 - n_l}\frac{A}{\Delta}\right)$$

(2.96)

In this equation, v_e refers to the erosion velocity, k_l is the permeability, n_0 is the porosity prior, n_l is the porosity in the sheared zone (keyword *pormax*) and the parameter A (keyword *rheeA*) is equal to 3/4 for single particles and approximately 1.7 for a continuum.

The larger the permeability of the bed, the smaller the dilatancy effect. Van Rhee (2010) suggests using the equation proposed by Den Adel (1987):

$$k_l = \frac{g}{160\nu}D_{15}^2\frac{n_0^3}{\left(1 - n_0^2\right)}$$

(2.97)

Finally, the erosion velocity v_e, is the velocity at which the bottom level decreases:

$$v_e = \begin{cases} -\dfrac{dz_b}{dt} & \text{if} & \dfrac{dz_b}{dt} < 0 \\ 0 & \text{else} \end{cases}$$

(2.98)

2.7.6 Bed slope effect

The bed slope affects the sediment transport in various ways (Walstra, 2007):

1   The bed slope influences the local near-bed flow velocity;
2   The bed slope may change the transport rate once the sediment is in motion;
3   The bed slope may change the transport direction once the sediment is in motion;
4   The bed slope will change the threshold conditions for initiation of motion.

Two possible expressions are implemented to change the magnitude of the sediment transport resulting from bed slope effects. The first method is the default one in XBeach:

$$q_{x,slope} = q_x - \alpha hC\sqrt{\left(u^L\right)^2 + \left(v^L\right)^2}\frac{\partial z_b}{\partial x}$$

$$q_{y,slope} = q_y - \alpha hC\sqrt{\left(u^L\right)^2 + \left(v^L\right)^2}\frac{\partial z_b}{\partial y}$$

(2.99)

Where q_x and q_y are calculated in equation (2.110), where α is 1.6 (keyword *facsl*). This method could be applied on either the total sediment transport (keyword: bdslpeffmag = roelvink_total) or only on the bed load transport (keyword: bdslpeffmag = roelvink_bed). The second method is based on the engineering formula of Soulsby (1997):

$$q_{slope} = q\left(1 - \alpha\frac{\partial z_b}{\partial s}\right)$$

(2.100)

Also this method could be applied on the total transport (keyword: bdslpeffmag = soulsby_total) or on the bed load transport only (keyword: bdslpeffmag = soulsby_total). To change the direction of the bed load transport, the expressions of Van Bendegom (1947) and Talmon et al. (1995) could be used (keyword: bdslpeffdir = talmon):

$$\tan\left(\alpha_{\psi,new}\right) = \frac{\sin\left(\alpha_\psi\right) - f\left(\theta\right)\dfrac{dz_b}{dy}}{\cos\left(\alpha_\psi\right) - f\left(\theta\right)\dfrac{dz_b}{dx}}$$

(2.101)

$$f\left(\theta\right) = \frac{1}{9\left(D_{50}/h\right)^{0.3}\theta^{0.5}}$$

(2.102)

$$q_{b,x} = \left|q_b\right|\cos\left(\alpha_{\psi,new}\right)$$

$$q_{b,y} = \left|q_b\right|\sin\left(\alpha_{\psi,new}\right)$$

(2.103)

Where α_ψ is the angle between the fluid velocity vector and the x-axis. Finally, it is possible to adjust the initiation of motion criteria for the total transport (keyword bdslpeffini = total) or the bed load transport only (keyword bdslpeffini = bed) through (Soulsby, 1997):

$$\theta_{cr}^{adjusted} = \theta_{cr}\frac{\cos\left(\psi\right)\sin\left(\beta\right) + \sqrt{\cos^2\left(\beta\right)\tan^2\left(\phi_i\right) - \sin^2\left(\psi\right)\sin^2\left(\beta\right)}}{\tan\left(\phi_i\right)}$$

(2.104)

In this equation is ψ the difference in angle between the flow direction and the on-slope directed vector, β the bed slope and ϕ_i the angle of repose.

De Vet (2014) provides a detailed overview on how the bed slope and flow direction are calculated and how the bed slope effect is combined with the dilatancy concept if the adjustment to the initiation of motion is considered (Section 2.7.5).

2.8 Bottom updating

2.8.1 Due to sediment fluxes
Based on the gradients in the sediment transport the bed level changes according to:

$$\frac{\partial z_b}{\partial t} + \frac{f_{mor}}{(1-p)}\left(\frac{\partial q_x}{\partial x} + \frac{\partial q_y}{\partial y}\right) = 0 \qquad (2.105)$$

In (2.105) ρ is the porosity, f_{mor} (keyword: *morfac*) is a morphological acceleration factor of O(1-10) (Reniers et al., 2004) and q_x and q_y represent the sediment transport rates in x- and y-direction respectively. Sediment transport can be activated with the keyword: *sedtrans*.

The morphological acceleration factor speeds up the morphological time scale relative to the hydrodynamic timescale. It means that if you have a simulation of 10 minutes with a *morfac* of 6 you effectively simulate the morphological evolution over one hour. There are now two ways in which you can input the time-varying parameters in combination with *morfac*:

- All times are prescribed on input in morphological time. If you apply a *morfac* all input time series and other time parameters are divided internally by *morfac*. This is determined with keyword *morfacopt = 1*. If you now specify a *morfac* of 6, the model just runs for 10 (hydrodynamic) minutes each hour, during which the bottom changes per step are multiplied by a factor 6. This of course saves a factor of 6 in computation time.

  This method is appropriate for short-term simulations with extreme events. This approach is only valid as long as the water level changes that are now accelerated by *morfac* do not modify the hydrodynamics too much. This is the case if the tide is perpendicular to the coast and the vertical variations do not lead to significant currents. If you have an alongshore tidal current, as is the case in shallow seas, you cannot apply this method because you would affect the inertia terms and thus modify the tidal currents.

- Alternatively you run the model over, say, over a tidal cycle, and apply the *morfac* without modifying the time parameters. This means you leave all the hydrodynamic parameters unchanged and just exaggerate what happens within a tidal cycle. As long as the evolution over a single tidal cycle is limited, the mean evolution over a tidal cycle using a morfac is very similar to running *morfac* tidal cycles without *morfac*. See Roelvink (2006) for a more detailed description of this approach. This option is enabled with keyword: *morfacopt = 0*.

  This method is more appropriate for longer-term simulations with not too extreme events.

2.8.2 Avalanching

To account for the slumping of sandy material from the dune face to the foreshore during storm-induced dune erosion avalanching (keyword: *avalanching*) is introduced to update the bed evolution. Avalanching is introduced via the use of a critical bed slope for both the dry and wet area (keyword: *wetslp* and *dryslp*). It is considered that inundated areas are much more prone to slumping and therefore two separate critical slopes for dry and wet points are used. The default values are 1.0 and 0.3 respectively. When this critical slope is exceeded, material is exchanged between the adjacent cells to the amount needed to bring the slope back to the critical slope (m_{cr}).

$$\left| \frac{\partial z_b}{\partial x} \right| > m_{cr} \tag{2.106}$$

with a similar expression for the y-direction. To prevent the generation of large shockwaves due to sudden changes of the bottom level, bottom updating due to avalanching has been limited to a maximum speed of $v_{av,max}$ (keyword: *dzmax*). Equation (2.107) shows the resulting bed level change within one time step.

$$\Delta z_b = \min\left(\left(\left| \frac{\partial z_b}{\partial x} \right| - m_{cr} \right) \Delta x, \quad v_{av,max} \Delta t \right) \quad , \frac{\partial z_b}{\partial x} > 0$$

$$\Delta z_b = \max\left(-\left(\left| \frac{\partial z_b}{\partial x} \right| - m_{cr} \right) \Delta x, -v_{av,max} \Delta t \right) \quad , \frac{\partial z_b}{\partial x} < 0 \tag{2.107}$$

2.8.3 Bed composition

If the effect of different sediment fractions, sorting and armoring are of importance, a bed composition constituting multiple sediment fractions can be defined. Each sediment fraction is characterized by a median grain size (D_{50}) and possible a D_{15} and D_{90} as well. When using multiple sediment fractions, multiple bed layers are needed as well to describe the vertical distribution of the sediment fractions in the bed.

By specifying multiple bed layers, XBeach can keep track of the different sediment fractions both in the horizontal and in the vertical. Coarse sediments may be deposited on top of fine sediment after which erosion of the coarse sediment is needed to expose the fine sediment again, effectively armoring the bed. Three types of bed layers are distinguished: 1) the top layers 2) the variable or "breathing" layer and 3) the bottom layers. The top layer is the only layer that interacts with the water column and can be eroded, but preserves its thickness. The bottom layers are layers of constant thickness that move with the top layer. A single variable or "breathing" layer is defined that adapts its thickness to the erosion and sedimentation of the bed. For example: if a grid cell is eroded, particular fractions of sediment are removed from the top layer, but the top layer preserves its thickness and thus it takes the same volume of sediment, likely of different composition than the eroded sediment, from the layer below. If this layer is a top layer as well, the thickness is preserved and again the same volume of sediment is taken form a lower bed layer. This continues until the variable or "breathing" layer is reached. This layer adapts its thickness to the amount of erosion. If the thickness of the layer becomes too small, the variable layer is merged with an adjacent bottom layer and a new bottom layer is defined underneath the existing ones to ensure a constant number of bed layers. Reversely, if a grid cell is accreting, the thickness of the variable layer will be increased and with sufficient increase the variable layer will be split in two effectively creating a new bottom layer. The lowest existing bottom layer is then discarded to ensure a constant

number of bed layers. The "breathing" layer can be the upper or bottom layer in which case the top layer or bottom layer class does not exist. The thickness of the different layer classes can be set separately (keyword: *dzg1, dzg2* and *dzg3*) or at once (keyword: *dzg*).

Each grid cell in XBeach holds its own sediment distribution and the sediment transport formulations are used differentiate between fractions. Therefore the distribution of sediment may change over time and processes like armoring and sorting can be simulated. Due to the shifting of sediment between bed layers numerical mixing of sediment occurs. Choosing bed layer thicknesses that are in balance with the expected erosion and deposition during the simulation should keep the numerical mixing to a minimum. A bed layer thickness that is too large will result in relatively uniform behavior, while a bed layer thickness that is too small will result in a lot of shifting and thus numerical mixing

2.9 Ship-induced wave motions

A specific application for XBeach is the generation and propagation of waves induced by sailing vessels. This functionality has been implemented recently (Zhou, 2013), and has currently been used in several studies (e.g. Zhou et al., 2014, De Jong et al., 2013).

For computing ship-induced waves the non-hydrostatic version of XBeach is used. A moving ship is represented as a pressure head that moves along a pre-defined track through the model domain. The ship is defined on a separate grid, where the ship draft is specified per grid point. Each computational time step the ship draft is interpolated from the ship grid to the global grid, where the ship volume is kept constant. Then the water pressure head in each global grid cell is updated based on the interpolated ship draft. By moving the pressure fields, the waves are generated and will propagate further through the global domain.

In Figure 2.9 an example XBeach setup for ship waves is shown. The ship track is user defined and can, for instance, be obtained from the Automatic Identification System (AIS) for marine traffic. In this example, the model results were compared with measurements taken at Bath, The Netherlands. A filtered time series of the measured and computed water level is shown in Figure 2.10. The time series was filtered to focus on the computation of the primary ship wave.
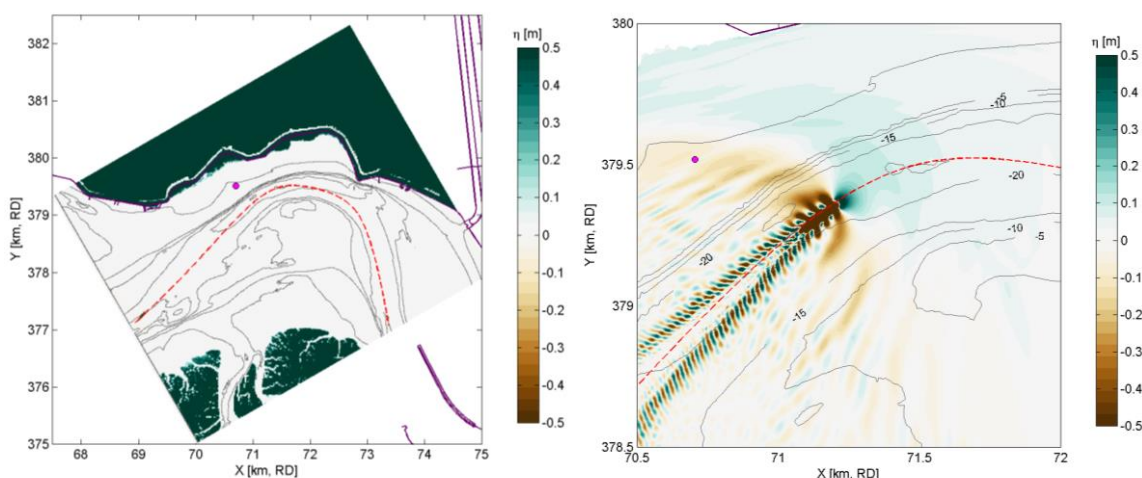
Figure 2.9   Example XBeach setup (left) and result (right) for a ship wave simulation in the Scheldt Estuary (The Netherlands). The ship track (red dashed line) is user-defined, and the measurement location is indicated (magenta dot).

Deltares
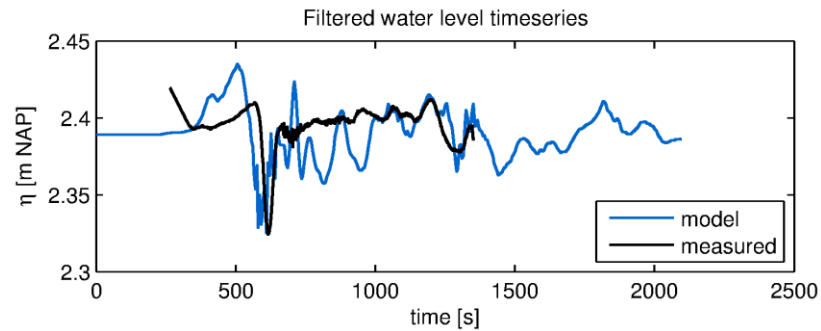
Figure 2.10 Example XBeach result for ship-induced waves. Measurements are taken at Bath, in the Scheldt Estuary, The Netherlands (Schroevers et al., 2011).

In addition to the propagation of ship-induced waves, XBeach computes the forces and moments acting on the ship body. With this functionality, passing ship effects can be analyzed (e.g. Zhou, 2013).

3 Boundary conditions

3.1 Waves
XBeach allows users to include two different options for the seaward wave boundary conditions in the model. (keyword: *wbctype*). First of all, in Section 3.1.1 the method to specify wave spectra is discussed. Secondly, in Section 3.1.2 the method to apply non-spectra, such as stationary wave conditions or time-series is elaborated. In Section 3.1.4 the lateral boundary conditions for waves are discussed. There is currently not a possibility to force waves on the landward boundary of a model. These seaward and lateral boundary conditions for waves can be applied for all hydrodynamic options, i.e. stationary, instationary and non-hydrostatic mode (Section 2.2).

3.1.1 Spectral conditions
The most-used wave boundary conditions in XBeach are spectral conditions. The input description of spectral wave boundary conditions can be found in Section 4.5.1. XBeach allows the user to define these with three possibilities:

1 Parameterized spectrum: With this option you define the boundary condition as parametric spectral input. The parameters (i.e. wave height, wave period, peak-enhancement factor, mean direction en directional spreading) can be specified. Here are two options:
1.1 Specify a single parametric spectrum (keyword *wbctype* = *jons*).
1.2 Specify a series of parametric spectra (keyword *wbctype* = *jons_table*).

2 SWAN spectrum input: In this case the two-dimensional (frequency-direction) output by the spectral wave model SWAN (.sp2 files) can be specified. (keyword *wbctype* = *swan*). This option is especially convenient when nesting XBeach into a SWAN model.

3 Formatted variance density spectrum: In this case a more general type spectrum can be specified. (keyword *wbctype* =*vardens*). This option is often used when a measured spectrum is available.

The details of the possible spectral inputs are described in Chapter 4.

3.1.2 Non-spectral conditions
XBeach also allows the user to define non-spectral wave boundary conditions. These can be stationary boundary conditions where an integral wave height is specified, or a specification as time series. The input description of non-spectral wave boundary conditions can be found in Section 4.5.2. XBeach allows the user to define these with two possibilities:

4 Stationary wave boundary condition. This means that a uniform and constant wave energy is specified, based on the given values of H_{rms}, T_{m01}, direction and power of the directional distribution function. The station boundary condition will not contain wave groups. Here there are two options:
4.1 Specify a single sea state (keyword *wbctype* = *stat*)
4.2 Specify a series of sea states (keyword *wbctype* = *stat_table*)

5 Time series of waves. The user can also specify the variation in time of the wave energy. There are three options:
5.1 First-order time series of waves (keyword *wbctype* = *ts_1*). XBeach will calculate the bound long wave based on the theory of Longuet-Higgins and Stewart (1964).

5.2 Second-order time series of waves (keyword *wbctype* = *ts_2*). The bound long wave is specified by the user via a long wave elevation.

5.3 It is also possible to specify a variation in time of the horizontal velocity, vertical velocity and the free surface elevation (keyword: *wbctype* = *ts_nonh*). Last two terms are optional in this boundary conditions type.

3.1.3 Special conditions

Besides clear spectral or non-spectral wave boundary conditions, there are also three special boundary condition types implemented in XBeach.

6 <u>Bichromatic (two short-wave components) waves</u> (keyword *wbctype* = *bichrom*). In this case, XBeach will be forced with regular wave groups as the two short-wave components force one difference (infragravity) wave period. The user needs to specify not only variables of the stationary situation but also a wave period for the long wave. This wave period will be used to calculate the long wave based on the theory of Longuet-Higgins and Stewart (1964). The bichromatic boundary condition is the most simplified form of a wave spectrum.

7 <u>No wave boundary conditions</u> (keyword *wbctype* = *off*). This is a simple no wave action boundary condition. It still allows for a tidal record to be specified.

8 <u>Reuse previous boundary conditions</u> (keyword: *wbctype* = *reuse*). If the user does not wish to recalculate boundary condition files or specifically wants to reuse the boundary condition files of another XBeach simulation this option should be used. No further wave boundary condition data need to be given. Obviously, the calculation grid should remain the same between runs, as the angles and number of grid points are embedded in the boundary condition files.

3.1.4 Lateral boundary conditions

There are three options to set the lateral boundaries for the wave model:

1. Neumann boundaries (keyword: *lateralwave* = *neumann)*: here the longshore gradient is set to zero.
2. Wave crest boundaries (keyword: *lateralwave* = *wavecrest)*: here the gradient in the wave energy along the wave crest is set to zero.
3. Cyclic boundaries (*keyword: cyclic*): where conditions on the lateral boundaries are copied to each other.

For the stationary wave mode Neumann boundaries are the only option. It allows a correct representation of the wave propagation near the lateral boundaries, without the usual shadow zones in e.g. SWAN. By neglecting the longshore gradients, the model automatically computes a consistent 1D solution.

For the surfbeat mode, Neumann leads to shadow zones, not so much in the wave height, but in the groupiness; the 'blobs' propagating in the mean wave direction turn into elongated, longshore uniform patches. To reduce this effect, the gradient along the wave crests of the wave energy can be set to zero, instead of the longshore gradient (keyword: *lateralwave* = *wavecrest)*. This way the crests of the wave groups have approximately the right orientation, though the along-crest groupiness also disappears. In the *wavecrest* case, the wave refraction may be overestimated leading to somewhat too large longshore currents. The effects of both boundary conditions are shown in Figure 3.1.
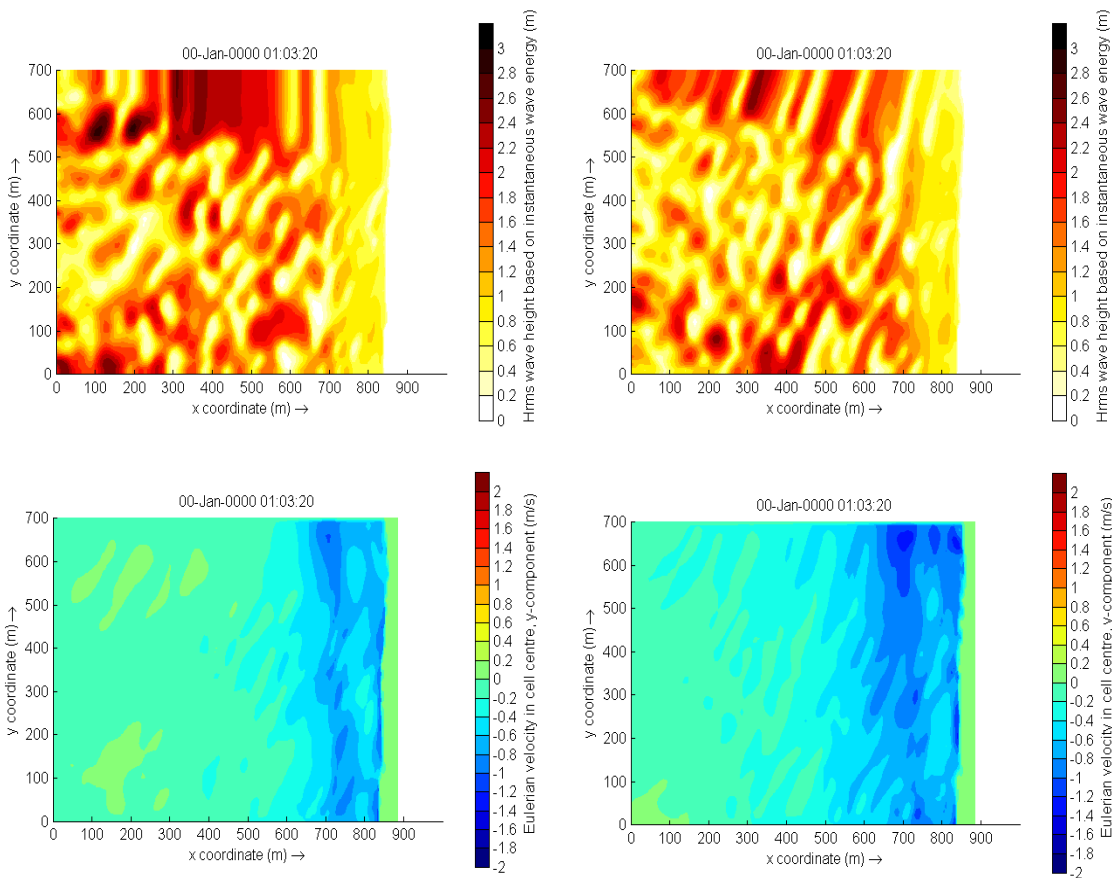
Figure 3.1   Effect of the lateral wave boundary conditions on root-mean square wave height patterns (top) and longshore velocity (bottom) for the Delilah test case. In this figure the left panels are used for simulations with Neumann boundaries and the right panel with the wavecrest boundary.

3.2   Shallow water equations

3.2.1   Offshore boundary

Typically, an offshore or lateral boundary is an artificial boundary which has no physical meaning. On the offshore boundary wave and flow conditions are imposed. In the domain waves and currents will be generated which need to pass through the offshore boundary to the deep sea with minimal reflection. One way to do this is to impose a weakly reflective-type boundary condition (absorbing-generating)(keyword: *front*). This method can be applied in 1D or 2D, is recommended and therefore the default value for XBeach.

In XBeach, there are two options with regard to the offshore absorbing-generating boundary condition. With the parameter setting *front = abs1d* a simple one-dimensional absorbing-generating boundary condition is activated. This option allows for a time-varying water level (surge and/or infragravity waves) to be specified at the boundary while allowing any waves propagating perpendicularly towards the boundary to be absorbed (i.e., passed through the boundary with a minimum of reflection. It is therefore only useful for 1D (flume like) simulations.

With option *front = abs2d* (default value) the formulation by Van Dongeren and Svendsen (1997) is activated which in turn is based on Verboom et al. (1981) and is based on the 'Method of Characteristics'. This boundary condition allows for obliquely-incident and

obliquely-reflected waves to pass through the boundary. It is possible to account for situations with boundary-perpendicular and boundary-parallel currents. In order to differentiate between the particle velocities, the keyword *epsi* must be set. This parameter affects a simple Kalman-update filter which controls whether the particle velocity is current or wave-related. By default XBeach computes the value for epsi automatically using offshore boundary conditions (keyword: *epsi = -1*).

There are four other possibilities implemented besides the absorbing-generating boundary conditions:

1. No flux wall (keyword: *front = wall*). This boundary condition type is a simple no flux boundary condition.
2. Water level specification (keyword: *front = wlevel*). This boundary sets the water level at a prescribed value. This can be constant or time-varying. With this option the outgoing long waves are not absorbed.
3. Boundary condition for the non-hydrostatic option (keyword*: front = nonh_1d*). The user needs to provide a file containing time series for the velocity at the boundary.
4. Radiation boundary condition (keyword: *front = waveflume*). This boundary uses a continuity relation at the front boundary. This means that no net water can come into the model domain. The wave flume boundary condition is especially useful in lab experiments with a large set-up (e.g. coral reefs).

3.2.2 Lateral boundaries

Lateral boundaries are the boundaries perpendicular to the coastline. Usually these are artificial, because the model domain is limited but the physical coast will continue. At these boundaries (keywords: *left* & *right*) we need to prescribe information about the area beyond the numerical model domain in such a way that the boundary condition does not influence the results in an adverse way. One way to do this is to prescribe a so-called "no-gradient" or Neumann boundaries (XBeach default), which state that there is locally no change in surface elevation and velocity, but there are also other possibilities implemented into XBeach. This method is recommended and is therefore the default value for XBeach. Each lateral boundary is a separate condition, so it is possible to mix different type of lateral boundary per side.

Neumann boundary conditions are activated where the longshore water level gradient is prescribed. The alongshore gradient is prescribed by the difference in specified water levels at the offshore corner points, divided by the alongshore length of the domain. This type of Neumann boundary condition has been shown to work quite well with (quasi-) stationary situations, where the coast can be assumed to be uniform alongshore outside the model domain. So far we have found that also in case of obliquely incident wave groups this kind of boundary conditions appears to give reasonable results when a shadow zone is taken into account. This means that regions where the boundary conditions are not fully enforced the results are not taken into account. Neumann boundaries can be individually defined (keyword: *left, right = neumann).*

There are four other possibilities implemented:

1. Simple no-flux boundary conditions can also be applied (keyword: *left = wall*). Wall boundary conditions will result in a zero velocity at the lateral boundary.
2. Velocity at the boundary will be calculated from the non-linear shallow water equations, but only include the advective terms (keywords: *left = no_advec*). The effect is that only terms that decrease the velocity will be taken into account. The result is an intermediate form between a full Neumann boundary and a wall boundary.
3. Velocity at the boundary will simply be copied from the adjacent cell in the model domain (keyword: *left = neumann_v*).
4. Cyclic boundaries

The cyclic boundary condition (keyword: cyclic = 1) treats two lateral boundary regions as if they are physically connected. This makes the model cyclic for everything, just treating it the same way as with MPI domain boundaries. Waves, flow and sediment transport that exists the domain at one side will be transported toward to other side. The only thing the user needs to make sure is that the two grid rows of bathymetric data on the lateral boundaries are identical to the ones on the other side. The advantage of cyclic boundary conditions is that there are no shadow zones (see Figure 3.2). Note: it only works with the MPI version of XBeach since it uses the same routine; however cyclic boundary conditions shouldbe applied with a single domain.
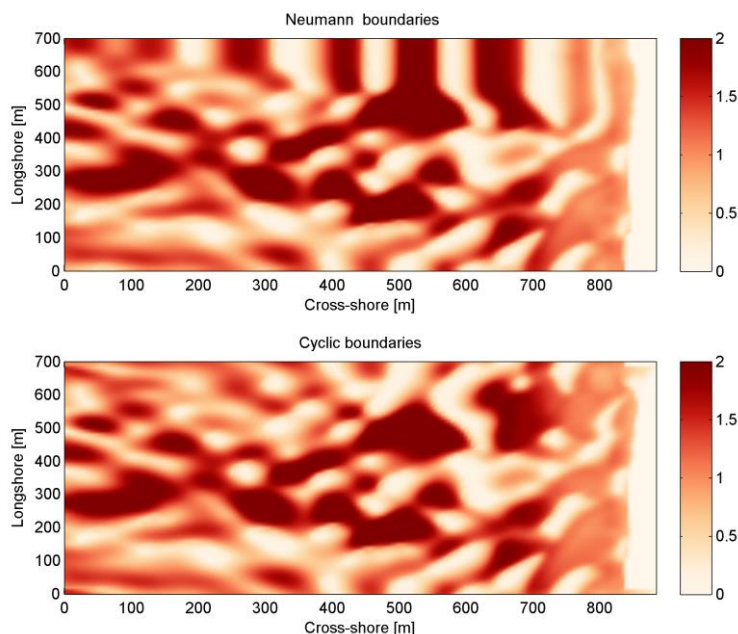
Figure 3.2   Effect of the lateral boundary conditions on root-mean square wave height patterns for the Delilah test case. In this figure the upper panel is used for simulations with Neumann boundaries and the right panel with the cyclic boundary. One can clearly see the 'bulbs' of wave height (shadow zone) in the upper panel as a result of oblique wave attack.

3.2.3   Time varying water level

XBeach can take in up to four time-vary tidal signals to be applied to the four boundaries (offshore-left, backshore-left, backshore-right, offshore-right). A time-varying water level signal is read into XBeach by reading the specified file in zs0file. The input signal will be interpolated to the local time step of the simulation; therefore the signals only need to be long enough and temporally-fine enough to resolve the water level phenomenon of interest (i.e. tide variations, surge event).

There are now four options for handling the tidal and/or surge contribution to the boundaries:
- Uniform water level (keyword: *tideloc = 0*)
- One time-varying water level signal (keyword: *tideloc = 1*)
- Two time-varying water level signals. (keyword: *tideloc = 2*)
- Four time-varying water level signals (keyword: *tideloc = 4*)

For the option with a uniform water level the value specified in the params.txt is applied in the complete model domain (keyword: *zs0*). For the option with one time-varying water level

signal the specified water level is applied (keyword: *zs0file = name_of_your_time_serie*) to the offshore boundary and a fixed value is applied at the backshore boundary (keyword: *zs0=value*). For the option with two time-varying water level signals two water level signals are read from the zs0file. Note: one tidal record is applied to both sea corners and one tidal record to both land corners. This means there is no alongshore variation. An alongshore variation can be applied when applying four time-varying water level signals.

3.2.4 River and point discharge

The effect of a river outflow or other discharges can be simulated with XBeach. Multiple discharge locations can be designated (keyword: *ndischarge*). At a discharge location the discharge orifice is defined as well as the discharge time series in m^3/s. The discharge orifice always constitutes an uninterrupted series of full grid abreast cell borders. It is not possible to define a discharge over half a grid cell nor is it possible to define a single discharge through grid cell borders that are not adjacent.

At each time step the model sets the discharge and velocities at the grid cell borders that constitute the discharge orifice, which can be computed given the size of the discharge orifice and discharge time series. The discharge is positive in positive x or y direction. An exception is made when discharges are defined at the domain border. In that case the discharge is positive towards the domain (influx).

When a discharge is defined with a zero size orifice the discharge is assumed to be in vertical direction where a positive discharge is into the domain (influx). In these cases the discharge is linked to the closest grid cell center and at each time step mass according to the discharge time series is added. No momentum is added in case of a vertical discharge.

3.3 Sediment transport

The boundary conditions for sediment transport are Neumann boundaries everywhere, implying that the cross-boundary gradients in the advection-diffusion equation are set to zero, as well as the gradients of the bed load transports in that direction. Cross-shore profile changes due to cross-shore transport gradients are possible, allowing the boundary to smoothly follow the rest of the model. Still, it is good modeling practice to have the boundaries away from the area of interest.

4 Input description

4.1 General

Upon running the XBeach executable *xbeach.exe*, the file *params.txt* in the current working directory will be read. The *params.txt* file contains grid and bathymetry info, wave input, flow input, morphological input, etc. in the form of keyword/value pairs. Each keyword/value pair may contain an actual model parameter or refer to another file with additional information on the model setup. If a *params.txt* file cannot be found then XBeach will not run.

In the *params.txt* file there can be a single keyword/value pair per line. The keywords can be specified in any order. A keyword/value pair is separated by an equal sign (=). Each line containing an equal sign is interpreted as a keyword/value pair. Reversely, any lines without an equal sign are ignored and may be used for comments. Only a few keywords are required for the model to run, others have default values that are used in case the keyword is not mentioned in the *params.txt* file. The essential parameters for a simulation with a JONSWAP spectrum are listed below:

- A <u>grid with values for x and y</u>. This can both in XBeach format (separate x and y files; keyword d: *xfile* and *yfile*) or Delft3D (one single xy file; keyword: *xyfile*). On top of that the user needs to specify the width of each domain (keyword: *nx* and *ny*)
- A <u>bathymetry</u> file (keyword: *depfile*) that matches with the grid you specified at 1)
- A <u>simulation time</u> (keyword: *tstop*) in seconds
- A <u>directional grid</u> for short waves and rollers. The grid is determined by a minimum and maximum angle and width per bin (keywords: *thetamin*, *thetamax* and *dtheta*).
- A <u>wave boundary condition type</u> (keyword: *wbctype = jons*). With a separate file containing the variables of the parametric (keyword: *bcfile*).

It is strongly recommended to specify as few parameters explicitly as possible and rely on the defaults for the other parameters. When running XBeach, a file called xbeach.log is created, which lists all the parameters set through the params.txt but also all parameters not set, for which the defaults are used. When the user starts the model, it generates a file named XBlog.txt. In this file all the different keyword available are determined. When no keyword is defined the default value will be applied.

This chapter describes the possibilities of the *params*.txt file and any auxiliary information files that are called from the *params.txt* file. These possibilities correspond all to the processes, model formulations and boundary conditions as elaborated in Chapters 2 and 3. The tables in this chapter contain a description of the keywords, the default values, its units and recommended value ranges, while the formats for additional input files are described in the relevant sections. Keyword marked with an astrix (*) are essential for XBeach to run. Keywords marked with a plus (+) are considered advanced expert options and should not be used for regular applications of XBeach.

In this chapter, any references to keywords refer to keywords that can be used in the *params.txt* file. Also any references to time indications are in seconds unless stated otherwise. A typical *params.txt* file for a 1D XBeach model is:

params.txt

```
%%%%%%%%%%%%%%%%%%%%%%%%%%%%%%%%%%%%%%%%%%%%%%%%%%%%%%%%%%%%%%%%%%%%%%%%%%%
%%% XBeach parameter settings input file                              %%%
%%%                                                                   %%%
%%% date:      01-Jan-2015 12:00                                      %%%
%%% function: xb_write_params                                         %%%
%%%%%%%%%%%%%%%%%%%%%%%%%%%%%%%%%%%%%%%%%%%%%%%%%%%%%%%%%%%%%%%%%%%%%%%%%%%

%%% Grid parameters %%%%%%%%%%%%%%%%%%%%%%%%%%%%%%%%%%%%%%%%%%%%%%%%%%%%%%%%

depfile      = bed.dep
posdwn       = 0
nx           = 265
ny           = 0
alfa         = 0
vardx        = 1
xfile        = x.grd
yfile        = y.grd
thetamin     = -90
thetamax     = 90
dtheta       = 15
thetanaut    = 0

%%% Model time %%%%%%%%%%%%%%%%%%%%%%%%%%%%%%%%%%%%%%%%%%%%%%%%%%%%%%%%%%%%%

tstop        = 3600

%%% Physical constants %%%%%%%%%%%%%%%%%%%%%%%%%%%%%%%%%%%%%%%%%%%%%%%%%%%%%%

rho          = 1025

%%% Tide boundary conditions %%%%%%%%%%%%%%%%%%%%%%%%%%%%%%%%%%%%%%%%%%%%%%%%

tideloc      = 2
zs0file      = tide.txt

%%% Wave boundary condition parameters %%%%%%%%%%%%%%%%%%%%%%%%%%%%%%%%%%%%%

wbctype      = jons
bcfile       = filelist.txt

%%% Output variables %%%%%%%%%%%%%%%%%%%%%%%%%%%%%%%%%%%%%%%%%%%%%%%%%%%%%%%%

outputformat = netcdf
tint         = 3600
tstart       = 0

nglobalvar   = 3
zb
zs
H
```

4.2 Physical processes

XBeach supports a variety of physical processes from generic, like waves and flow, to very specific, like ship motions and point discharge. Each process can be switched on or off. The commonly used processes are turned on by default. The table below lists the keywords used to switch on or off physical processes in XBeach.

Table 4.1 Input parameters for physical processes supported by XBeach. The symbol '+' indicates an advanced option.

keyword	description	default	range	units	remark
`avalanching`	Turn on avalanching	1	0 - 1	-	
`flow`	Turn on flow calculation	1	0 - 1	-	
`gwflow` +	Turn on groundwater flow	0	0 - 1	-	
`lwave`	Turn on short wave forcing on NLSW equations and boundary conditions	1	0 - 1	-	
`morphology`	Turn on morphology	1	0 - 1	-	
`nonh` +	Turn on non-hydrostatic pressure: 0 = NSWE, 1 = NSW + non-hydrostatic pressure compensation Stelling & Zijlema, 2003	0	0 - 1	-	
`sedtrans`	Turn on sediment transport	1	0 - 1	-	
`setbathy`	Turn on time series of prescribed bathy input	0	0 - 1	-	
`ships` +	Turn on ship waves	0	0 - 1	-	
`single_dir` +	Turn on stationary model for refraction, surfbeat based on mean direction	0	0 - 1	-	
`snells` +	Turn on Snell's law for wave refraction	0	0 - 1	-	
`Swave`	Turn on short waves	1	0 - 1	-	
`swrunup` +	Turn on short wave runup	0	0 - 1	-	
`vegetation` +	Turn on interaction of waves and flow	0	0 - 1	-	

keyword	description	default	range	units	remark
	with vegetation				

4.3 Physical constants

The parameters listed in the table below involve physical constants used by XBeach. The gravitational acceleration and density of water are universally used coefficient. The *depthscale* is a factor in order to set different cut-off values like *eps* and *hswitch*. A value of the *depthscale* lower than one means the cut-off values will increase.

Table 4.2   Overview of available keyword related to physics

keyword	description	default	range	units	remark
depthscale+	Depthscale of (lab)test simulated, affects eps, hmin, hswitch and dzmax	1.0	0.1 200.0	–	–
g	Gravitational acceleration	9.81	9.7 – 9.9	ms^-2	
rho	Density of water	1025.0	1000.0 – 1040.0	kgm^-3	

4.4 Grid and bathymetry

XBeach' spatial grid size is defined by the keywords *nx* and *ny*. Here nx are the number of grid points in the cross-shore direction and ny the number in the alongshore direction. The size of the computational grid will be *nx+1* by *ny+1* cells large. The initial bathymetry is provided using a separate file that is referred to by the *depfile* keyword, which has to have a size of [nx+1, ny+1]. This file contains an initial bed level for each grid cell where each line corresponds to a transect in x-direction (cross-shore). The values are positive down by default (e.g. a value of '10' is 10 meters of water depth), but this can be changed using the *posdwn* keyword.

Three main types of XBeach grids are supported: fast 1D, 1D and 2DH. Fast 1D grids have a single alongshore grid cell and thus a value *ny=0* and thus a single row (ny+1=1) in the *depfile*. The 1D grids have 3 alongshore grid cells and thus a value *ny=2* and three rows in the *depfile*. The 2DH grids have more than 3 alongshore grid cells, a value *ny>2* and as many rows in the *depfile*. In general, the bathymetry file has the following space-separated format:

bed.dep

```
<z 1,1> <z 2,1> <z 3,1> ... <z nx,1> <z nx+1,1>
<z 1,2> <z 2,2> <z 3,2> ... <z nx,2> <z nx+1,2>
<z 1,3> <z 2,3> <z 3,3> ... <z nx,3> <z nx+1,3>
...
<z 1,ny> <z 2,ny> <z 3,ny> ... <z nx,ny> <z nx+1,ny>
<z 1,ny+1> <z 2,ny+1> <z 3,ny+1> ... <z nx,ny+1> <z nx+1,ny+1>
```

XBeach spatial grids can be equidistant or non-equidistant. In the former case the grid size is defined by the keywords *dx* and *dy*. In the latter case the keyword *vardx* should be set to *1* and x- and y-coordinates of the grid cells should be provided through the files referenced by the *xfile* and *yfile* keywords. These files take exactly the same format as the *depfile* file where all coordinates along the x-direction are in one row and each row represents a cell in y-

direction. XBeach grids are defined in a coordinate system of choice and can be either rectangular or curvilinear grids. This section can be found in 2.1.

Delft3D grids created with tools like RFGRID are also supported. To use Delft3D grids, choose *gridform=delft3d* and provide a grid file via the keyword *xyfile*. The format of Delft3D grids is not described here, but can be found in the Delft3D manual (Deltares, 2011). Also forced updating of bathymetries is supported as described in Section 5A.7.

Apart for the spatial grid, XBeach also uses a directional grid for short waves and rollers. The grid is determined by a minimum and maximum angle and a directional bin size using the keywords *thetamin*, *thetamax* and *dtheta* respectively. The *thetamin* and *thetamax* angles are either defined according to the Cartesian convention (angle w.r.t. the computational x-axis) or according to the nautical convention (angle w.r.t. deg. N, so from W is 270 deg. N). The convention is chosen using the keyword *thetanaut* (thetanaut=0 for Cartesian and thetanaut=1 for Nautical)

Examples of typical input for a non-equidistant, fast 1D XBeach model, together with the *params.txt* example at the start of this chapter, are:

depfile = bed.dep

```
-20.00 -20.00 -19.90 -19.80 -19.70 ... 14 14 15 15 15
```

xfile = x.grd

```
0.00 10.00 20.00 30.00 40.00 ... 1992.00 1994.00 1996.00 1998.00 2000.00
```

yfile = y.grd

```
0.00 0.00 0.00 0.00 0.00 0.00 0.00 ... 0.00 0.00 0.00 0.00 0.00 0.00 0.00
```

All keywords related to grid and bathymetry input are listed in the following table:

Table 4.3   Input parameters for grid and bathymetry supported by XBeach

Keyword	description	default	range	units	remark
Alfa	Angle of computational x-axis relative to "East"	0.0	0.0 – 360.0	deg	
Depfile	Name of the input bathymetry file			<file>	
Dtheta	Directional resolution	10.0	0.1 – 20.0	deg	
dtheta_s	Directional resolution in case of stationary refraction	10.0	0.1 – 20.0	deg	
dx	Regular grid spacing in x-direction	-1.0	0.0 – 1000000000.0	m	
dy	Regular grid spacing in y-direction	-1.0	0.0 – 1000000000.0	m	

Keyword	description	default	range	units	remark
gridform	Grid definition format	xbeach	xbeach, delft3d		
nx	Number of computational cell corners in x-direction	50	2 - 10000	-	
ny	Number of computational cell corners in y-direction	2	0 - 10000	-	
posdwn	Bathymetry is specified positive down (1) or positive up (-1)	1.0	-1.0 - 1.0	-	
thetamax	Higher directional limit (angle w.r.t computational x-axis)	90.0	-180.0 - 180.0	deg	
thetamin	Lower directional limit (angle w.r.t computational x-axis)	-90.0	-180.0 - 180.0	deg	
thetanaut	specify thetamin and thetamax in cartesian (0) or nautical (1) convention	0	0 - 1	-	
vardx	Switch for variable grid spacing	0	0 - 1	-	
xfile*	Name of the file containing x-coordinates of the calculation grid			<file>	
xori	X-coordinate of origin of axis	0.0	-100000000.0 - 1000000000.0	m	
xyfile	Name of the file containing Delft3D xy-coordinates of the calculation grid			<file>	
yfile*	Name of the file containing y-coordinates of the			<file>	

Keyword	description	default	range	units	remark
	calculation grid				
yori	Y-coordinate of origin of axis	0.0	-1000000000.0 - 1000000000.0	m	

4.5 Waves input

An XBeach model is generally forced by waves on its offshore boundary. These waves are described by the wave boundary conditions discussed in this section. The details of the wave motions within the model are described by the wave numerics in terms of the wave action balance (see Section 2.3.1), wave dissipation model (see Section 2.3.2) and wave roller model (see Section 2.3.6)

XBeach supports a variety of wave boundary condition types that are divided in two main groups: stationary and spectral boundary conditions. The *wbctype* keyword can be used to select one particular type of wave boundary conditions. In Section 3.1 all types of wave boundary conditions available for XBeach are given, see Table 4.4 for an overview. Figure 4.1 can be used to help determine what type of wave boundary conditions is appropriate for your case. Each wave boundary condition type is explained in the following subsections. Note that most spectral wave boundary conditions can vary both in space and time using a *FILELIST* and/or *LOCLIST* construction as described in Section 4.5.4.

Table 4.4   *Overview of wave boundary conditions supported by XBeach*

wbctype	Type	description
off	Special	no wave boundary condition
stat	Non-spectral	stationary wave boundary condition (sea state)
bichrom	Special	bichromatic (two wave component) waves
ts_1	Non-spectral	first-order time series of waves (generated outside XBeach), this option specifies free surface elevation and short wave energy
ts_2	Non-spectral	second-order time series of waves (generated outside XBeach), this option specifies free surface elevation and short wave energy
jons	Spectral	wave groups generated using a parametric (JONSWAP) spectrum
swan	Spectral	wave groups generated using a SWAN 2D output file
vardens	Spectral	wave groups generated using a formatted file
ts_nonh	Non-spectral	boundary conditions initially meant for the non-hydrostatic wave type, this option specifies free surface elevation and velocity
reuse	Special	reuse of wave conditions
stat_table	Non-spectral	a sequence of stationary conditions (sea states)
jons_table	Spectral	a sequence of time-varying wave groups

Apart from keywords specific to the various wbctypes, there are a few general keywords

*Table 4.5   General input parameters for wave boundary conditions supported by XBeach. The symbol '+'
indicates an advanced option*

keyword	description	default	range	units	remark
lateralwave	Switch for lateral boundary at left	neumann	neumann, wavecrest, cyclic		
taper	Spin-up time of wave boundary conditions, in morphological time	100.0	0.0 1000.0	– s	This is the spinup time.
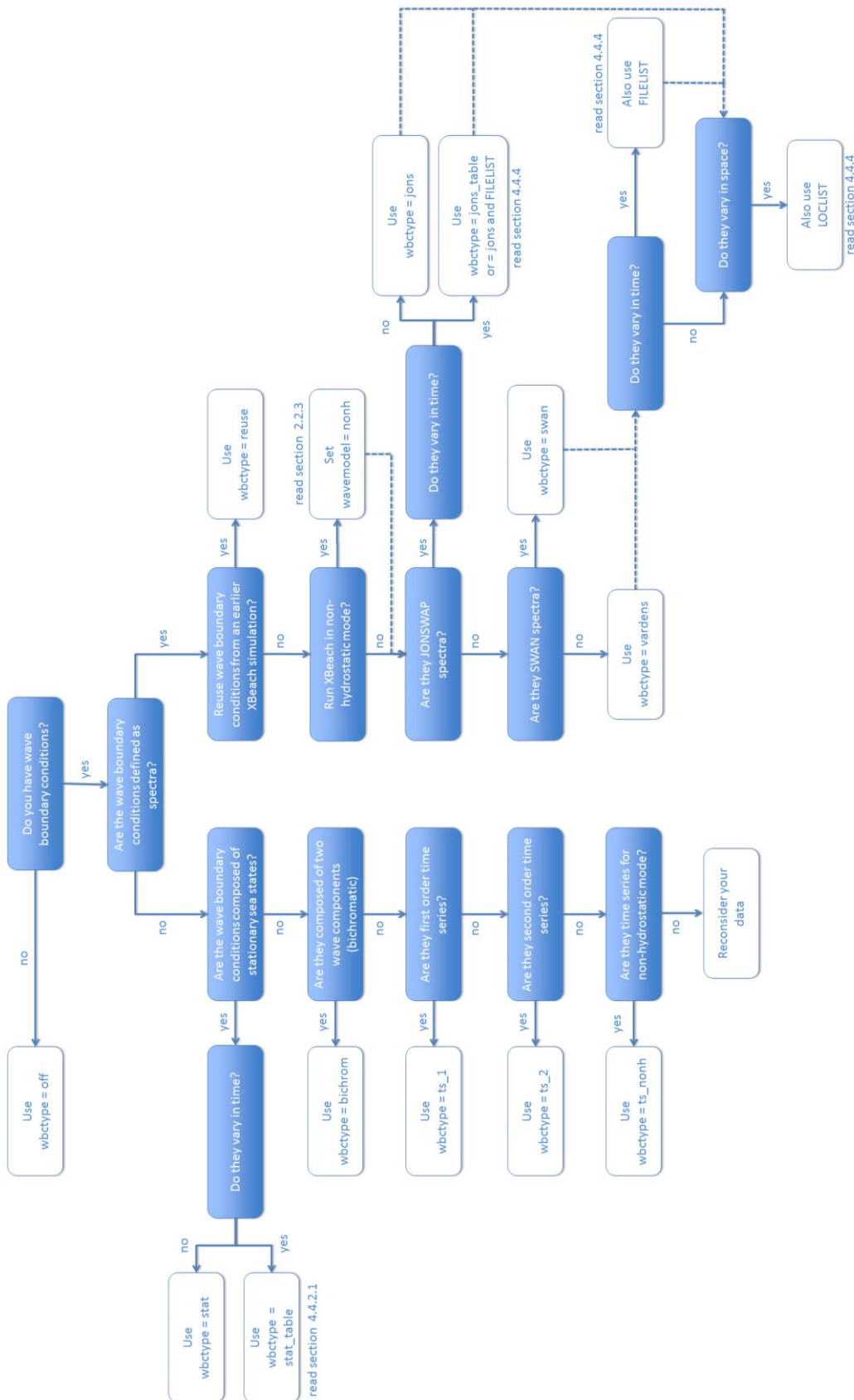
Figure 4.1   Decision tree for selecting the appropriate type of wave boundary conditions

4.5.1 Spectral wave boundary conditions

Spectral wave boundary conditions are enabled using *wbctype* values *jons*, *swan*, *vardens* or *jons_table*. The conditions are defined in separate files referenced from the *params.txt* file using the *bcfile* keyword. A spectral wave boundary condition describes a spectrum *shape* that XBeach uses to generate a (random) wave time series. The length and resolution of the generated time series is determined by the keywords *rt* and *dtbc* respectively. XBeach will reuse the generated time series until the simulation is completed. The resolution of the time series should be enough to accurately represent the bound long wave, but need not be as small as the time step used in XBeach.

An overview of all keywords relevant for spectral wave boundary conditions is given in the table below. The necessary file formats for each type of spectral wave boundary condition is explained in the following subsections.

Table 4.6   Input parameters for spectral wave boundary conditions supported by XBeach. The symbol '+' indicates an advanced option

Keyword	description	default	range	units	remark
Tm01switch +	Switch to enable Tm01 rather than Tm-10	0	0 - 1	-	
Bcfile	Name of spectrum file			<file>	
correctHm0 +	Switch to enable Hm0 correction	1	0 - 1	-	
dtbc+	Time step used to describe time series of wave energy and long wave flux at offshore boundary (not affected by morfac)	1.0	0.1 - 2.0	s	
dthetaS_XB +	The (counter-clockwise) angle in the degrees needed to rotate from the x-axis in SWAN to the x-axis pointing East	0.0	-360.0 - 360.0	deg	
fcutoff +	Low-freq cutoff frequency for wbctype = jons, swan or vardens boundary conditions	0.0	0.0 - 40.0	Hz	
Wbctype	Wave boundary condition type	bichrom	stat, bichrom, ts_1, ts_2, jons,		

Keyword	description	default	range	units	remark
			swan, vardens, reuse, ts_nonh, off, stat_table, jons_table		
Nonhspectrum +	Spectrum format for wave action balance of non-hydrostatic waves	0	0 - 1	-	
Nspectrumloc +	Number of input spectrum locations	1	1 - ny+1	-	
nmax+	Maximum ratio of cg/c for computing long wave boundary conditions	0.8	0.5 - 1.0	-	This option is used to prevent the bound long wave to become too large when the offshore depth is too shallow
random +	Switch to enable random seed for wbctype = jons, swan or vardens boundary conditions	1	0 - 1	-	
Rt	Duration of wave spectrum at offshore boundary, in morphological time	3600	1200-7200	s	
sprdthr +	Threshold ratio to maximum value of S above which spectrum densities are read in	0.08	0.0 - 1.0	-	

Deltares

Keyword	description	default	range	units	remark
Trepfac +	Compute mean wave period over energy band: for wbctype jons, swan or vardens; converges to Tm01 for trepfac = 0.0	0.01	0.0 – 1.0	–	

4.5.1.1 *JONSWAP wave spectra*

JONSWAP spectrum input is enabled using *wbctype = jons*. A JONSWAP wave spectrum is parametrically defined in a file that is referenced using the *bcfile* keyword. This file contains a single parameter per line in arbitrary order. The parameters that can be defined are listed in Table 4.7. All variables are optional. If no value is given, the default value as specified in the table is used. It is advised not to specify the keyword *dfj* and allow XBeach to calculate the default value.

A typical JONSWAP definition file looks as follows:

jonswap.txt

```
Hm0       = 0.8
Tp        = 8
mainang   = 285.
gammajsp  = 3.3
s         = 10.
fnyq      = 0.3
```

For the definitions see the table below.

It is possible to use an alternative file format for time-varying JONSWAP spectra. To enable this option use the *wbctype* value *jons_table*. In this case, each line in the spectrum definition file contains a parametric definition of a spectrum, like in a regular JONSWAP definition file, plus the duration for which that spectrum is used during the simulation. XBeach does not reuse time-varying spectrum files. Therefore the total duration of all spectra should at least match the duration of the simulation. The name of the file can be chosen freely, but the file format is fixed as follows and all parameters should be present in all lines:

jonswap.txt

```
<Hm0> <Tp> <mainang> <gammajsp> <s> <duration> <dbtc>
```

Note that we refer to the keywords used in a regular JONSWAP definition file in this example, with three differences: 1) the peak period rather than the peak frequency is defined 2) the duration is added (similar to *rt* in *params.txt*) 3) the time resolution is added (similar to *dtbc* in *params.txt*). The duration and boundary condition time step in this file overrules *rt* and *dtbc* in *params.txt*.

As an example, the JONSWAP spectrum definition file presented above would look as follows if the significant wave height should be increased with 0.2 m every hour:

jonswap.txt

```
0.8 8. 285. 3.3 10. 3600. 1
```

```
1.0 8. 285. 3.3 10. 3600. 1
1.2 8. 285. 3.3 10. 3600. 1
```

A more generic way of providing time-varying spectral wave boundary conditions is using a FILELIST construction as described in Section 4.5.4. This approach is compatible with all spectral wave boundary condition types as well as spatially varying boundary conditions as described in the same section.

The parameter *s* in the JONSWAP spectrum definition is related to the directional spreading (in deg.) through the following relation $\sigma = \sqrt{\dfrac{2}{s+1}}$, $s = \dfrac{2}{\sigma^2} - 1$, see Figure 4.2. Here σ is the directional spreading in radians and s the JONSWAP spreading parameter.
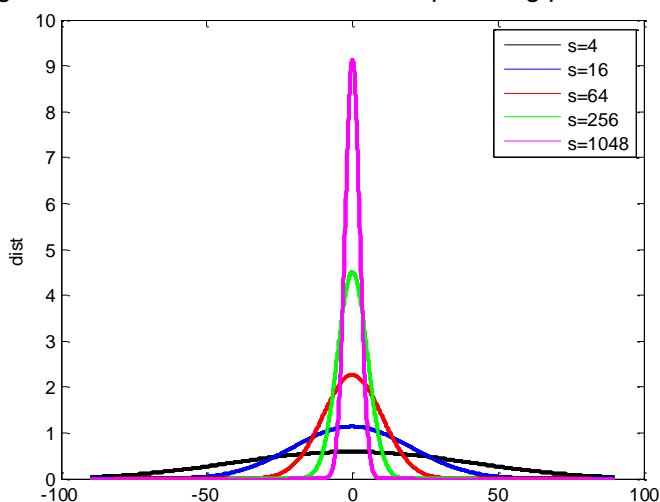
Figure 4.2   Effects of a variation in s for the directional spreading of wave energy. The x-axis shows degrees, the y-axis the distribution where the integral under the curves is unity.

Table 4.7   Overview of available keywords in JONSWAP definition file

keyword	Description	default	minimum	maximum
Hm0	Hm0 of the wave spectrum, significant wave height [m]	0.0	0.0	5.0
fp	Peak frequency of the wave spectrum [s-1]	0.08	0.0625	0.4
gammajsp	Peak enhancement factor in the JONSWAP expression [-]	3.3	1.0	5.0
s	Directional spreading coefficient [-]	10.	1.0	1000.
mainang	Main wave angle (nautical convention) [°]	270.	180.	360.
fnyq	Highest frequency used to create JONSWAP spectrum [s-1]	0.3	0.2	1.0
dfj	Step size frequency used to create JONSWAP spectrum [s-1]	fnyq/200	fnyq/1000	fnyq/20

4.5.1.2 *SWAN wave spectra*

XBeach can read standard SWAN 2D variance density or energy density output files (+.sp2 files) as specified in the SWAN v40.51 manual. This option is enabled using *wbctype = swan* in *params.txt* and a reference to the spectrum file via the keyword *bcfile*. XBeach assumes the directional information in the SWAN file is according to the nautical convention. If the file uses the Cartesian convention for directions, the user must specify the angle in degrees to rotate the x-axis in SWAN to the x-axis in XBeach (by the Cartesian convention). This value is specified in *params.txt* using the keyword *dthetaS_XB*.

Note that time-varying and spatially varying SWAN spectra can be provided using the FILELIST and LOCLIST constructions as described in Section 4.5.4.

An example of a 2D SWAN spectrum is given below:

swan.txt

```
SWAN   1                                Swan standard spectral file
$ Data produced by SWAN version 40.51
$ Project:'projname'     ;   run number:'runnum'
LOCATIONS                               locations in x-y-space
1                                       number of locations
22222.22        0.00
RFREQ                                   relative frequencies in Hz
23                                      number of frequencies
0.0545
0.0622
0.0710
0.0810
0.0924
0.1055
0.1204
0.1375
0.1569
0.1791
0.2045
0.2334
0.2664
0.3040
0.3470
0.3961
0.4522
0.5161
0.5891
0.6724
0.7675
0.8761
1.0000
CDIR                                    spectral Cartesian directions in
degr
  12                                    number of directions
 30.0000
 60.0000
 90.0000
```

```
120.0000
150.0000
180.0000
210.0000
240.0000
270.0000
300.0000
330.0000
360.0000
QUANT
1                                    number of quantities in table
VaDens                               variance densities in m2/Hz/degr
m2/Hz/degr                           unit
-0.9900E+02                          exception value
FACTOR
0.675611E-06
  51    242    574    956   1288   1482   1481   1286    957    579    244     51
 129    610   1443   2402   3238   3725   3724   3234   2406   1454    613    128
 273   1287   3054   5084   6846   7872   7869   6837   5091   3076   1295    271
 665   3152   7463  12402  16712  19229  19221  16690  12419   7518   3172    662
1302   6159  14608  24275  32688  37618  37603  32644  24309  14716   6198   1296
2328  10989  26020  43341  58358  67109  67080  58281  43401  26213  11058   2317
3365  15922  37712  62733  84492  97150  97110  84380  62820  37991  16021   3349
3426  16230  38440  63939  86109  99010  98969  85995  64027  38724  16331   3410
2027   9612  22730  37790  50909  58529  58505  50841  37843  22898   9672   2018
 672   3178   7538  12535  16892  19440  19432  16870  12552   7594   3198    669
 101    479   1135   1890   2542   2924   2923   2539   1892   1144    482    101
   2     11     26     43     57     66     66     57     43     26     11      2
   0      0      0      0      0      0      0      0      0      0      0      0
   0      0      0      0      0      0      0      0      0      0      0      0
   0      0      0      0      0      0      0      0      0      0      0      0
   0      0      0      0      0      0      0      0      0      0      0      0
   0      0      0      0      0      0      0      0      0      0      0      0
   0      0      0      0      0      0      0      0      0      0      0      0
   0      0      0      0      0      0      0      0      0      0      0      0
   0      0      0      0      0      0      0      0      0      0      0      0
   0      0      0      0      0      0      0      0      0      0      0      0
   0      0      0      0      0      0      0      0      0      0      0      0
   0      0      0      0      0      0      0      0      0      0      0      0
   0      0      0      0      0      0      0      0      0      0      0      0
```

4.5.1.3   Variance density spectra

2D spectral information that is not in SWAN format can be provided using a formatted variance density spectrum file and *wbctype* = *vardens*. The spectrum file itself is again referenced using the keyword *bcfile*. The contents of the file must adhere to a specific format:

vardens.txt

```
<number of frequencies (n)>
<frequency 1>
<frequency 2>
<frequency 3>
```

```
...
<frequency n-1>
<frequency n>
<number of directions (m)>
<directions 1>
<directions 2>
<directions 3>
...
<directions m-1>
<directions m>
<variance density 1,1> <variance density 2,1> ... <variance density m,1>
<variance density 1,2> <variance density 2,2> ... <variance density m,2>
...
<variance density 1,n> <variance density 2,n> ... <variance density m,n>
```

Note that the directions must be defined according to the Cartesian convention and in the coordinate system used by XBeach. In this coordinate system 0° corresponds to waves travelling in the direction of the x-axis, while 90° corresponds to the direction of the y-axis. Also, the directions must be defined in increasing order. Time-varying and spatially varying variance density spectra can be provided using the FILELIST and LOCLIST constructions as described in Section 4.5.4.

An example of a formatted variance density file is given below:

vardens.txt

```
15
0.0418
0.0477
0.0545
0.0622
0.0710
0.0810
0.0924
0.1055
0.1204
0.1375
0.1569
0.1791
0.2045
0.2334
0.2664
13
-180.0000
-150.0000
-120.0000
-90.0000
-60.0000
-30.0000
0.0000
30.0000
60.0000
90.0000
```

```
120.0000
150.0000
180.0000
    0       0       0       0       0       0       0       0       0       0       0       0
   51     242     574     956    1288    1482    1481    1286     957     579     244      51
  129     610    1443    2402    3238    3725    3724    3234    2406    1454     613     128
  273    1287    3054    5084    6846    7872    7869    6837    5091    3076    1295     271
  665    3152    7463   12402   16712   19229   19221   16690   12419    7518    3172     662
 1302    6159   14608   24275   32688   37618   37603   32644   24309   14716    6198    1296
 2328   10989   26020   43341   58358   67109   67080   58281   43401   26213   11058    2317
 3365   15922   37712   62733   84492   97150   97110   84380   62820   37991   16021    3349
 3426   16230   38440   63939   86109   99010   98969   85995   64027   38724   16331    3410
 2027    9612   22730   37790   50909   58529   58505   50841   37843   22898    9672    2018
  672    3178    7538   12535   16892   19440   19432   16870   12552    7594    3198     669
  101     479    1135    1890    2542    2924    2923    2539    1892    1144     482     101
    2      11      26      43      57      66      66      57      43      26      11       2
    0       0       0       1       1       1       1       1       1       0       0       0
    0       0       0       0       0       0       0       0       0       0       0       0
    0       0       0       0       0       0       0       0       0       0       0       0
```

4.5.2 Non-spectral wave boundary conditions

Non-spectral wave boundary conditions are enabled using *wbctype* values *stat*, *ts_1*, *ts_2*, *ts_nonh* or *stat_table, as explained in Section 3.1.2*. The conditions are generally defined within the *params.txt* file directly using the keywords described in the table below. In addition, in case of *wbctype* values *ts_1* or *ts_2* the file *bc/gen.ezs* should be present that describes the infragravity wave forcing generated outside of XBeach. For the *wbctype ts_nonh* also a separate file is needed. For more information about these files. see Section 4.5.2.2.

4.5.2.1 Stationary wave boundary conditions

Only in case of *wbctype = stat_table* the time-varying stationary wave boundary conditions are fully described in an external file referenced by the *bcfile* keyword. The *bcfile* keyword is part of the spectral wave boundary condition input and also the referenced file is designed for time-varying spectral input in the form of JONSWAP spectra (see Section 4.5.1.1). In stationary mode only the relevant data from this file is used (*Hm0, Tp, mainang, s and duration*) and irrelevant data like *gamma* and *dfj* are discarded.

Table 4.8   Overview of available keywords for stationary boundary conditions

keyword	description	default	range	units	remark
Hrms	Hrms wave height for wbctype = stat, bichrom, ts_1 or ts_2	1.0	0.0 – 10.0	m	
Tlong	Wave group period for case wbctype = bichrom	80.0	20.0 – 300.0	s	
Trep	Representative wave period for wbctype = stat, bichrom, ts_1 or ts_2	10.0	1.0 – 20.0	s	T_{m01} by default using keyword *Tm01switch=1*, and $T_{m-1,0}$ for

keyword	description	default	range	units	remark
					Tm01switch=0.
dir0	Mean wave direction for wbctype = stat, bichrom, ts_1 or ts_2 (nautical convention)	270.0	180.0 360.0	- deg	
lateralwave	Switch for lateral boundary at left	neumann	neumann, wavecrest, cyclic		
M	Power in cos^m directional distribution for wbctype = stat, bichrom, ts_1 or ts_2	10	2 - 128	-	
taper	Spin-up time of wave boundary conditions, in morphological time	100.0	0.0 1000.0	- s	This is the spinup time.
wavint	Interval between wave module calls (only in stationary wave mode)	60.0	1.0 3600.0	- s	

4.5.2.2 Time series

The wave boundary condition types of *ts_1* and *ts_2* need a separate file containing short wave energy and free surface elevation (including long wave motions). This file should be included in the current working directory of the model, i.e. where the *params.txt* file is located, with the particular name. The format of this file is as follows:

bc/gen.ezs

```
<time 1> <zs 1> <E 1>
<time 1> <zs 2> <E 2>
<time 2> <zs 3> <E 3>
...
```

This file needs to be in a subdirectory "bc" in the directory where params.txt is placed, and should have the name "gen.ezs".

The wave boundary condition type of ts_*nonh* also needs a separate file in order to run the simulation. This file, however, needs to contain free surface elevations and velocities (both in u and v).

Boun_u.bcf

```
< scalar/vector        >
< number of variables >
< variables: t,U,Zs,W >
```

$$
\left.\begin{array}{ccccccccccc}
t^0 & U_1^0 & \cdots & U_J^0 & \eta_1^0 & \cdots & \eta_J^0 & W_1^0 & \cdots & W_J^0 \\
\vdots & \vdots & & \vdots & \vdots & & \vdots & \vdots & & \vdots \\
t^n & U_1^N & \cdots & U_J^N & \eta_1^N & \cdots & \eta_J^N & W_1^N & \cdots & W_J^N
\end{array}\right\}[\text{Data}]
$$

4.5.3 Special types of wave boundary conditions

Two special types of wave boundary conditions are available that makes XBeach skip the generation of new wave time series. The first is *wbctype* = *off* which simply does not provide any wave forcing on the model and hence no wave action in the model.

The second is *wbctype* = *reuse* which makes XBeach reuse wave time series that were generated during a previous simulation. This can be a simulation using the same or a different model as long as the computational grids are identical. In order to reuse boundary conditions, all relevant files should be copied to the current working directory of the model (where the *params.txt* file is located). Relevant files are the *ebcflist.bcf* and *qbcflist.bcf* files, see Appendix C.6, and all files referenced therein. No further wave boundary condition data need be given in *params.txt*.

On top of that bichromatic waves are also supported. Currently the same input parameters as non-spectral waves (see 4.5.2) are required.

4.5.4 Temporally and/or spatially varying wave boundary conditions

Time-varying spectral wave boundary conditions can be defined by feeding in multiple spectrum definition files rather than a single definition file. In addition, the duration for which these spectra should occur needs to be defined.

To make use of this option, the user must specify a regular *wbctype* value for spectral wave boundary conditions (*jons*, *swan* or *vardens*), but instead of referencing a single spectrum definition file using the *bcfile* keyword, an extra file listing all spectrum definition files is now referenced.

The first word in this extra file must be the keyword *FILELIST*. In the following lines, each line contains the duration of this wave spectrum condition in seconds (similar to *rt* in *params.txt*), the required time step in this boundary condition file in seconds (similar to *dtbc* in *params.txt*) and the name of the spectral definition file used to generate these boundary conditions. The duration and boundary condition time step in this file overrules *rt* and *dtbc* in *params.txt*. XBeach does not reuse time-varying spectrum files. Therefore the total duration of all spectra should at least match the duration of the simulation.

A typical input file contains the following:

filelist.txt

```
FILELIST
1800 0.2 jonswap1.inp
1800 0.2 jonswap1.inp
1350 0.2 jonswap2.inp
1500 0.2 jonswap3.inp
```

```
1200 0.2 jonswap2.inp
3600 0.2 jonswap4.inp
```

Similar to time-varying spectral wave boundary conditions, also spatially varying wave boundary conditions can be defined using a similar approach. In order to apply spatially varying spectra on the offshore boundary, the user must specify set the keywords *wbcversion =3* and *nspectrumloc=ns* in *params.txt* where *ns* is the number of locations in which a spectrum is defined. By default the number of defined spectra is one.

Similar to time-varying spectral wave boundary conditions, its spatially varying sibling uses an extra file listing all relevant spectrum definition files. The first word in this extra file must be the keyword *LOCLIST* . This line should be followed by one line per spectrum definition location containing the world x-coordinate and world y-coordinate of the location that the input spectrum should apply, and the name of the file containing spectral wave information.

A typical input file for a run with three JONSWAP spectra contains the following:

loclist.txt

```
LOCLIST
0. 0.    jonswap1.inp
0. 100.  jonswap2.inp
0. 200.  jonswap3.inp
```

The user is reminded that along the offshore boundary of the model, the wave energy, rather than the wave height, is interpolated linearly between input spectra without consideration of the physical aspects of the intermediate bathymetry. In cases with large gradients in wave energy, direction or period, the user should specify sufficient wave spectra for the model to accurately represent changes in offshore wave conditions.

Note that it is not possible to use a mix of JONSWAP, SWAN and variance density files in either a *FILELIST* or a *LOCLIST* construction. It is also not possible to vary *dthetaS_XB* between files in case of non-nautical SWAN spectra. However, it is possible to combine *FILELIST* and *LOCLIST* files by referencing *FILELIST* files from the *LOCLIST* file. In this case all *FILELIST* files should adhere to the same time discretization, so the duration and time step values should be constant over al *FILELIST* files as well as the number of wave spectra definitions.

4.6 Flow, tide and surge input

An XBeach model needs flow boundary conditions on all boundaries of the model domain. Moreover, on each boundary tidal elevations and/ or surges may be imposed. The flow boundary conditions and time-varying tide or surge input are discussed in this section. The details on how the flow is computed within the model are described in the sections on bedfriction and viscosity parameters (see Section 2.4).

4.6.1 Flow boundary conditions

Flow boundary conditions need to be specified on all sides of the domain. We will differentiate between the offshore, lateral and landward boundaries that are set using the keywords *front*, *back* and *left*/*right,* respectively. From Table 4.9 to Table 4.12 an overview is given of the available flow boundary condition types for each of these boundaries.

The keyword *freewave* can be used to switch from bound to free long waves, which can be useful when time series of the free long wave incident on the offshore boundary need to be specified. The file *bc/gen.ezs* can be used to describe the free long waves at the offshore boundary as discussed in Section 3.1.

Table 4.9   Overview of available offshore flow boundary condition types

front	description
abs1d	absorbing-generating (weakly-reflective) boundary in 1D
abs2d	absorbing-generating (weakly-reflective) boundary in 2D
wall	no flux wall
wlevel	water level specification (from file)
nonh_1d	boundary condition for non-hydrostatic option
waveflume	boundary condition for flume experiments based on a continuity relation

Table 4.10   Overview of available landward flow boundary condition types

back	description
wall	no flux wall
abs1d	absorbing-generating (weakly-reflective) boundary in 1D
abs2d	absorbing-generating (weakly-reflective) boundary in 2D
wlevel	water level specification (from file)

Table 4.11   Overview of available lateral flow boundary condition types

left/right	description
wall	no flux wall
neumann	Neumann boundary condition (constant water level gradient)
neumann_v	velocity is determined by the adjacent cell
no_advec	Neumann boundary condition, but only the advective terms are taken into account. Intermediate form between wall and neumann

Table 4.12   Preview of all keywords related to the flow boundary conditions

keyword	description	default	range	units	remark
ARC +	Switch for active wave reflection compensation at seaward boundary	1	0 - 1	-	
back	Switch for boundary at bay side	abs_2d	wall, abs_1d, abs_2d, wlevel		
epsi +	Ratio of mean current to time varying current through offshore boundary	-1.0	-1.0 - 0.2	-	
freewave +	Switch for free wave propagation 0 = use cg	0	0 - 1	-	

keyword	description	default	range	units	remark
	(default); 1 = use sqrt(gh) in wbctype = ts_2				
front	Switch for seaward flow boundary	abs_2d	abs_1d, abs_2d, wall, wlevel, nonh_1d, waveflume		
left	Switch for lateral boundary at ny+1	neumann	neumann, wall, no_advec, neumann_v		
order +	Switch for order of wave steering, 1 = first order wave steering (short wave energy only), 2 = second order wave steering (bound long wave corresponding to short wave forcing is added)	2.0	1.0 – 2.0	–	
right	Switch for lateral boundary at 0	neumann	neumann, wall, no_advec, neumann_v		
tidetype+	Switch for offshore boundary, velocity boundary or instant water level boundary	velocity	instant, velocity		

4.6.2 Time-varying water level

Time-varying tidal (or surge) signals can be applied at all four boundaries in a number of ways, as explained in Section 3.2.3 and shown in Table 4.11.

The number of tidal signals is determined by the keyword *tideloc* that can take the values 0, 1, 2 or 4. Specifying three tidal signals is not an option. Setting *tideloc=0* disables the time-varying tide/surge option. In this case a constant and uniform water level is used specified by the keyword *zs0*. With *tideloc =1* the specified tidal record is specified on all four corners of the domain and interpolated along the boundaries. Using tideloc=1, the signal is imposed on both offshore corners of the domain, while a constant water level defined by the keyword *zs0* is imposed on the landward corners.

Using *tideloc = 2*, two tidal signals are specified and there are two options available: 1) the first signal is imposed on the offshore boundary and the second on the landward boundary or 2) the first signal is imposed on the left lateral boundary and the second on the right lateral

boundary. The choice between the two options is made using the keyword *paulrevere* where a value *0* indicates the first option and a value *1* indicates the second option. Also in the case of two tidal signals the signals are spatially interpolated along the boundaries.

Using *tideloc=4,* four tide/surge signals are to be specified on each corner of the model domain and spatially interpolated along the boundaries. The first signal is imposed to the left offshore boundary seen from sea (x=1,y=1) and the others according to a clockwise rotation. Therefore the columns in the *zs0file* must follow the order of: (x=1,y=1), (x=1,y=N), (x=N,y=N), (x=N,y=1).

The length of the tidal signals is determined by the keyword *tidelen*. This is the number of water levels specified in the file referenced with the *zs0file* keyword. The tidal signal will be interpolated to the local time step of the XBeach simulation; therefore the resolution of the signals only needs to be enough to resolve the water level phenomenon of interest (i.e. tide variations, surge event). The tidal signals are not re-used, therefore the signal should be at least as long as the simulation time.

The *zs0file* file must adhere to the following format where the last three columns are optional depending on the value of *tideloc* and *tlen* represents the value of *tidelen*:

tide.txt

```
<time 1> <zs 1,1> [<zs 2,1> [<zs 3,1> <zs 4,1>]]
<time 2> <zs 1,2> [<zs 2,2> [<zs 3,2> <zs 4,2>]]
<time 3> <zs 1,3> [<zs 2,3> [<zs 3,3> <zs 4,3>]]
...
<time tlen> <zs 1,tlen> [<zs 2,tlen> [<zs 3,tlen> <zs 4,tlen>]]
```

Table 4.13 Overview of all keywords related to the tide boundary conditions

keyword	description	default	range	units	remark
paulrevere	Specifies tide on sea and land or two sea points if tideloc = 2	sea	land, sea		
tideloc	Number of corner points on which a tide time series is specified	0	0,1,2,3 4	–	
zs0	Initial water level	0.0	–5.0 – 5.0	m	
zs0file	Name of tide boundary condition series				<file>

4.7   Water level (dam break)

Water levels can be imposed on the model boundaries as explained in Section 4.6.2 Time-varying after which the shallow water equations force the water body in the model domain. Specific applications may require the initialization of the entire water body in the model domain at the start of the simulation. For example, an initial significant gradient in the water level that "collapses" at the start of the simulation may simulate a dam break. The initialization of the water level in the model domain is governed by the keywords listed in the table below.

The keyword *zsinitfile* references an external file describing the initial water levels in the entire model domain. The file should have the same format as the bathymetry input files described in Section 4.4.

Table 4.14 Overview of all keywords related to the water levels

keyword	description	default	range	units	remark
hotstartflow+	Switch for hotstart flow conditions with pressure gradient balanced by wind and bed stress	0	0 – 1	–	
zs0	Initial water level	0.0	−5.0 – 5.0	m	
zsinitfile	Name of initial water level file			<file>	

4.8 Wave dissipation

The parameters listed in the table below involve the wave dissipation process. For instationary model runs use either *break=roelvink1*, *roelvink2* or *roelvink_daly.* Note that the standard value *gamma=0.55* and *n=10* was calibrated for option *break=roelvink1*. For *break=roelvink2* the wave dissipation is proportional to H^3/h instead of H^2; this affects the calibration. For stationary runs the *break=baldock* option is suitable. The *break=roelvink_daly* option is a model in which waves start and stop breaking. Reducing *gammax* will reduce wave heights in very shallow water, probably 2 is a reasonable value.

Table 4.15 Overview of available keyword related to the wave dissipation model

keyword	description	default	range	units	remark
alpha+	Wave dissipation coefficient in Roelvink formulation	1.0	0.5 – 2.0	–	
break	Type of breaker formulation	roelvink2	roelvink1, baldock, roelvink2, roelvink_daly, janssen		
breakerdelay+	Switch to enable breaker delay model	1	0 – 1	–	
delta+	Fraction of wave height to add to water depth	0.0	0.0 – 1.0	–	
facrun+	Calibration coefficient for short wave runup	1.0	0.0 – 2.0	–	
facsd+	Fraction of the local	1.0	0.0 – 2.0	–	

keyword	description	default	range	units	remark
	wave length to use for shoaling delay depth				
fw+	Short wave friction factor	0.0	0.0 – 1.0	–	
fwcutoff	Depth greater than which the bed friction factor is not applied	1000.0	0.0 – 1000.0	m	
gamma	Breaker parameter in Baldock or Roelvink formulation	0.55	0.4 – 0.9	–	
gamma2	End of breaking parameter in Roelvink Daly formulation	0.3	0.0 – 0.5	–	
gammax+	Maximum ratio wave height to water depth	2.0	0.4 – 5.0	–	
n+	Power in Roelvink dissipation model	10.0	5.0 – 20.0	–	
shoaldelay+	Switch to enable shoaling delay	0	0 – 1	–	

4.9 Bed friction and viscosity

The parameters listed in the table below involve the settings for bed friction and viscosity influencing the flow in XBeach. The bed friction is influenced by the dimensionless friction coefficient *cf* or other formulation like the dimensional Chézy or Manning. The bed friction formulation applied needs to be determined with the keyword *bedfriction*. It is possible both to define one value (keyword: *bedfriccoef*) or to apply, spatially varying values for the bed friction. A spatial varying friction can be provided through an external file referenced via the keyword *bedfricfile*. The file has the same format as the bathymetry file explained in Section 4.4.

The horizontal viscosity is composed of an overall background viscosity *nuh* and a viscosity depending on the roller dissipation tuned by *nuhfac*. In the alongshore direction the viscosity may be multiplied by a factor *nuhv* to account for additional advective mixing. It is also possible to use a user-defined value for the horizontal viscosity (keyword *smag = 0*)

Table 4.16 Overview of available keyword related to the bed friction and viscosity

keyword	description	default	range	units	remark
bedfriccoef	Bed friction coefficient	0.003	3.5e-05 0.9	– –	See Table 2.2
bedfricfile	Bed friction file			<file>	
bedfriction	Bed friction formulation	chezy	chezy, cf, white-colebrook, manning, white-colebrook-grainsize		
nuh	Horizontal background viscosity	0.1	0.0 – 1.0	m^2s^-1	
nuhfac+	Viscosity switch for roller induced turbulent horizontal viscosity	1.0	0.0 – 1.0	–	
nuhv+	Longshore viscosity enhancement factor, following Svendsen	1.0	1.0 – 20.0	–	
smag+	Switch for smagorinsky sub grid model for viscosity	1	0 – 1	–	

4.10 Wind input

Spatially-uniform winds can be parametrically defined using the keywords *windv* and *width* that represent the wind velocity and direction (nautical convention) respectively (Section 2.4.4). Time-varying winds can be defined in an external file referenced by the *windfile* keyword. The file should adhere to the format indicated below. The total length of the time series is automatically determined and should be at least as long as the simulation time.

wind.txt

```
<time 1> <windv 1> <windth 1>
<time 2> <windv 2> <windth 2>
<time 3> <windv 3> <windth 3>
...
```

The table below gives an overview of all keywords related to the wind:

Table 4.17 Overview of all keywords related to the wind input

keyword	description	default	range	units	remark
Cd+	Wind drag	0.002	0.0001	– –	

keyword	description	default	range	units	remark
	coefficient		0.01		
rhoa+	Air density	1.25	1.0 - 2.0	kgm^-3	
windfile	Name of file with non-stationary wind data			<file>	
windth	Nautical wind direction, in case of stationary wind	270.0	-360.0 - 360.0	deg	
windv	Wind velocity, in case of stationary wind	0.0	0.0 - 200.0	ms^-1	

4.11   Sediment input

The sediment input determines the (initial) composition of the bed and the detail in which processes related to sediment sorting are resolved. This is different from how the sediment transport processes are handled in the model itself, as described in 2.7 and 2.8

The simplest situation is an XBeach simulation with uniform sediment. In this case it is sufficient to specify the uniform grain size using the keyword *D50* indicating the median grain size. The effects of a specific sediment distribution can be parametrically defined by additionally specifying values for *D15* and *D90* and optionally the bed composition can be fine-tuned by specifying the porosity and sediment density using the keywords *por* and *rhos* respectively. In this case no sorting of sediment will be simulated.

If the effect of different sediment fractions, sorting and armoring are of importance, multiple sediment fractions can be defined. The number of sediment fraction is determined by the keyword *ngd*. For each sediment fraction a value for *D50,* and optionally *D15* and *D90*, should be defined separated by a space. Moreover, when using multiple sediment fractions, multiple bed layers are needed as well. The number of bed layers can be defined using the keyword *nd*.

Three types of bed layers are distinguished: 1) the top layer 2) the variable or "breathing" layer and 3) the bottom layers. At least one of each type of bed layer is needed, which makes that at least three bed layers are required (see Section 2.8.3). Each bed layer has a thickness. Choosing bed layer thicknesses that are in balance with the expected erosion and deposition during the simulation should keep the numerical mixing to a minimum. A bed layer thickness that is too large will result in relatively uniform behavior, while a bed layer thickness that is too small will result in a lot of shifting and thus numerical mixing. The bed layer thicknesses are determined by the three keywords *dzg1*, *dzg2* and *dzg3* for the top, variable and bottom layers respectively.

Apart from the discretization of the grain size distribution and the vertical structure of the bed, the initial bed composition needs to be defined. The bed composition is defined using external files that are not explicitly referenced from *params.txt*, but are assumed to be located in the working directory of the model (next to *params.txt*). There is one file for each sediment fraction specified by *ngd.* The file corresponding to the first sediment fraction is named *gdist1.inp*, the second *gdist2*.inp, et cetera.

The bed composition files hold information on how much sediment of a specific fraction is in each grid cell and bed layer at the start of the simulation. The values are a volumetric fraction that implies that they should add up to unity over all fractions. For example, if a specific grid cell is filled with the first sediment fraction only, the value corresponding to this grid cell will be

one in the *gdist1.inp* file and zero in all others. Alternatively, if we defined five sediment fractions and a specific grid cell is filled equally with all fractions, the value corresponding to this grid cell will be 1/5 = 0.2 in all files. The *gidst<N>.inp* files are formatted comparable to the bathymetry files (see Section 4.4, but now holds values over the three dimensions x (nx+1), y (ny+1) and the bed layers (nd). The file format is as follows:

gdist1.inp

```
<p 1,1,1> <p 1,2,1> <p 1,3,1> ... <p 1,nx,1> <p 1,nx+1,1>
<p 1,1,2> <p 1,2,2> <p 1,3,2> ... <p 1,nx,2> <p 1,nx+1,2>
<p 1,1,3> <p 1,2,3> <p 1,3,3> ... <p 1,nx,3> <p 1,nx+1,3>
...
<p 1,1,ny> <p 1,2,ny> <p 1,3,ny> ... <p 1,nx,ny> <p 1,nx+1,ny>
<p 1,1,ny+1> <p 1,2,ny+1> <p 1,3,ny+1> ... <p 1,nx,ny+1> <p 1,nx+1,ny+1>


...


<p 2,1,1> <p 2,2,1> <p 2,3,1> ... <p 2,nx,1> <p 2,nx+1,1>
<p 2,1,2> <p 2,2,2> <p 2,3,2> ... <p 2,nx,2> <p 2,nx+1,2>
<p 2,1,3> <p 2,2,3> <p 2,3,3> ... <p 2,nx,3> <p 2,nx+1,3>
...
<p 2,1,ny> <p 2,2,ny> <p 2,3,ny> ... <p 2,nx,ny> <p 2,nx+1,ny>
<p 2,1,ny+1> <p 2,2,ny+1> <p 2,3,ny+1> ... <p 2,nx,ny+1> <p 2,nx+1,ny+1>


...


<p nd,1,1> <p nd,2,1> <p nd,3,1> ... <p nd,nx,1> <p nd,nx+1,1>
<p nd,1,2> <p nd,2,2> <p nd,3,2> ... <p nd,nx,2> <p nd,nx+1,2>
<p nd,1,3> <p nd,2,3> <p nd,3,3> ... <p nd,nx,3> <p nd,nx+1,3>
...
<p nd,1,ny> <p nd,2,ny> <p nd,3,ny> ... <p nd,nx,ny> <p nd,nx+1,ny>
<p nd,1,ny+1> <p nd,2,ny+1> ... <p nd,nx,ny+1> <p nd,nx+1,ny+1>
```

The table below gives an overview of all keywords related to working with multiple sediment fractions and bed layers:

Table 4.18 Overview of all keywords related to the sediment input

keyword	description	default	range	units	remark
D15	D15 grain size per grain type	0.00015	0.0001–0.0008	m	
D50	D50 grain size per grain type	0.0002	0.0001–0.0008	m	
D90	D90 grain size per grain type	0.0003	0.0001–0.0015	m	
dzg+	Thickness of top sediment class layers	0.1	0.01 – 1.0	m	
dzg2+	Nominal thickness of variable sediment class layer	0.1	0.01 – 1.0	m	
dzg3+	Thickness of bottom sediment	0.1	0.01 – 1.0	m	

keyword	description	default	range	units	remark
	class layers				
nd+	Number of computational layers in the bed	3	3 - 1000	-	
ngd	Number of sediment classes	1	1 - 20	-	
por	Porosity	0.4	0.3 - 0.5	-	
Rhos	Solid sediment density (no pores)	2650.0	2400.0 - 2800.0	kgm^-3	
sedcal+	Sediment transport calibration coefficient per grain type	1	None	-	
smax+	Maximum Shields parameter for equilibrium sediment concentration	-1.0	-1.0 - 3.0	-	
ucrcal+	Critical velocity calibration coefficient per grain type	1	None	-	

4.12 Morphology

The parameters listed in the table below involve the morphological processes. The *dryslp* and *wetslp* keyword define the critical avalanching slope above and below water respectively. If the bed exceeds the relevant critical slope it collapses and slides downward (avalanching). To reduce the impact of these landslides the maximum bed level change due to avalanching is limited by the *dzmax* value. Which of the two slopes is applied to a grid cell is determined by the *hswitch* keyword.

The keyword *morfac* enables the user to decouple the hydrodynamical and the morphological time. This is suitable for situations where the morphological process is much slower than the hydrodynamic process. The factor defined by the *morfac* keyword is applied to all morphological change. A *morfac=10* therefore results in 10 times more erosion and deposition in a given time step than usual. The simulation time is however then shortened with the same factor to obtain an approximate result more quickly. The user can prevent the simulation time to be adapted to the *morfac* value by setting *morfacopt* to zero. The keywords *morstart* and *morstop* let the user enable the morphological processes in XBeach only for a particular period during the (hydrodynamic) simulation. These options can be useful if a spin-up time is needed for the hydrodynamics.

The *struct* and *ne_layer* keywords enable the user to specify non-erodible structures in the model. To switch on non-erodible structures use *struct=1*. The location of the structures is specified in an external file referenced by the *ne_layer* keyword. The file has the same format as the bathymetry file explained in Section 4.4 The values of the file define the thickness of the erodible layer on top of the non-erodible layer. A *ne_layer* file with only zeros therefore defines a fully non-erodible bathymetry and a file with only tens means a erodible layer of 10 meters. Only at the grid cells where the value in the *ne_layer* file is larger than zero erosion

can occur. Non-erodible layers are infinitely deep and thus no erosion underneath these layers can occur.

Table 4.19 Overview of available keyword related to morphology

keyword	description	default	range	units	remark
dryslp	Critical avalanching slope above water (dz/dx and dz/dy)	1.0	0.1 - 2.0	-	
dzmax+	Maximum bed level change due to avalanching	0.05	0.0 - 1.0	m/s/m	
hswitch+	Water depth at which is switched from wetslp to dryslp	0.1	0.01 - 1.0	m	
morfac	Morphological acceleration factor	1.0	0.0 - 1000.0	-	
morfacopt+	Switch to adjusting output times for morfac	1	0 - 1	-	
morstart	Start time morphology, in morphological time	120.0	0.0 - 10000000.0	s	
morstop	Stop time morphology, in morphological time	2000.0	0.0 - 10000000.0	s	
ne_layer	Name of file containing depth of hard structure			<file>	
struct	Switch for enabling hard structures	0	0 - 1	-	
wetslp	Critical avalanching slope under water (dz/dx and dz/dy)	0.3	0.1 - 1.0	-	

4.13 Vegetation input

Short wave dissipation, long wave dissipation and flow interaction due to vegetation is supported. The user can define multiple vegetation species. The number of vegetation species is set by the keyword *nveg*. Furthermore, two files should be created and specified in the params.txt-file: a vegetation characteristics file (keyword *veggiefile*) and a vegetation location file (keyword *veggiemapfile*).

The veggiefile is a text file listing the names of the vegetation characteristics files that should be created for every individual vegetation species that should be accounted for. These property files contain the vegetation parameters *nsec*, *ah*, C_d, b_v and *N* that represent the number of vertical sections, height of vegetation section relative to the bed , the drag coefficient, stem diameter and vegetation density per vegetation section, respectively. An example of a set of files describing two different vegetation species is given below.

veggiefile.txt

```
seagrass.txt
mangrove.txt
```

seagrass.txt

```
ah = 0.2
Cd = 1.0
bv = 0.02
N = 1200
```

mangrove.txt

```
nsec = 3
ah = 0.5 0.8 1.3
Cd = 2.0 1.0 2.0
bv = 0.05 0.15 0.1
N = 1000 50 500
```

The *nsec* keyword in the species property file allows the user to define multiple height segments of the species with different properties. The height per vegetation section is defined relative to the bed level. For all properties, the values are given from bottom to top. A definition sketch is given in Figure 4.3.
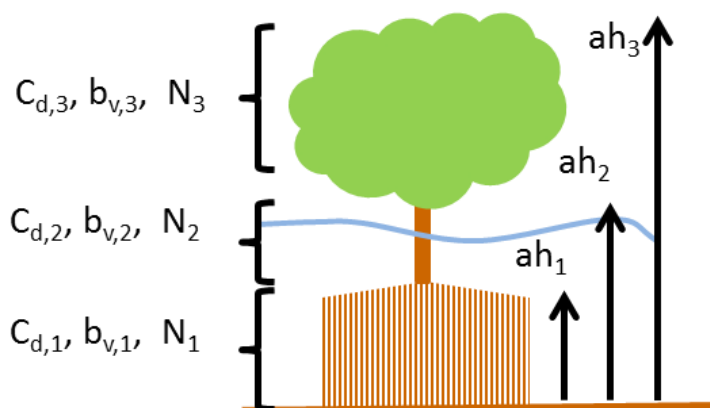
Figure 4.3   Definition sketch of vegetation specification in XBeach (example for mangrove type vegetation schematized in three vertical sections).

Finally, the *veggiemapfile* indicates in what grid cell which vegetation species can be found. The format of this file is similar to the bathymetry files described in Section 4.4, but the values are integers referring to a species where 1 refers to the first listed species, 2 to the second, et cetera. A zero indicates no vegetation at that particular location.

In summary, the following files should be created when the effect of vegetation is modeled:

•   1 x Veggiemapfile: file similar to bathymetry file containing 0, 1 etc. (up to *nveg*)
•   1 x Veggiefile: list of file names of vegetation property files per species
•   *Nveg* x vegetation property file(s): describing vegetation properties per species

Below the relevant keywords in the params.txt are given. In addition, the keyword *vegetation* should be set to 1.

Table 4.20 Overview of all keywords related to the vegetation module

keyword	description	default	range	units	remark
nveg	Number of vegetation species	-123		–	
veggiefile	Name of vegetation species list file			<file>	
veggiemapfile	Name of vegetation species map file			<file>	

4.14 Discharge input

Discharge of water at the model boundaries or directly in the model domain is defined along specific grid sections. The keywords *ndischarge* and *ntdischarge* define the number of discharge sections and the length of the discharge time series respectively. The *disch_loc_file* keyword references a file that defines the discharge sections. Each line in this file corresponds to a grid section and each line contains four numbers being the start and end coordinates of the section. The file is formatted as follows, where *ndisch* refers to the keyword *ndischarge*:

disch_loc.txt

```
<x_start 1> <y_start 1> <x_end 1> <y_end 1>
<x_start 2> <y_start 2> <x_end 2> <y_end 2>
<x_start 3> <y_start 3> <x_end 3> <y_end 3>
...
<x_start ndisch> <y_start ndisch> <x_end ndisch> <y_end ndisch>
```

The world coordinates specified in this file must be chosen such that they are close to the desired grid cell borders, since the grid cell borders are eventually used as discharge section. Discharge sections can be located along grid cell borders that are either oriented cross-shore or alongshore, but not a combination of the two. In a regular grid this implies that either the start or end x-coordinates are equal, or the start and end y-coordinates are equal. Alternatively, both are equal. In this case a vertical discharge from above is assumed, rather than a horizontal discharge. Vertical discharges only add mass and no momentum to the water body.

The keyword *disch_time series_file* references a file defining the time series imposed on the discharge locations. The file lists the timings in the first column and a discharge value in m^3/s for each discharge section as follows, where *ntdisch* refers to the keyword *ntdischarge*:

disch_time series.txt

```
<t 1> <Q 1,1> <Q 2,1> ... <Q ndisch,1>
<t 2> <Q 1,2> <Q 2,2> ... <Q ndisch,2>
<t 3> <Q 1,3> <Q 2,3> ... <Q ndisch,3>
...
<t ntdisch> <Q 1,ntdisch> <Q 2,ntdisch> ... <Q ndisch,ntdisch>
```

Discharges defined at the domain borders are positive in direction towards the domain (influx). Discharges defined in the domain itself are positive in direction of the positive x or y direction. Vertical discharges are positive into the domain (influx).
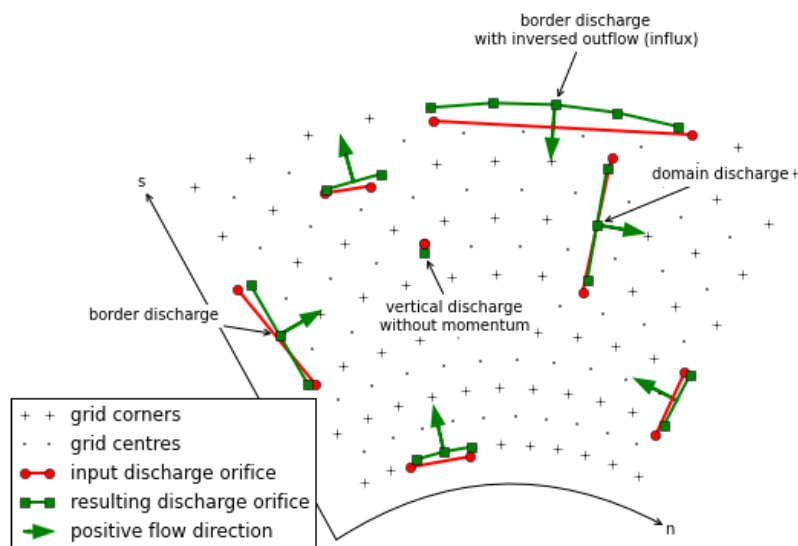
Figure 4.4 Possible discharge orifices. A discharge orifice is defined as line in between two points (red). The resulting discharge orifice constitutes out of full abreast grid cells (green). The discharge direction is in positive grid direction (s or n), except at the domain border where the discharge is an influx in the domain (green arrows).

The table below gives an overview of all keywords related to discharges:

Table 4.21 Overview of all keywords related to the discharge input

keyword	description	default	range	units	remark
disch_loc_file+	Name of discharge locations file			<file>	
disch_time series_file+	Name of discharge time series file			<file>	
ndischarge+	Number of discharge locations		0 - 100	–	
ntdischarge+	Length of discharge time series		0 - 100	–	

4.15 Drifters input

Drifters can be deployed during the model simulation by specifying the number of drifters using the keyword *ndrifter* and the location, start and end time of the drifter deployment in a separate file referenced by the *drifterfile* keyword. The file format is as follows:

drifter.txt

```
<x 1> <y 1> <t_start 1> <t_end 1>
<x 2> <y 2> <t_start 2> <t_end 2>
<x 3> <y 3> <t_start 3> <t_end 3>
...
<x ndrifter> <y ndrifter> <t_start ndrifter> <t_end ndrifter>
```

The table below gives an overview of all keywords related to drifters:

Table 4.22 Overview of all keywords related to drifters

keyword	description	default	range	units	remark
drifterfile	Name of drifter data file			<file>	
ndrifter	Number of drifters	ndrifter	0 – 50	–	

4.16 Ship-induced wave motions

Ship waves can be simulated by defining the ships' geometries and trajectories in a collection of files. The user can define multiple ships. The number of ships is set by the keyword *nship*. In the file referenced by the keyword *shipfile* each ship is given a name. The properties of each ship are summarized in another textfile with the name of the ship (*shipname.txt*). This properties file defines the parameters for the discretization of the ships geometry. The ship grid is determined by the keywords *dx, dy, nx*, and *ny*, and the ship geometry itself is given in a separate file, referenced by the keyword *shipgeom*. This file contains the ship draft per ship grid point, and should have a size of *nx*+1 by *ny*+1. The center of gravity of the ship is also defined in the ship properties file using the keywords *xCG, yCG* and *zCG*. The ships trajectory is defined in a file referenced from the ship properties file by the keyword *shiptrack*. Each row in this file contains a time, x- and y-coordinate indicating the ships position as function of time.

To avoid numerical problems, the full ship track should be within the model domain (i.e. a vessel cannot sail through the model boundary). Furthermore, it is advised to start the ship track with a very low velocity and gradually increase the sailing speed. When not taking into account a spin up period, the impact of the ship on the water level can be too abrupt, resulting in unrealistic wave patterns. In addition, it is advised to maintain a relatively deep edge of a few grid cells at both model boundaries (i.e. front and back side).

Another way to avoid numerical issues at the initialization of a ship simulation is to use the 'flying' option, which can be specified in the ship file (*flying* = 1). In case the option *flying* is enabled, also a z-coordinate is defined in the shiptrack-file indicating the vertical position of the ship. In this way, the vessel can 'land' on the water with its correct sailing speed, thereby avoiding unwanted disturbance to the water level. Also, the ship can 'fly out' of the model domain before reaching the back boundary. By using this method the spin-up time can be reduced considerably and both inflow and outflow boundaries are unaffected by the ship

The two keywords *compute_force* and *compute_motion* enable the computation of forces on the ship and the ships motions due to wave forcing respectively; the latter has not been

implemented yet. Forces on a ship in motion may be unreliable due to near-field effects; forces on a ship at rest are much more reliable. An example of ship definition files is:

shipfile.txt

```
containership.txt
oiltanker.txt
```

containership.txt

```
dx = 10
dy = 10
nx = 30
ny = 10
shipgeom = container_geom.dep
xCG = 120
yCG = 50
zCG = 30
shiptrack = container_track.txt
flying = 1
compute_force = 1
compute_motion = 1
```

pannamax_geom.txt

```
<z 0,0> <z 1,0> <z 2,0> <z 3,0> ... <z nx,0> <z nx+1,0>
<z 0,1> <z 1,1> <z 2,1> <z 3,1> ... <z nx,1> <z nx+1,1>
...
<z 0,ny> <z 1,ny> <z 2,ny> <z 3,ny> ... <z nx,ny> <z nx+1,ny>
<z 0,ny+1> <z 1,ny+1> <z 2,ny+1> <z 3,ny+1> ... <z nx,ny+1> <z nx+1,ny+1>
```

pannamax_track.txt

```
<t 1> <x 1> <y 1> <z 1>
<t 2> <x 2> <y 2> <z 2>
<t 3> <x 3> <y 3> <z 3>
...
```

oiltanker.txt

```
dx = 2
dy = 2
nx = 20
ny = 4
shipgeom = tanker_geom.dep
xCG = 20
yCG = 40
zCG = 1.5
shiptrack = tanker_track.txt
flying = 0
```

tanker_track.txt

```
<t 1> <x 1> <y 1>
<t 2> <x 2> <y 2>
<t 3> <x 3> <y 3>
```

```
...
```

Table 4.23 Overview of all keywords related to the ship module

Keyword	description	default	range	units	remark
nship	Number of ships	123		–	
shipfile	Name of ship data file			<file>	

4.17 Output selection

Output selection determines what data computed by XBeach is written to a file in terms of location and time and in what format. The output types, output times and output formats supported by XBeach are explained in more detail in the following subsections. The table below gives an overview of all keywords related to model output:

Table 4.24 Overview of all keywords related to the output definitions

keyword	description	default	range	units	remark
ncfilename+	Xbeach netcdf output file name			<file>	
ncross+	Number of output cross sections	0	0 – 50	–	
nglobalvar	Number of global output variables (as specified by user)	-1	-1 – 20	–	
nmeanvar	Number of mean, min, max, var output variables	0	0 – 15	–	
npoints	Number of output point locations	0	0 – 50	–	
npointvar	Number of point output variables	0	0 – 50	–	
nrugauge	Number of output runup gauge locations	0	0 – 50	–	
nrugdepth+	Number of depths to compute runup in runup gauge	1	1 – 10	–	
outputformat+	Output file format	fortran	fortran, netcdf, debug		
rugdepth+	Minimum depth for determination of last wet point in runup gauge	0	0 – 0.1	m	
timings+	Switch enable progress output	1	0 – 1	–	

keyword	description	default	range	units	remark
	to screen				
tintc+	Interval time of cross section output	1.0	0.01 – 100000.0	s	
tintg	Interval time of global output	1.0	0.01 – 100000.0	s	
tintm	Interval time of mean, var, max, min output	tstop-tstart	1 – [tstop – start]	s	
tintp	Interval time of point and runup gauge output	1.0	0.01 – 100000.0	s	
tscross+	Name of file containing timings of cross section output	None	None None	–	–
tsglobal+	Name of file containing timings of global output	None	None None	–	–
tsmean+	Name of file containing timings of mean, max, min and var output	None	None None	–	–
tspoints+	Name of file containing timings of point output	None	None None	–	–
tstart	Start time of output, in morphological time	1.0	0.0 – 1000000.0	s	

4.17.1 Output types

XBeach supports four different types of output: 1) instantaneous spatial output 2) time-averaged spatial output 3) fixed point output or 4) runup gauge output, which will be further elaborated in the next subsections. In principle any variable in XBeach can be outputted as long as it is part of the *spaceparams* structure defined in *spaceparams.tmpl* in the XBeach source code. An overview of all currently supported parameters in this file is presented in Table 4.25.

The amount of output variables used for each type is determined by the keywords *nglobalvar*, *nmeanvar*, *npoints* and *nrugauge*. Each of these keywords takes a number indicating the number of parameters or locations that should be written to file. If any of the keywords is set to zero, the output type is effectively disabled. If *nglovalvar* is set to *-1* then a standard set of output variables is used, being *H, zs, zs0, zb, hh, u, v, ue, ve, urms, Fc, Fy, ccg, ceqsg, ceqbg, Susg, Svsg, E, R, D* and *DR*. If *nglobalvar* is not set it defaults to *-1*. The lines in the *params.txt* file immediately following these keywords determine what parameters or locations are used, as will be explained in more detail in the following subsections.

Table 4.25 Possible output parameters

keyword	description	units
alfau	Grid orientation at u-point	rad
alfav	Grid orientation at v-point	rad
alfaz	Grid orientation at z-point	rad
As	Asymmetry of short waves	-
bedfriccoef	Dimensional/dimensionless input bed friction coefficient; depends on value of parameter bedfriction	-
bi	Incoming bound long wave	m
BR	Maximum wave surface slope used in roller dissipation formulation	-
breaking	Indicator whether cell has breaking nonh waves	-
c	Wave celerity	m/s
ccg	Depth-averaged suspended concentration for each sediment fraction	m3/m3
cctot	Sediment concentration integrated over bed load and suspended and for all sediment grains	m3/m3
ceqbg	Depth-averaged bed equilibrium concentration for each sediment class	m3/m3
ceqsg	Depth-averaged suspended equilibrium concentration for each sediment class	m3/m3
cf	Dimensionless friction coefficient flow	-
cfu	Dimensionless friction coefficient flow in u-points	-
cfv	Dimensionless friction coefficient flow in v-points	-
cg	Group velocity	m/s
cgx	Group velocity, x-component	m/s
cgx_s	Group velocity, x-component	m/s
cgy	Group velocity, y-component	m/s
cgy_s	Group velocity, y-component	m/s
costh	Cos of wave angles relative to grid direction	-
costh_s	Cos of wave angles relative to grid direction	-
ctheta	Wave celerity theta-direction (refraction)	rad/s
ctheta_s	Wave celerity theta-direction (refraction)	rad/s
cx	Wave celerity, x-component	m/s
cy	Wave celerity, y-component	m/s
D	Dissipation	W/m2
D15	D15 grain diameters for all sediment classses, lodewijk	m
D50	D50 grain diameters for all sediment classses	m
D50top	Friction coefficient flow	-
D90	D90 grain diameters for all sediment classses	m
D90top	Friction coefficient flow	-
Dc	Diffusion coefficient	m2/s
dcbdx	Bed concentration gradient x-dir.	kg/m3 /m
dcbdy	Bed concentration gradient y-dir.	kg/m3 /m
dcsdx	Suspended concentration gradient x-dir.	kg/m3 /m
dcsdy	Suspended concentration gradient y-dir.	kg/m3 /m
depo_ex	Explicit bed deposition rate per fraction	m/s

keyword	description	units
depo_im	Implicit bed deposition rate per fraction	m/s
dinfil	Infiltration layer depth used in quasi-vertical flow model for groundwater	m
dnc	Grid distance in n-direction, centered around c-point	m
dnu	Grid distance in n-direction, centered around u-point	m
dnv	Grid distance in n-direction, centered around v-point	m
dnz	Grid distance in n-direction, centered around z-point (=eta-point)	m
DR	Roller energy dissipation	W/m2
dsc	Grid distance in s-direction, centered around c-point	m
dsdnui	Inverse of grid cell surface, centered around u-point	1/m2
dsdnvi	Inverse of grid cell surface, centered around v-point	1/m2
dsdnzi	Inverse of grid cell surface, centered around z-point	1/m2
dsu	Grid distance in s-direction, centered around u-point	m
dsv	Grid distance in s-direction, centered around v-point	m
dsz	Grid distance in s-direction, centered around z-point (=eta-point)	m
dtheta	Wave direction bin size	rad
Dveg	Dissipation due to short wave attenuation by vegetation	W/m2
dx	Grid size x-direction	m
dy	Grid size y-direction	m
dzav	Total bed level change due to avalanching	m
dzbdt	Rate of change bed level	m/s
dzbdx	Bed level gradient in x-direction	-
dzbdy	Bed level gradient in y-direction	-
dzbed	Vertical dimension of each bed sediment layer (nd), per grid cell (nx,ny)	-
dzbnow	Bed level change in current time step	m
dzsdt	Rate of change water level	m/s
dzsdx	Water surface gradient in x-direction	m/s
dzsdy	Water surface gradient in y-direction	m/s
E	Wave energy	Nm/m2
ee	Directionally distributed wave energy	J/m2/rad
ee_s	Directionally distributed wave energy	J/m2/rad
ero	Bed erosion rate per fraction	m/s
Fvegu	X-forcing due to long wave attenuation by vegetation	N/m2
Fvegv	Y-forcing due to long wave attenuation by vegetation	N/m2
Fx	Wave force, x-component	N/m2
Fy	Wave force, y-component	N/m2
gwbottom	Level of the bottom of the aquifer	m

keyword	description	units
gwcurv	Curvature coefficient of groundwater head function	-
gwhead	Groundwater head (differs from gwlevel)	m
gwheadb	Groundwater head at bottom (differs from gwlevel)	m
gwheight	Vertical size of aquifer through which groundwater can flow	m
gwlevel	Groundwater table (min(zb,gwhead))	m
gwqx	Groundwater discharge in x-direction	m/s
gwqy	Groundwater discharge in y-direction	m/s
gwu	Groundwater flow in x-direction	m/s
gwv	Groundwater flow in y-direction	m/s
gww	Groundwater flow in z-direction (interaction between surface and ground water)	m/s
H	Hrms wave height based on instantaneous wave energy	m
hh	Water depth	m
hold	Water depth previous time step	m
Hrunup	Short wave height used in runup formulation	m
hu	Water depth in u-points	m
hum	Water depth in u-points	m
hv	Water depth in v-points	m
hvm	Water depth in v-points	m
idrift	Drifter x-coordinate in grid space	-
infil	Rate of exchange of water between surface and groundwater (positive from sea to groundwater)	m/s
istruct	Location of revetments toe	-
iwl	Location of water line (including long wave runup)	-
jdrift	Drifter y-coordinate in grid space	-
k	Wave number	rad/m
L1	Wave length (used in dispersion relation)	m
maxzs	Maximum elevation in simulation	m
minzs	Minimum elevation in simulation	m
n	Ratio group velocity/wave celerity	-
nd	Number of bed layers (can be different for each computational cell)	-
ndist	Cum. distance from right boundary along n-direction	m
ntheta	Number of wave direction bins	-
nuh	Horizontal viscosity coefficient	m2/s
nx	Local number of grid cells x-direction	-
ny	Local number of grid cells y-direction	-
pbbed	Concentration of every sediment type, per bed sediment layer, per grid cell	-
pdisch	Discharge locations	-
ph	Pressure head due to ship	m
pntdisch	Point discharge locations (no momentum)	-
Qb	Fraction breaking waves	-
qx	Discharge in u-points, x-component	m2/s
qy	Discharge in u-points, y-component	m2/s
R	Roller energy	Nm/m2
rolthick	Long wave roller thickness	m
rr	Directionally distributed roller energy	J/m2/

keyword	description	units
		rad
runup	Short wave runup height	m
sdist	Cum. distance from offshore boundary along s-direction	m
sedcal	Equilibrium sediment concentartion factor for each sediment class	-
sedero	Cum. sedimentation/erosion	m
setbathy	Prescribed bed levels	m
shipFx	Force on ship in x-direction	m
shipFy	Force on ship in y-direction	m
shipFz	Force on ship in z-direction	m
shipMx	Moment on ship around x-axis	m
shipMy	Moment on ship around y-axis	m
shipMz	Moment on ship around z-axis	m
shipchi	Turning angle arround y-axis	m
shipphi	Turning angle arround x-axis	m
shippsi	Turning angle arround z-axis	m
shipxCG	X-coordinate of ship center of gravity	m
shipyCG	Y-coordinate of ship center of gravity	m
shipzCG	Z-coordinate of ship center of gravity	m
sigm	Mean frequency	rad/s
sigt	Relative frequency	rad/s
sinth	Sin of wave angles relative to grid direction	-
sinth_s	Sin of wave angles relative to grid direction	-
Sk	Skewness of short waves	-
strucslope	Slope of structure	-
structdepth	Depth of structure in relation to instantaneous bed level	m
Subg	Bed sediment transport for each sediment class (excluding pores), x-component	m2/s
Susg	Suspended sediment transport for each sediment class (excluding pores), x-component	m2/s
Sutot	Sediment transport integrated over bed load and suspended and for all sediment grains, x-component	m2/s
Svbg	Bed sediment transport for each sediment class (excluding pores), y-component	m2/s
Svsg	Suspended sediment transport for each sediment class (excluding pores), y-component	m2/s
Svtot	Sediment transport integrated over bed load and suspended and for all sediment grains, y-component	m2/s
Sxx	Radiation stress, x-component	N/m
Sxy	Radiation stress, y-component	N/m
Syy	Radiation stress, y-component	N/m
Tbore	Wave period interval associated with breaking induced turbulence	s
tdisch	Discharge time series	-
tdriftb	Drifter release time	s
tdrifte	Drifter retrieval time	s
thet	Wave angles	rad
thet_s	Wave angles	rad
theta	Wave angles directional distribution w.r.t. comp. x-axis	rad

keyword	description	units
theta_s	Wave angles directional distribution w.r.t. comp. x-axis	rad
thetamean	Mean wave angle	rad
tideinpt	Input time of input tidal signal	s
tideinpz	Input tidal signal	m
tsetbathy	Points in time of prescibed bed levels	s
Tsg	Sediment response time for each sediment class	s
u	Glm velocity in cell centre, x-component	m/s
ua	Time averaged flow velocity due to wave assymetry	m/s
ucrcal	Calibration factor for u critical for each sediment class	-
ue	Eulerian velocity in cell centre, x-component	m/s
ueu	Eulerian velocity in u-points, x-component	m/s
ui	Incident bound wave velocity in, x-component	m/s
umean	Longterm mean velocity at bnds in u-points, x-component	m/s
umwci	Velocity (time-averaged) for wci, x-component	m/s
ur	Reflected velocity at bnds in u-points	m/s
urepb	Representative flow velocity for sediment advection and diffusion, x-component	m/s
ureps	Representative flow velocity for sediment advection and diffusion, x-component	m/s
urms	Orbital velocity	m/s
usd	Return flow due to roller after breaker delay	m/s
ust	Stokes drift	m/s
ustr	Return flow due to roller	m/s
uu	Glm velocity in u-points, x-component	m/s
uv	Glm velocity in v-points, x-component	m/s
uwf	Stokes drift, x-component	m/s
v	Glm velocity in cell centre, y-component	m/s
ve	Eulerian velocity in cell centre, y-component	m/s
vev	Eulerian velocity in u-points, y-component	m/s
vi	Incident bound wave velocity in, y-component	m/s
vmag	Velocity magnitude in cell centre	m/s
vmageu	Eulerian velocity magnitude u-points	m/s
vmagev	Eulerian velocity magnitude v-points	m/s
vmagu	Glm velocity magnitude u-points	m/s
vmagv	Glm velocity magnitude v-points	m/s
vmean	Longterm mean velocity at bnds in u-points, y-component	m/s
vmwci	Velocity (time-averaged) for wci, y-component	m/s
vrepb	Representative flow velocity for sediment advection and diffusion, y-component	m/s
vreps	Representative flow velocity for sediment advection and diffusion, y-component	m/s
vu	Glm velocity in u-points, y-component	m/s
vv	Glm velocity in v-points, y-component	m/s
vwf	Stokes drift, y-component	m/s
wb	Vertical velocity at the bottom	m/s
wetu	Mask wet/dry u-points	-
wetv	Mask wet/dry v-points	-
wetz	Mask wet/dry eta-points	-
windinpt	Input time of input wind signal	s

keyword	description	units
windnv	Wind velocity in n direction in v point at current time step	m/s
windsu	Wind velocity in s direction in u point at current time step	m/s
windvelts	Input wind velocity	m/s
windxts	Time series of input wind velocity (not s direction), x-component	m/s
windyts	Time series of input wind velocity (not n direction), y-component	m/s
wm	Mean abs frequency	rad/s
ws	Vertical velocity at the free surface	m/s
wscrit	Critial vertical velocity at the free surface for breaking	m/s
x	X-coord. original comp. grid	m
xHrunup	Location at which short wave height for runup is taken	m
xu	X-coord. comp. grid u-points	m
xv	X-coord. comp. grid v-points	m
xyzs01	Global xy coordinates of corner (x=1,y=1)	–
xyzs02	Global xy coordinates of corner (x=1,y=n)	–
xyzs03	Global xy coordinates of corner (x=n,y=n)	–
xyzs04	Global xy coordinates of corner (x=n,y=1)	–
xz	X-coord. comp. grid (positive shoreward, perp. to coastline)	m
y	Y-coord. original comp. grid	m
yu	Y-coord. comp. grid u-points	m
yv	Y-coord. comp. grid v-points	m
yz	Y-coord. comp. grid	m
z0bed	Reference level for the bed, located at the initial bottom of the bed sediment layers	–
zb	Bed level	m
zb0	Initial bed level	m
zs	Water level	m
zs0	Water level due to tide alone	m
zs01	Initial water level first sea boundary	m
zs02	Initial water level second sea boundary	m
zs03	Initial water level first land boundary	m
zs04	Initial water level second land boundary	m
zs0fac	Relative weight of offshore boundary and bay boundary for each grid point is stored in zs0fac	–
zswci	Waterlevel (time-averaged) for wci	m

4.17.1.1 Instantaneous spatial output

Instantaneous spatial output describes the instantaneous state of variables across the entire model domain at various points in time. To make use of this option the user must specify the output time (see Section 4.17.2 under the keywod *tintg*) and the number of output variables required using the *nglobalvar* keyword in *params.txt*, immediately followed by the names of the requested variables on a separate line each. The output of three instantaneous grids can look as follows:

params.txt

```
nglobalvar = 3
zs
zb
H
```

4.17.1.2 *Time-averaged spatial output*

Time-averaged spatial output describes the time-averaged state of variables across the entire model domain at various points in time. The user can define the averaging period in *params.txt*. To make use of this option the user must specify the output time (see Section 4.17.2 under *tintm*) and the number of output variables required using the *nmeanvar* keyword in *params.txt*, immediately followed by the names of the requested variables on a separate line each. The output of two time-averaged grids may look as follows:

params.txt

```
nmeanvar = 2
u
v
```

4.17.1.3 *Fixed point output*

Fixed point output allows the user to select one or more locations for which a time series of data is stored. This output describes a time-series of one or more variables at one point in the model domain. To make use of this option, the user must specify the number of output locations using the *npoints* keyword in *params.txt*, immediately followed by one line per output location describing the location coordinates given as the x-coordinate and y-coordinate and in world coordinates, as well as (optionally) a name for the output point. XBeach will link the output location to the nearest computational point. If no name is given for the output point, a generic name, e.g., point001, will be given to the output point.

The user can specify the number and selection of output variables for all points (and runup gauges, discussed in the following section) using the *npointvar* keyword in *params.txt* to specify the number of output variables, immediately followed by the names of the requested variables on a separate line each. Fixed point output significantly reduces the amount of data written to file in each time step and is therefore particularly suitable for high temporal resolution output.

An example with two output locations is given below. The first point ("offshore1") is located on the offshore boundary (x = 0.0) and somewhere in the middle of the model domain in y-direction (y = 800.0). The second point ("PT1") is located slightly off the centre of the model (y = 900.0) and somewhere in the middle of the domain in x-direction (x = 2000.0). Both locations have four output variables: *H, zs, zb* and *D*.

params.txt

```
npoints = 2
0. 800.      offshore1
2000. 900.  PT1

npointvar = 4
H
zs
zb
D
```

4.17.1.4 *Runup gauge output*

Runup gauge output describes a time-series of a number of variables at the (moving) waterline. In this case XBeach scans in an x-directional transect defined by the user for the location of the waterline. Output information is recorded for this moving point. This is particularly useful to keep track of runup levels in cross-shore transects.

The definition of runup gauges is similar to the definition of fixed point output. The user needs to specify the number of runup gauges using the *nrugauge* keyword in *params.txt*, immediately followed by one line per runup gauge location describing the coordinates of the initial location of the runup gauge, as well as (optionally) a name for the runup gauge. XBeach will subsequently link the initial runup gauge location to the nearest computational cross-shore transect rather than just the nearest computational point. If no name is given for the runup gauge, a generic name, e.g., rugau001, will be given to the runup gauge. It is also possible for the user to set a minimum depth for determination of the last wet point in the runup gauge (keyword: *rugdepth*).

Runup gauges share their selection of output variables with regular point output. However, in the case of runup gauges, XBeach will automatically also include the variables *xw*, *yw* and *zs* to the point output variables, if these variables were not specified using the *npointvar* keyword

in *params.txt*. Note that the user should refer to the *pointvars.idx* output file, which automatically generated, to check the order of output variables for points and runup gauges.

An example of a runup gauge input is given below. The runup gauge is initially located on the offshore boundary (x = 0.0) and somewhere in the middle of the model domain in y-direction (y = 800.0). The name of the runup guage is "transect1". The runup gauge will display standard output variables (*xw*, *yw* and *zs*, as well as any output variables specified by the *npointvar* keyword).

params.txt

```
nrugauge = 1
0. 800. transect1
```

4.17.2 Output times
The user may determine the output times for regular spatial output variables, time averaged spatial variables and point location variables individually. Runup gauge output and fixed point output are given at the same moments in time. For all three types of output the user may choose to either state a fixed interval time at which output is given or supply an external file containing times at which output should be given or a combination of both.

4.17.2.1 *Output at fixed intervals*
The user can define a point in time after the start of the simulation at which the first output is generated for fixed interval output. The user can do this by using the *tstart* keyword in *params.txt*. All output that is being generated at fixed intervals uses *tstart* as their base. The interval for instantaneous spatial output is given by the *tintg* keyword. The keywords for the interval of time-averaged spatial output and point output are *tintm* and *tintp* respectively, where *tintp* is used both for fixed point and runup gauge output. Note that *tintg*, *tintm* and *tintp* supersede the older *tint* parameter that is valid for all types of output. If *tintp* or *tintm* is not stated, but output is declared (*npoints*, *nrugauge* or *nmeanvar* is stated larger than zero), XBeach assumes the same output interval as *tintg*. An example of the definition of fixed intervals is given below.

params.txt

```
tstart = 100.
tintg = 100.
tintp = 2.
tintm = 3600.
```

In the case of instantaneous spatial output and point output, the first output is given at *tstart*. In the case of time-averaged spatial variables, the first output is given at *tstart*+*tintm*. This output represents the average condition over the interval between *tstart* and *tstart*+*tintm*.

4.17.2.2 *Output times defined by external file*
The user is given the option to have output at a set of points in time that are not separated by regular intervals. In this case the user must supply an additional file for each output type. The user specifies the name of the output time series file for instantaneous spatial output using the *tsglobal* keyword. The keywords for time series files for time-averaged spatial output and point output are *tsmean* and *tspoint* respectively, where *tspoint* is again used for both fixed point and runup gauge output. All time series files must contain on the first line the number of output times followed by every output time on a new line. An example of such irregular output time definition is given below.

params.txt

```
tsglobal= timeseries1.txt
tspoints = timeseries2.txt
tsmean= timeseries3.txt
```

time series1.txt

```
18
0.05
0.15
0.2
0.8
12.0
12.5
19.124
30.
60.
90.
120.
150.
160.
170.
177.
178.
179.
180.
```

In the case of instantaneous spatial output and point output, the first output is given at the first stated point in time. In the case of time-averaged spatial variables, the first output is given at the second stated point in time. This output represents the average condition over the interval between first and second stated point in time. Subsequent averaging is done over every interval.

4.17.2.3   Combinations of fixed internal and external files

The user is allowed to define certain types of output using fixed intervals and others using external files. The use of an external file supersedes the use of fixed intervals. Note that *tstart* will only apply to output of fixed interval type. An example of mixing fixed and varying output time intervals is given below.

param.txt

```
tstart = 100.
tintg = 100.
tspoints = time series2.txt
tintm = 3600.
```

4.17.3   Output format

XBeach supports two types of output: 1) Fortran binary and 2) netCDF. The output format used is determined by the keyword *outputformat*. The use of netCDF output is more convenient since all output (and input) is stored in a single, easy accessible file. Also the netCDF file format is compatible with many programming languages (e.g. Matlab, Python) as well as many visualization tools (e.g. QuickPlot, Morphan).

4.17.3.1   Fortran binary

Output files in Fortran binary format are bare matrix dumps of XBeach' computational matrices. At each output time, one such matrix block is added to the output file. These files can generally be read by binary read functions, like *fread* in Matlab and the *struct* package in Python.

Output files written in Fortran binary format are given the name *<variable>.dat*, for example *zs.dat*, for instantaneous spatial output. The only exception is that files containing information about the wave height of the short waves are called *hrms.dat* instead of *H.dat* to maintain backward compatibility. Time-averaged spatial output is stored similarly, but the file names have a suffix indicating the type of averaging *<variable>_mean.dat*. For time-averaged spatial output also the variance, minimum and maximum values are stored using the suffixes *_var*, *_min* and *_max* respectively.

All data corresponding to fixed point locations will be stored in files called *point<NNN>.dat*. *<NNN>* represents a number between 001 and 999 corresponding to the order in which the points are declared in *params.txt*. The data files are plain text and contain one row for each output time step. The first position on each row is the time at which the output is given. The subsequent positions in the row are the instantaneous values of the variables at the given point. The order of the variables is equal to the order in which they are defined for that point in *params.txt*. Data corresponding to runup gauge locations are stored in the same format as fixed point output, but the files are named *rugau<NNN>.dat*.

An extra file called *dims.dat* is always written at the start of the simulation in Fortran binary output mode. This file contains the dimensions of the XBeach model. It simply states the following dimensions in order: *nt* (number of output time steps)*, nx* (number of grid cells in x-direction)*, ny* (number of grid cells in y-direction)*, ngd* (number of sediment fractions)*, nd* (number of bed layers)*, ntp* (number of point output time steps)*, ntm* (number of time-averaged output time steps). Subsequently, the irregular time series are stored, if applicable: *tsglobal* (irregular output times)*, tspoints* (irregular point output times) and *tsmean* (irregular time-averaged output times). Similarly, a file *xy.dat* is written containing the x- and y-coordinates of the full computational grid.

4.17.3.2   netCDF

All data in netCDF output is stored in a single output file. By default this file is named *xboutput.nc*, but this name can be chosen freely using the keyword *ncfilename*. The netCDF file holds all output data, dimensions and input data in a single file. It should be noted that netCDF files can hold a multiple time axes. The temporal unit can be specified in the *params.txt* file using the keyword *tunits*. This unit does not affect calculations and is only used for output. An example of the layout of the netcdf file is given below:

xboutput.nc (structure only, no real contents)

```
netcdf xboutput {
dimensions:
    x = 565 ;
    y = 101 ;
    wave_angle = 9 ;
    bed_layers = 3 ;
    sediment_classes = 1 ;
    inout = 2 ;
    globaltime = 2 ;
    tidetime = 435 ;
    tidecorners = 2 ;
```

```
    windtime = 2 ;
variables:
    double x(x) ;
          x:units = "m" ;
          x:long_name = "local x coordinate" ;
    double y(y) ;
          y:units = "m" ;
          y:long_name = "local y coordinate" ;
    double globaltime(globaltime) ;
          globaltime:units = "s" ;
    double H(globaltime, y, x) ;
          H:units = "m" ;
          H:long_name = "wave height" ;
    double zs(globaltime, y, x) ;
          zs:units = "m" ;
          zs:long_name = "water level" ;
    double zb(globaltime, y, x) ;
          zb:units = "m" ;
          zb:long_name = "bed level" ;
    double ue(globaltime, y, x) ;
          ue:units = "m/s" ;
```

4.18   Time parameters

In all XBeach simulations the hydrodynamic simulation starts at time 0. Model output can be postponed until the time specified by the keyword *tstart* (see 4.17.2). The time step of the simulation is determined based on a given maximum Courant number using the keyword *CFL*. The table below gives an overview of all keywords related to time management:

Table 4.26   Overview of all keywords related to time management

keyword	description	default	range	units	remark
CFL	Maximum Courant-Friedrichs-Lewy number	0.7	0.1 – 0.9	–	
tstop	Stop time of simulation, in morphological time	2000.0	1.0 – 1000000.0	s	
tunits+	Time units in udunits format (seconds since 1970-01-01 00:00:00.00 +1:00)	's'		–	

5 References

Andrews, D. G., & Mcintyre, M. E. (1978). An exact theory of nonlinear waves on a Lagrangian-mean flow. Journal of Fluid Mechanics, 89, 609. doi:10.1017/S0022112078002773

Baldock, T. E., Holmes, P., Bunker, S., & van Weert, P. (1998). Cross-shore hydrodynamics within an unsaturated surfzone. Coastal Engineering, 34, 173–196.

Battjes, J. A. (1975). Modelling of turbulence in the surfzone. Symposium on Modelling Techniques, San Francisco, 1050–1061.

Daly, C., Roelvink, J. A., van Dongeren, A. R., & McCall, R. T. (2010). Short wave breaking effects on law frequency waves. Proceedings 30th International Conference on Coastal Engineering, San Diego, 1–13.

Daly, C., Roelvink, J. A., van Dongeren, A. R., van Thiel de Vries, J. S. M., & McCall, R. T. (2012). Validation of an advective-deterministic approach to short wave breaking in a surf-beat model. Coastal Engineering, 60, 69–83. doi:10.1016/j.coastaleng.2011.08.001

Darcy, H. (1856). Les fontaines publiques de la ville de dijon. Tech. Rep., Dalmont, Paris.

De Jong, M. P. C., Roelvink, J. A., & Breederveld, C. (2013). Numerical modelling of passing-ship effects in complex geometries and on shallow water. Pianc Smart Rivers 2013.

De Vet, P. L. M. (2014). Modelling sediment transport and morphology during overwash and breaching events. MSc thesis, Delft University of Technology, Delft.

Deigaard, R. (1993). A note on the three-dimensional shear stress distribution in a surf zone. Coastal Engineering, 20, 157–171. doi:10.1016/0378-3839(93)90059-H

Deltares. (2011). Delft3D-FLOW: user manual.

Den Adel, H. (1987). Heranalyse doorlatendheidsmetingen door middel van de forchheimer relatie. Technical Report M 1795/H 195, CO 272550/56, Grondmechanica Delft, Waterloopkundig Laboratorium. Dutch.

Galappatti, R., & Vreugdenhill, C. B. (1985). A depth integrated model for suspended transport. Journal for Hydraulic Research, 23(4), 359–377.

Guza, R. T., & Thornton, E. B. (1985). Velocity moments in the nearshore. Coastal Engineering, 111(2), 235–256.

Halford, K. (2000). Simulation and interpretation of borehole flowmeter results under laminar and turbulent flow conditions. Proceedings of the Seventh International Symposium on Logging for Minerals and Geotechnical Applications, Golden, Colorado, The Minerals and Geotechnical Logging Society, 157–168.

Hallermeier, R. J. (1981). Terminal settling velocity of commonly occurring sand grains. Sedimentology, 28, 859–865.

Harbaugh, A. W. (2005). MODFLOW-2005 , The USGS Modular Ground-Water Model. U.S. Geological Survey Techniques and Methods, 253.

Hirsch, C. (2007). Numerical computation of internal and external flows. New York John Wiley & Sons.

Holthuijsen, L. H., Booij, N., & Herbers, T. H. C. (1989). A prediction model for stationary, short-crested waves in shallow water with ambient currents. Coastal Engineering, 13(1), 23–54. doi:10.1016/0378-3839(89)90031-8

Janssen, T. T., & Battjes, J. A. (2007). A note on wave energy dissipation over steep beaches. Coastal Engineering, 54, 711–716. doi:10.1016/j.coastaleng.2007.05.006

Komar, P. D., & Miller, M. C. (1975). On the comparison between the threshold of sediment motion under waves under unidirectional currents with a discussion of the practical evaluation of the threshold. Journal of Sedimentary Research, 362–367.

Lam, D. C. L., & Simpson, R. B. (1976). Centered differencing and the box scheme for diffusion convection problems. Journal of Computational Physics, 22, 486–500.

Lee, K. H., Mizutani, N., Hur, D. S., & Kamiya, A. (2007). The effect of groundwater on topographic changes in a gravel beach. Ocean Engineering, 34, 605–615. doi:10.1016/j.oceaneng.2005.10.026

Li, L., & Barry, D. A. (2000). Wave-induced beach groundwater flow. Advances in Water Resources, 23, 325–337. doi:10.1016/S0309-1708(99)00032-9

Longuet-Higgins, M. S., & Stewart, R. W. (1962). Radiation stress and mass transport in gravity waves, with application to "surf beats." Journal of Fluid Mechanics, 13, 481–504.

Longuet-Higgins, M. S., & Stewart, R. W. (1964). Radiation stress in water waves: a physical discussion with applications. Deep-Sea Research, 529–562.

Longuet-Higgins, M. S., & Turner, J. S. (1974). An "entraining plume" model of a spilling breaker. Journal of Fluid Mechanics, 63(01), 1–20.

Lowe, R. J., Falter, J. L., Koseff, J. R., Monismith, S. G., & Atkinson, M. J. (2007). Spectral wave flow attenuation within submerged canopies: Implications for wave energy dissipation. Journal of Geophysical Research: Oceans, 112, 1–14. doi:10.1029/2006JC003605.

MacCormack, R. W. (1969). The effect of viscocity in hypervecloity impact cratering. AIAA Hyper Velocity Impact Conference, 69–354.

McCall, R. T., Masselink, G., Poate, T. G., Roelvink, J. a., Almeida, L. P., Davidson, M., & Russell, P. E. (2014). Modelling storm hydrodynamics on gravel beaches with XBeach-G. Coastal Engineering, 91, 231–250. doi:10.1016/j.coastaleng.2014.06.007

Mendez, F. J., & Losada, I. J. (2004). An empirical model to estimate the propagation of random breaking and nonbreaking waves over vegetation fields. Coastal Engineering, 51, 103–118. doi:10.1016/j.coastaleng.2003.11.003.

Deltares

Nairn, R. B., Roelvink, J. A., & Southgate, H. N. (1990). Transition zone width and implications for modeling surfzone hydrodynamics. Proceedings 22th International Conference on Coastal Engineering, 68–81. doi:10.9753/icce.v22.

Nederhoff, C. M., Lodder, Q. J., Boers, M., Den Bieman, J. P., & Miller, J. K. (2015). Modeling the effects of hard structures on dune erosion and overwash - a case study of the impact of Hurricane Sandy on the New Jersey coast. Proceedings Coastal Sediments, San Diego, CA.

Phan, L., van Thiel de Vries, J. S. M., & Stive, M. J. F. (2014). Coastal Mangrove Squeeze in the Mekong Delta. Journal of Coastal Research.

Phillips, O. M. (1977). The dynamics of the upper ocean. Cambridge University Press, 366.

Quataert, E., Storlazzi, C. S., van Rooijen, A. A., Cheriton, O., & van Dongeren, A. R. The influence of coral reefs and climate change on wave-driven flooding of tropical coastlines. Geophysical Research Letters (in Press).

Raubenheimer, B., Guza, R. T., & Elgar, S. (1999). Tidal water table fluctuations in a sandy ocean beach. Water Resources Research, 35(8), 2313. doi:10.1029/1999WR900105

Reniers, A. J. H. M., MacMahan, J. H., Thornton, E. B., & Stanton, T. P. (2007). Modeling of very low frequency motions during RIPEX. Journal of Geophysical Research: Oceans, 112(February), 1–14. doi:10.1029/2005JC003122

Reniers, A. J. H. M., Roelvink, J. A., & Thornton, E. B. (2004). Morphodynamic modeling of an embayed beach under wave group forcing. Journal of Geophysical Research, 109, 1–22. doi:10.1029/2002JC001586

Rienecker, M. M., & Fenton, J. D. (1981). A Fourier approximation method for steady water waves. Journal of Fluid Mechanics, 104, 119. doi:10.1017/S0022112081002851

Roelvink, J. A. (1993a). Dissipation in random wave group incident on a beach. Coastal Engineering, 19, 127–150.

Roelvink, J. A. (1993b). Surf beat and its effect on cross-shore profiles. PhD thesis, Delft Unversity of Technology, Delft.

Roelvink, J. A. (2006). Coastal morphodynamic evolution techniques. Coastal Engineering, 53, 277–287. doi:10.1016/j.coastaleng.2005.10.015

Roelvink, J. A., & Stive, M. J. F. (1989). Bar-generating cross-shore flow mechanisms on a beach. Journal of Geophysical Research, 94, 4785–4800.

Rowe, P. N. (1987). A convenient empirical equation for estimation of the richardson-zaki exponent. Chemical Engineering Science, 42(11), 2795 – 2796.

Ruessink, B. G., Miles, J. R., Feddersen, F., Guza, R. T., & Elgar, S. (2001). Modeling the alongshore current on barred beaches. Journal of Geophysical Research, 106(22), 451–463.

Ruessink, B. G., Ramaekers, G., & van Rijn, L. C. (2012). On the parameterization of the free-stream non-linear wave orbital motion in nearshore morphodynamic models. Coastal Engineering, 65, 56–63. doi:10.1016/j.coastaleng.2012.03.006

Schroevers, M., Huisman, B. J., van der Wal, A., & Terwindt, J. (2011). Measuring ship induced waves and currents on a tidal flat in the Western Scheldt Estuary. Current, Waves and Turbulence Measurements (CWTM), 2011 IEEE/OES 10th, 123–129.

Shields, A. (1936). Anwendung der Aehnlichkeitsmechanik under der Turbulenzforschung auf die Geschiebebewegung. Preussischen Versuchsanstalt Fur Wasserbau and Schiffbau, 26, 524–526.

Smagorinsky, J. (1963). General circulation experiments wiht the primitive equations I. The basic experiment. Monthly Weather Review, 91, 99–164. doi:10.1126/science.27.693.594

Smit, P. B., Stelling, G. S., Roelvink, J. A., van Thiel de Vries, J. S. M., McCall, R. T., van Dongeren, A. R., Jacobs, R. (2010). XBeach: Non-hydrostatic model. Validation, verification and model description.

Smit, P. B., Janssen, T. T., Holthuijsen, L. H., & Smith, J. (2014). Non-hydrostatic modeling of surf zone wave dynamics. Coastal Engineering, 83, 36–48. doi:10.1016/j.coastaleng.2013.09.005

Soulsby, R. L. (1997). Dynamics of Marine Sands. London: Thomas Telford Publications.

Stelling, G. S., & Zijlema, M. (2003). An accurate and efficient finite-difference algorithm for non-hydrostatic free-surface flow with application to wave propagation. International Journal for Numerical Methods in Fluids, 43(1), 1–23.

Stelling, G. S., & Duinmeijer. (2003). A staggered conservative scheme for every Froude number in rapidly varied shallow water flows. International Journal for Numerical Methods in Fluids, 43(12), 1329–1354.

Stive, M. J. F., & De Vriend, H. J. (1994). Shear stresses and mean flow in shoaling and breaking waves. Proceedings 24th International Conference on Coastal Engineering, 594–608. doi:10.9753/icce.v24.

Suzuki, T., Zijlema, M., Burger, B., Meijer, M. C., & Narayan, S. (2012). Wave dissipation by vegetation with layer schematization in SWAN. Coastal Engineering, 59(1), 64–71. doi:10.1016/j.coastaleng.2011.07.006

Svendsen, I. A. (1984a). Mass flux and undertow in a surf zone. Coastal Engineering, 8, 347–365.

Svendsen, I. A. (1984b). Wave heights and set-up in a surf zone. Coastal Engineering, 8, 303–329. doi:10.1016/0378-3839(84)90028-0

Talmon, A. M., van Mierlo, M. C., & Struiksma, N. (1995). Laboratory measurements of the direction of sediment transport on transverse alluvial-bed slope. Journal of Hydraulic Research, 33(4), 495–517.

Van Bendegom, L. (1947). Enige beschouwingen over riviermorphologie en rivierverbetering.

Van der Zwaag, J. (2014). Modelling sediment sorting near the large scale nourishment ' The Sand Motor '. MSc thesis, Delft University of Technology, Delft.

Van Dongeren, A. R., & Svendsen, I. A. (1997). Absorbing-generating boundary condition for shallow water models. Journal of Waterway, Port, Coastal and Ocean Engeering, (123), 303–313.

Van Dongeren, A. R., Lowe, R. J., Pomeroy, A., Trang, D. M., Roelvink, J. A., Symonds, G., & Ranasinghe, R. (2013). Numerical modeling of low-frequency wave dynamics over a fringing coral reef. Coastal Engineering, 73, 178–190.

Van Rhee, C. (2010). Sediment entrainment at high flow velocity. Journal of Hydraulic Engineering, 136, 572–582.

Van Rijn, L. C. (1985). Sediment transport, part III: bed forms and alluvial roughness. Journal of Hydraulic Engineering, 110(12), 1733–1754.

Van Rijn, L. C. (2007). Unified View of Sediment Transport by Currents and Waves: part I and II. Journal of Hydraulic Engineering, (June), 649–667.

Van Rooijen, A. A., Van Thiel de Vries, J. S. M., McCall, R. T., van Dongeren, A. R., Roelvink, J. A., & Reniers, A. J. H. M. (2015). Modeling of wave attenuation by vegetation with XBeach. E-Proceedings of the 36th IAHR World Congress 28 June – 3 July, 2015, The Hague, The Netherlands.

Van Thiel de Vries, J. S. M. (2009). Dune erosion during storm surges. PhD thesis, Delft Unversity of Technology, Delft.

Verboom, G. K., Stelling, G. S., & Officer, M. J. (1981). Boundary conditions for the shallow water equations. Engineering Applications of Computational Hydraulics, 230–262.

Walstra, D. J. R., Roelvink, J. A., & Groeneweg, J. (2000). Calculation of wave-driven currents in a 3D mean flow model. In Proceedings 27th International Conference on Coastal Engineering (pp. 1050–1063).

Walstra, D. J. R., van Rijn, L. C., Van Ormondt, M., Briere, C., & Talmon, A. M. (2007). The Effects of Bed Slope and Wave Skewness on Sediment Transport and Morphology (pp. 137–150).

Zhou, M., Roelvink, J. A., Verheij, H. J., & Ligteringen, H. (2013). Study of Passing Ship Effects along a Bank by Delft3D-FLOW and XBeach. International Workshop on Nautical Traffic Models 2013, Delft, The Netherlands, July 5-7, 2013. Delft University of Technology.

Zhou, M., Roelvink, J. A., Zou, Z., & van Wijhe, H. J. (2014). Effects of Passing Ship With a Drift Angle on a Moored Ship. ASME 2014 33rd International Conference on Ocean, Offshore and Arctic Engineering.

Zijlema, M., & Stelling, G. S. (2005). Further experiences with computing non-hydrostatic free-surface flows involving water waves. INTERNATIONAL JOURNAL FOR NUMERICAL METHODS IN FLUIDS, (48), 169–197.

Zijlema, M., & Stelling, G. S. (2008). Efficient computation of surf zone waves using the nonlinear shallow water equations with non-hydrostatic pressure. Coastal Engineering, 55(10), 780–790.

Zijlema, M., Stelling, G. S., & Smit, P. B. (2011). SWASH: An operational public domain code for simulating wave fields and rapidly varied flows in coastal waters. Coastal Engineering, 58(10), 992–1012. doi:10.1016/j.coastaleng.2011.05.015

A   Advanced model coefficients

In 4.1 the main input parameters and files required by XBeach to start a simulation are explained. It explained how the user can switch on and off specific processes and how the user can define the model initial and boundary conditions. XBeach offers, however, many more parameters to fine-tune the simulation of different processes. These parameters are listed in the following subsections grouped by process. Most parameters are not relevant for the average XBeach user. Parameters marked with a plus (+) are considered advanced options that are recommended to stay untouched.

A.1   Wave numerics

The parameters listed in the table below involve the numerical aspects of the wave action balance that solves the wave propagation in the model. The keyword *scheme* can be used to set the numerical scheme. By default a higher-order upwind scheme is used to minimize numerical dissipation.

Table 5.1   Overview of available keyword related to wave numerics

keyword	description	default	range	units	remark
maxerror+	Maximum wave height error in wave stationary iteration	5e-05	1e-05 – 0.001	m	
maxiter+	Maximum number of iterations in wave stationary	500	2 – 1000	–	
scheme+	Numerical scheme for wave propagation	upwind_2	upwind_1, lax_wendroff, upwind_2		

A.2   Rollers

The parameters listed in the table below involve the wave roller model. Using the roller model will give a shoreward shift in wave-induced setup, return flow and alongshore current. This shift becomes greater for lower *beta* values.

Table 5.2   Overview of available keyword related to the roller model

keyword	description	default	range	units	remark
beta+	Breaker slope coefficient in roller model	0.1	0.05 – 0.3	–	
rfb+	Switch to feedback maximum wave surface slope in roller energy balance, otherwise rfb = Beta	0	0 – 1	–	
roller+	Switch to enable roller model	1	0 – 1	–	

A.3 Wave-current interaction

The parameters listed in the table below involve the process of wave-current interaction. With the switch *wci* one can turn off or on the wave-current interaction, the wave current interaction will result in a feedback of currents on the wave propagation. On top of that, *hwci* limits the computation of wave-current interaction in very shallow water where the procedure may not converge.

Table 5.3   Overview of available keyword related to the wave-current interaction (wci)

keyword	description	default	range	units	remark
cats+	Current averaging time scale for wci, in terms of mean wave periods	4.0	1.0 - 50.0	Trep	
hwci+	Minimum depth until which wave-current interaction is used	0.1	0.001 - 1.0	m	
wci	Turns on wave-current interaction	0	0 - 1	-	

A.4 Flow numerics

The parameters listed in the table below involve the numerical aspects of the shallow water equations that solve the water motions in the model. Especially in very shallow water some processes need to be limited to avoid unrealistic behavior. For example *hmin* prevents very strong return flows or high concentrations and the *eps* determines whether points are dry or wet and can be taken quite small.

Table 5.4   Overview of available keyword related to flow numerics

keyword	description	default	range	units	remark
eps	Threshold water depth above which cells are considered wet	0.005	0.001 – 0.1	m	
eps_sd	Threshold velocity difference to determine conservation of energy head versus momentum	0.5	0.0 – 1.0	m/s	
hmin	Threshold water depth above which Stokes drift is included	0.2	0.001 – 1.0	m	
oldhu+	Switch to enable old hu calculation	0	0 – 1	–	
secorder+	Use second order corrections to advection/non-linear terms based on MacCormack scheme	0	0 – 1	–	
umin	Threshold velocity for upwind velocity detection and for vmag2 in equilibrium sediment concentration	0.0	0.0 – 0.2	m/s	

A.5   Sediment transport

The parameters listed in the table below involve the process of sediment transport. The keywords *facAs* and *facSk* determine the effect of the wave form on the sediment transport, this is especially important in the nearshore. The *facua* is an alias setting in which both parameters can be varied at once. The wave form model itself is selected using the keyword *waveform*. Processes like short- and long-wave stirring and turbulence can be switched on or off using the keywords *sws, lws* and *lwt*. Several options for calibrating the sediment transport formulations are available as well as keywords to incorporate the bed slope effect.

Table 5.5   Overview of available keyword related to the sediment transport model

keyword	description	Default	Range	units	remark
BRfac+	Calibration factor surface slope	1.0	0.0 – 1.0	–	
Tbfac+	Calibration factor for bore interval	1.0	0.0 – 1.0	–	

keyword	description	Default	Range	units	remark
	Tbore: Tbore = Tbfac+Tbore				
Tsmin+	Minimum adaptation time scale in advection diffusion equation sediment	0.5	0.01 - 10.0	s	
bdslpeffdir	Modify the direction of the sediment transport based on the bed slope	none	none, talmon		
bdslpeffdir fac	Calibration factor in the modification of the direction	1.0	0.0 - 2.0	–	
bdslpeffini	Modify the critical shields parameter based on the bed slope	none	none, total, bed		
bdslpeffmag	Modify the magnitude of the sediment transport based on the bed slope, uses facsl	roelvink_to tal	none, roelvink_tot al, roelvink_bed , soulsby_tota l, soulsby_bed		
bed+	Calibration factor for bed transports	1	0 - 1	–	
betad+	Dissipation parameter long wave breaking turbulence	1.0	0.0 - 10.0	–	
bulk+	Switch to compute bulk transport	0	0 - 1	–	

keyword	description	Default	Range	units	remark
	rather than bed and suspended load separately				
dilatancy	Switch to reduce critical shields number due dilatancy	0	0 - 1	-	
facAs+	Calibration factor time averaged flows due to wave asymmetry	0.1	0.0 - 1.0	-	
facDc+	Option to control sediment diffusion coefficient	1.0	0.0 - 1.0	-	
facSk+	Calibration factor time averaged flows due to wave skewness	0.1	0.0 - 1.0	-	
facsl+	Factor bedslope effect	1.6	0.0 - 1.6	-	
facua+	Calibration factor time averaged flows due to wave skewness and asymmetry	0.1	0.0 - 1.0	-	
fallvelred	Switch to reduce fall velocity for high concentrations	0	0 - 1	-	
form	Equilibrium sediment concentration formulation	vanthiel_vanrijn	soulsby_vanrijn, vanthiel_vanrijn		
jetfac+	Option to mimic turbulence production	0.0	0.0 - 1.0	-	

keyword	description	Default	Range	units	remark
	near revetments				
lws+	Switch to enable long wave stirring	1	0 – 1	–	
lwt+	Switch to enable long wave turbulence	0	0 – 1	–	
pormax	Max porosity used in the expression of Van Rhee	0.5	0.3 – 0.6	–	
reposeangle	Angle of internal friction	30.0	0.0 – 45.0	deg	
rheeA	A parameter in the Van Rhee expression	0.75	0.75 – 2.0	–	
sus+	Calibration factor for suspensions transports	1	0 – 1	–	
sws+	Switch to enable short wave and roller stirring and undertow	1	0 – 1	–	
tsfac+	Coefficient determining Ts = tsfac + h/ws in sediment source term	0.1	0.01 – 1.0	–	
turb+	Switch to include short wave turbulence	bore_averaged	none, wave_averaged, bore_averaged		
turbadv+	Switch to activate turbulence advection model for short and or long wave turbulence	none	none, lagrangian, eulerian		
waveform	Wave shape	vanthiel	ruessink_van		

keyword	description	Default	Range	units	remark
	model		rijn, vanthiel		
z0+	Zero flow velocity level in Soulsby and van Rijn (1997) sediment concentration	0.006	0.0001 – 0.05	– m	

A.6 Sediment transport numerics

The parameters listed in the table below involve the numerical aspects of sediment transport that are all considered advanced options. For example the maximum allowed sediment concentration can be varied with the keyword *cmax*. It is however not recommended varying these settings.

Table 5.6   Overview of available keyword related to sediment transport numerics

keyword	Description	default	range	units	remark
cmax+	Maximum allowed sediment concentration	0.1	0.0 – 1.0		
sourcesink+	Switch to enable source-sink terms to calculate bed level change rather than suspended transport gradients	0	0 – 1	–	
thetanum+	Coefficient determining whether upwind (1) or central scheme (0.5) is used.	1.0	0.5 – 1.0	–	

A.7 Bed update

The parameters listed in the table below involve the settings for the bed update process especially in the case multiple sediment fractions and bed layers are involved. The *frac_dz, split* and *merge* keywords determine the fraction of the variable bed layer thickness at which the layer is split or merged respectively with the surrounding bottom layers. The variable layer is chosen using the *nd_var* keyword.

Pre-defined bed evolution can be used with the keywords *setbathy* that is used to turn user-imposed bed level change on, *nsetbathy* that determines the number of imposed bed level conditions and *setbathyfile* that references a file that specifies the time series of imposed bed levels. If the *setbathy* option is used, XBeach will automatically interpolate the bed level at each computational time step from the imposed bed level time series.

The *setbathyfile* file must contain a time series (of length *nsetbathy*) of the bed level at every grid point in the XBeach model. The format of the *setbathyfile* file is such that each imposed bed level starts with the time at which the bed level should be applied (in seconds relative to the start of the simulation), followed on a new line by the bed level in each grid cell in an identical manner to the normal initial bathymetry file (e.g., one line per transect in the x-direction). The following imposed bed level condition starts on a new line with the time at which the condition is imposed and the bed levels at that time, etc. An example of a *setbathyfile* is given below.

setbathyfile.dep (generalized)

```
<t 0>
<z 1,1> <z 2,1> <z 3,1> ... <z nx,1> <z nx+1,1>
<z 1,2> <z 2,2> <z 3,2> ... <z nx,2> <z nx+1,2>
<z 1,3> <z 2,3> <z 3,3> ... <z nx,3> <z nx+1,3>
...
<z 1,ny> <z 2,ny> <z 3,ny> ... <z nx,ny> <z nx+1,ny>
<z 1,ny+1> <z 2,ny+1> <z 3,ny+1> ... <z nx,ny+1> <z nx+1,ny+1>
<t 1>
<z 1,1> <z 2,1> <z 3,1> ... <z nx,1> <z nx+1,1>
<z 1,2> <z 2,2> <z 3,2> ... <z nx,2> <z nx+1,2>
<z 1,3> <z 2,3> <z 3,3> ... <z nx,3> <z nx+1,3>
...
<z 1,ny> <z 2,ny> <z 3,ny> ... <z nx,ny> <z nx+1,ny>
<z 1,ny+1> <z 2,ny+1> <z 3,ny+1> ... <z nx,ny+1> <z nx+1,ny+1>
...
...
<t nsetbathy>
<z 1,1> <z 2,1> <z 3,1> ... <z nx,1> <z nx+1,1>
<z 1,2> <z 2,2> <z 3,2> ... <z nx,2> <z nx+1,2>
<z 1,3> <z 2,3> <z 3,3> ... <z nx,3> <z nx+1,3>
...
<z 1,ny> <z 2,ny> <z 3,ny> ... <z nx,ny> <z nx+1,ny>
<z 1,ny+1> <z 2,ny+1> <z 3,ny+1> ... <z nx,ny+1> <z nx+1,ny+1>
```

setbathyfile.dep (short 1D example, nx = 20, ny = 0, nsetbathy = 4)

```
0
-20 -18 -16 -14 -12 -10 -8 -6 -5 -4 -3 -2 -1 -0.5 0 0.5 1 2 3 4 5
1200
-20 -18 -16 -14 -12 -10 -8 -6 -5 -4 -3 -1.8 -0.75 -0.25 0 0.2 0.7 2 3 4 5
2400
-20 -18 -16 -14 -12 -10 -8 -6 -5 -4 -2.5 -1.6 -0.5 -0.3 0 0.1 0.6 1.5 3 4 5
3600
-20 -18 -16 -14 -12 -10 -8 -6 -5 -4 -2 -1.4 -0.3 0 0.05 0.1 0.6 1 2.2 3.5 5
```

Note that if the *setbathy* option is used, the initial bed level is derived from an interpolation of the *setbathyfile* file time series, not from the *depfile* file. It is strongly advised to turn of the computation of morphological updating (keyword: *morphology = 0*) if the *setbathy* option is used, as the computed morphological change will be overridden by the imposed morphological change.

Table 5.7   Overview of available keyword related to the bed update module

keyword	description	default	range	units	remark
frac_dz*	Relative thickness to split time step for bed updating	0.7	0.5 – 0.98	–	–
merge*	Merge threshold for variable sediment layer (ratio to nominal thickness)	0.01	0.005 – 0.1	–	–
nd_var*	Index of layer with variable thickness	2	2 – nd	–	
nsetbathy*	Number of prescribed bed updates	1	1 – 1000	–	
setbathyfile*	Name of prescribed bed update file				<file>
split*	Split threshold for variable sediment layer (ratio to nominal thickness)	1.01	1.005 – 1.1	–	–

A.8   Groundwater flow

The parameters listed in the table below involve the process of groundwater flow. The vertical permeability coefficient in the vertical can be set differently than that of the horizontal using the keywords *kz* and *kz* respectively. The initial bed level of the aquifer is read from an external file referenced by the *aquiferbotfile* keyword and the initial groundwater head can be set to either a uniform value using the *gw0* keyword or to spatially varying values using an external file referenced by the *gw0file* keyword. Both files have the same format as the bathymetry file explained in Section 4.4).

Table 5.8   Overview of available keyword related to the groundwater module

keyword	description	default	range	units	remark
aquiferbot+	Level of uniform aquifer bottom	–10.0	–100.0 – 100.0	m	
aquiferbotfile+	Name of the aquifer bottom file				<file>
dwetlayer+	Thickness of the top soil layer interacting more freely with the surface	0.1	0.01 – 1.0	m	

keyword	description	default	range	units	remark
	water				
gw0+	Level initial groundwater level	0.0	-5.0 - 5.0	m	
gw0file+	Name of initial groundwater level file			<file>	
gwReturb+	Reynolds number for start of turbulent flow in case of gwscheme = turbulent	100.0	1.0 - 600.0	-	
gwfastsolve+	Reduce full 2D non-hydrostatic solution to quasi-explicit in longshore direction	0	0 - 1	-	
gwheadmodel+	Model to use for vertical groundwater head	parabolic	parabolic, exponential		
gwhorinfil+	Switch to include horizontal infiltration from surface water to groundwater	0	0 - 1	-	
gwnonh+	Switch to turn on or off non-hydrostatic pressure for groundwater	0	0 - 1	-	
gwscheme+	Scheme for momentum equation	laminar	laminar, turbulent		
kx+	Darcy-flow permeability coefficient in x-direction	0.0001	1e-05 - 0.1	ms^-1	
ky+	Darcy-flow permeability coefficient in y-direction	0.0001	1e-05 - 0.1	ms^-1	

keyword	description	default	range	units	remark
kz+	Darcy-flow permeability coefficient in z-direction	0.0001	1e-05 – 0.1	ms^-1	

A.9   Non-hydrostatic correction

The parameters listed in the table below involve the settings for the non-hydrostatic option. These are all considered advanced options and it is thus recommended not to change these

Table 5.9   Overview of available keyword related to the non-hydrostatic module

keyword	description	default	range	units	remark
Topt+	Absolute period to optimize coefficient	10.0	1.0 – 20.0	s	
breakviscfac+	Factor to increase viscosity during breaking	1.5	1.0 – 3.0	–	
breakvisclen+	Ratio between local depth and length scale in extra breaking viscosity	1.0	0.75 – 3.0	–	
dispc+	Coefficient in front of the vertical pressure gradient	1.0	0.1 – 2.0	?	
kdmin+	Minimum value of kd (pi/dx > min(kd))	0.0	0.0 – 0.05	–	
maxbrsteep+	Maximum wave steepness criterium	0.6	0.3 – 0.8	–	
nhbreaker+	Non-hydrostatic breaker model	2	0 – 3	–	
reformsteep+	Wave steepness criterium to reform after breaking	0.25 + maxbrsteep	0.0 – 0.95+ maxbrsteep	–	
secbrsteep+	Secondary maximum wave steepness	0.5 + maxbrsteep	0.0 – 0.95+ maxbrsteep	–	

keyword	description	default	range	units	remark
	criterium				
solver+	Solver used to solve the linear system	tridiag	sip, tridiag		
solver_acc+	Accuracy with respect to the right-hand side used in the following termination criterion: ||b-Ax || < acc+||b||	0.005	1e-05 - 0.1	-	
solver_maxit+	Maximum number of iterations in the linear sip solver	30	1 - 1000	-	
solver_urelax+	Under relaxation parameter	0.92	0.5 - 0.99	-	

A.10 Coriolis force

The parameters listed in the table below involve the settings for incorporating the effect of Coriolis on the shallow water equations. The keywords are universally used coefficients.

Table 5.10   Overview of available keyword related to the Coriolis force

keyword	description	default	range	units	remark
lat+	Latitude at model location for computing Coriolis	0.0	-90.0 - 90.0	deg	
wearth+	Angular velocity of earth calculated as: 1/rotation_time (in hours)	0.0417	0.0 - 1.0	hour^-1	

A.11 MPI

The parameters listed in the table below involve the settings for parallelization of XBeach. When running XBeach in parallel mode, the model domain is subdivided in sub models and each sub model is then computed on a separate core. This will increase the computational speed of the model. The sub models only exchange information over their boundaries when necessary. The MPI parameters determine how the model domain is subdivided. The keyword *mpiboundary* can be set to *auto, x, y* or *man*. In *auto* mode the model domain is subdivided such that the internal boundary is smallest. In *x* or *y* mode the model domain is subdivided in sub models extending to either the full alongshore or the full cross-shore extent of the model domain. In *man* mode the model domain is manually subdivided using the

values specified with the *mmpi* and *nmpi* keywords. The number of sub models is not determined by XBeach itself, but by the MPI wrapper (e.g. MPICH2 or OpenMPI).

Table 5.11 Overview of available keyword related to MPI

keyword	description	default	range	units	remark
mmpi+	Number of domains in cross-shore direction when manually specifying mpi domains	2	1 - 100	-	
mpiboundary+	Fix mpi boundaries along y-lines, x-lines, use manual defined domains or find shortest boundary automatically	auto	auto, x, y, man		
nmpi+	Number of domains in alongshore direction when manually specifying mpi domains	4	1 - 100	-	

A.12 Output projection

The parameters listed in the table below involve the projection of the model output. These settings do not influence the model results in anyway. The *rotate* keyword can be used to rotate the model output with an angle specified by the keyword *alfa*. The *projection* string can hold a string specifying the coordinate reference system used and is stored in the netCDF output file as metadata.

Table 5.12 Overview of available keyword related to the output projection

keyword	description	default	range	units	remark
projection+	Projection string	' '		-	
rotate	Rotate output as post processing with given angle	1	0 - 1	-	

B Numerical implementation

B.1 Grid set-up

The new implementation utilizes a curvilinear, staggered grid where depths, water levels, wave action and sediment concentrations are given in the cell centers (denoted by subscript z) and velocities and sediment fluxes at the cell interfaces (denoted by subscript u or v). In Figure 5.1 the z, u, v and c (corner) points with the same numbering are shown. The grid directions are named s and n; grid distances are denoted by *Δs* and *Δn*, with subscripts referring to the point where they are defined. A finite-volume approach is utilized where mass, momentum and wave action are strictly conserved. In the middle panel of Figure 5.1, the control volume for the mass balance is shown with the corresponding grid distances around the *u*- and *v*-points. The right panel explains the numbering of the fluxes *Q* and the volume *V*.
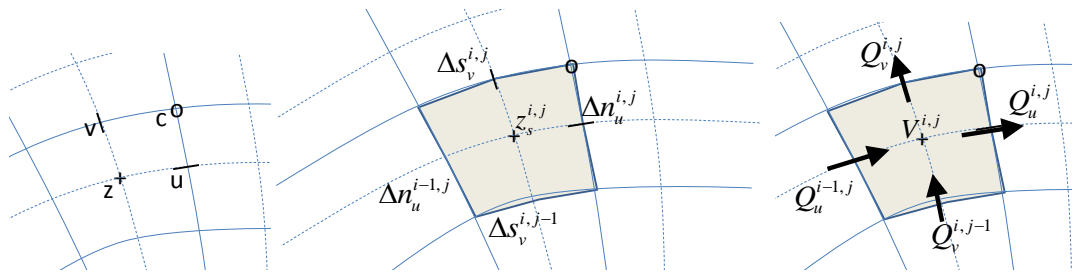
Figure 5.1 Location of staggered grid points (left panel); definition of grid distances (middle) and terms in volume balance (right)

B.2 Wave action balance

B.2.1 Surfbeat solver

The time-varying wave action balance solved in XBeach is as follows:

$$\frac{\partial A}{\partial t} + \frac{\partial c_x A}{\partial x} + \frac{\partial c_y A}{\partial y} + \frac{\partial c_\theta A}{\partial \theta} = -SINK \tag{B.1}$$

Where A is the wave energy or wave action, c_g is the group velocity, c_Θ the refraction speed in theta-space and *SINK* refers to effects of wave breaking, vegetation and bottom friction. Again, the advection terms are the only ones affected by the curvilinear scheme so we will discuss their treatment in detail. The control volume is the same as for the mass balance. In (B.1) the procedure to compute the wave energy fluxes across the cell boundaries is outlined. All variables should also have an index *itheta* referring to the directional grid, but for brevity these are omitted here.

The component of the group velocity normal to the cell boundary, at the cell boundary, is interpolated from the two adjacent cell center points. Depending on the direction of this component, the wave energy at the cell boundary is computed using linear extrapolation based on the two upwind points, taking into account their grid distances. This second order upwind discretization preserves the propagation of wave groups with little numerical diffusion.

$$c_{gu,u}^{i,j} = \frac{1}{2}(c_{gu}^{i,j} + c_{gu}^{i+1,j})$$

$$FLUX_u^{i,j} = c_{gu,u}^{i,j} A_u^{i,j} \Delta n_u^{i,j}$$

if $c_{gu,u}^{i,j} > 0$

$$A_u^{i,j} = A^{i,j} + \frac{1}{2}\Delta s_u^{i,j} \frac{A^{i,j} - A^{i-1,j}}{\Delta s_u^{i-1,j}} =$$

$$A_u^{i,j} = \left(\left(\Delta s_u^{i-1,j} + \frac{1}{2}\Delta s_u^{i,j} \right) A^{i,j} - \frac{1}{2}\Delta s_u^{i,j} A^{i-1,j} \right) / \Delta s_u^{i-1,j}$$

if $c_{gu,u}^{i,j} < 0$

$$A_u^{i,j} = A^{i+1,j} - \frac{1}{2}\Delta s_u^{i,j} \frac{A^{i+2,j} - A^{i+1,j}}{\Delta s_u^{i+1,j}} =$$

$$A_u^{i,j} = \left(\left(\Delta s_u^{i+1,j} + \frac{1}{2}\Delta s_u^{i,j} \right) A^{i+1,j} - \frac{1}{2}\Delta s_u^{i,j} A^{i+2,j} \right) / \Delta s_u^{i+1,j}$$

(B.2)

The other three fluxes are computed in a similar way; for brevity we will not present all formulations.

The time integration is explicit and the same as in the original implementation. The advection in u- and v-direction is computed simply by adding the four fluxes and dividing by the cell area. This procedure guarantees conservation of wave energy.

$$\frac{A^{i,j,n+1} - A^{i,j,n}}{\Delta t} + \frac{FLUX_u^{i,j,n} - FLUX_u^{i-1,j,n} + FLUX_v^{i,j,n} - FLUX_v^{i,j-1,n}}{A_z^{i,j}} + \left(\frac{\partial c_\theta A}{\partial \theta} \right)^{i,j,n} = -SINK^{i,j,n}$$

(B.3)

The procedure for the roller energy balance is identical to that for the wave energy balance and will not be repeated here.

B.2.2 Stationary solver
In the stationary solver the wave energy and roller energy balances are solved line by line, from the seaward boundary landward. For each line the automatic time step is computed and the quasi-time-dependent balance according to (B.3) is solved until convergence or the maximum number of iterations is reached, after which the solver moves to the next line. The iteration is controlled by the keywords *maxiter* and *maxerror.*

B.3 Shallow water equations

B.3.1 Mass balance equation
The mass balance reads as follows:

$$\frac{\partial V}{\partial t} = Q_u^{i,j} - Q_u^{i-1,j} + Q_v^{i,j} - Q_v^{i,j-1} \tag{B.4}$$

This is discretized according to:

$$A_{cell}^{i,j} \frac{z_s^{i,j,n+1} - z_s^{i,j,n}}{\Delta t} = u_u^{i,j,n+1/2} h_u^{i,j,n} \Delta n_u^{i,j} - u_u^{i-1,j,n+1/2} h_u^{i-1,j,n} \Delta n_u^{i-1,j}$$
$$+ v_v^{i,j,n+1/2} h_v^{i,j,n} \Delta s_v^{i,j} - v_v^{i,j-1,n+1/2} h_v^{i,j-1,n} \Delta s_v^{i,j-1} \tag{B.5}$$

Here, A_{cell} is the area of the cell around the cell center, z_s is the surface elevation, u_u is the u-velocity in the u-point, h_u the water depth in the u-point and v_v the v-velocity in the v-point. The indices *i,j* refer to the grid number in u resp. v direction; the index *n* refers to the time step.

B.3.2 Momentum balance equation
Second, we will outline the derivation of the u-momentum balance. The control volume is given in Figure 5.2. It is centered around the u-point. We now consider the rate of change of the momentum in the local u-direction as follows:

$$\frac{d(Vu)}{dt} - \sum Q_{in} u_{in} + \sum Q_{out} u + Vg \frac{\partial z_s}{\partial s} + A_{cell} \frac{\tau_{b,u}}{\rho} = A_{cell} \frac{\tau_{s,u}}{\rho} + A_{cell} \frac{F_u}{\rho} \tag{B.6}$$

Where V is the cell volume, u the velocity in local grid direction, Q the fluxes, ρ the density, g acceleration of gravity, τ_{bu} the bed shear stress, τ_{su}, wind shear stress and F_u wave force in u-direction. We consider that the outgoing fluxes carry the velocity inside the cell, u and that u_{in} is determined at each inflow boundary by interpolation, reconstructing the component in the same direction as u.

The volume balance for the same volume reads:

$$\frac{dV}{dt} - \sum Q_{in} + \sum Q_{out} = 0 \tag{B.7}$$

By multiplying the volume balance by *u*, subtracting it from the momentum balance and dividing the result by V (A_{cell}, h_{um}) we arrive at the following equation:

$$\frac{du}{dt} + \frac{\sum Q_{in}(u - u_{in})}{A_{cell} h_{um}} + g \frac{\partial z_s}{\partial s} + \frac{\tau_{b,s}}{\rho h_{um}} = \frac{\tau_{s,u}}{\rho h_{um}} + \frac{F_u}{\rho h_{um}} \tag{B.8}$$

Where A_{cell} is the cell area and h_{um} is the average depth of the cell around the *u*-point. The procedure for the second term (the others are straightforward) now boils down to integrating (only) the incoming fluxes over the interfaces and multiplying them with the difference between *u* in the cell and the component of velocity in the same direction at the upwind cell.
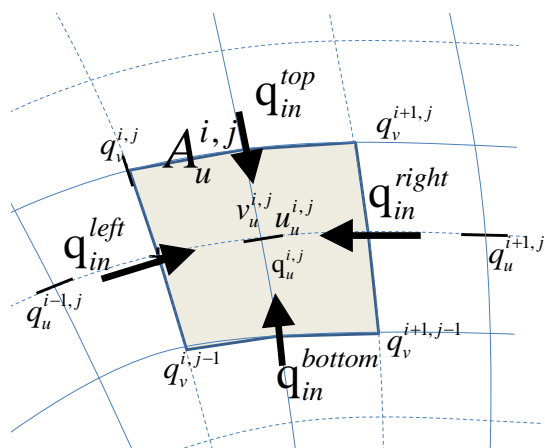
Figure 5.2   Control volume u-momentum balance and definition of fluxes

In (B.9) and (B.10) the procedure for computing the u-momentum balance is outlined. The discharges in the u-points are computed by multiplying the velocity in the u- or v-point by the water depth at that point. These discharges are then interpolated to the borders of the control volume around the u-point. The difference *Δa* in grid orientation between the incoming cell and the u-point is computed and used to compute the component of the incoming velocity in the local u-direction, from the left and right side of the control volume.

$$
\begin{aligned}
&\mathrm{q}_u^{i,j} = u_u^{i,j,n-1/2} h_u^{i,j,n} \\
&\mathrm{q}_{in}^{left} = \frac{1}{2}\left(\mathrm{q}_u^{i,j} + \mathrm{q}_u^{i-1,j}\right) && \mathrm{q}_{in}^{right} = -\frac{1}{2}\left(\mathrm{q}_u^{i+1,j} + \mathrm{q}_u^{i,j}\right) \\
&\Delta\alpha^{left} = \alpha_u^{i,j} - \alpha_u^{i-1,j} && \Delta\alpha^{right} = \alpha_u^{i+1,j} - \alpha_u^{i,j} \\
&u_{in}^{left} = u_u^{i-1,j}\cos\left(\Delta\alpha\right) - v_u^{i-1,j}\sin\left(\Delta\alpha\right) && u_{in}^{right} = u_u^{i+1,j}\cos\left(\Delta\alpha\right) - v_u^{i+1,j}\sin\left(\Delta\alpha\right)
\end{aligned}
$$
(B.9)

The same is done for the top and bottom of the control volume, based on the discharges in v-direction:

$$
\begin{aligned}
&\mathrm{q}_v^{i,j} = v_v^{i,j,n-1/2} h_v^{i,j,n} \\
&\mathrm{q}_{in}^{bottom} = \frac{1}{2}\left(\mathrm{q}_v^{i,j-1} + \mathrm{q}_v^{i+1,j-1}\right) && \mathrm{q}_{in}^{top} = -\frac{1}{2}\left(\mathrm{q}_v^{i,j} + \mathrm{q}_v^{i+1,j}\right) \\
&\Delta\alpha^{bottom} = \alpha_u^{i,j} - \alpha_u^{i,j-1} && \Delta\alpha^{top} = \alpha_u^{i,j+1} - \alpha_u^{i,j} \\
&u_{in}^{bottom} = u_u^{i,j-1}\cos\left(\Delta\alpha\right) - v_u^{i,j-1}\sin\left(\Delta\alpha\right) && u_{in}^{top} = u_u^{i,j+1}\cos\left(\Delta\alpha\right) - v_u^{i,j+1}\sin\left(\Delta\alpha\right)
\end{aligned}
$$
(B.10)

Finally, the advective term in the momentum balance is given in (B.11).

$$
\left(\frac{\sum Q_{in}\left(u-u_{in}\right)}{A_{cell}h_{um}} \right)^{i,j} = \max(q_{in}^{left},0)(u_u^{i,j}-u_{in}^{left})\frac{\Delta n_z^{i,j}}{h_{um}^{i,j}A_{cellu}^{i,j}}
$$

$$
+ \max(q_{in}^{right},0)(u_u^{i,j}-u_{in}^{right})\frac{\Delta n_z^{i+1,j}}{h_{um}^{i,j}A_{cellu}^{i,j}}
$$

$$
+ \max(q_{in}^{bottom},0)(u_u^{i,j}-u_{in}^{bottom})\frac{\Delta s_c^{i,j-1}}{h_{um}^{i,j}A_{cellu}^{i,j}}
$$

$$
+ \max(q_{in}^{top},0)(u_u^{i,j}-u_{in}^{top})\frac{\Delta s_c^{i,j}}{h_{um}^{i,j}A_{cellu}^{i,j}}
$$

(B.11)

B.3.3 Time integration scheme

The time integration of the mass and momentum balance equations is combined in an explicit leap-frog scheme, as depicted in Figure 5.3. The velocities (in the '-' points) are updated using the momentum balance. The water levels are updated using the mass balance. The water level gradients influence the momentum balance and the velocities and derived discharges affect the mass balance. Because of the leap-frog scheme these influences are always computed at the half time step level, which makes the scheme second order accurate.
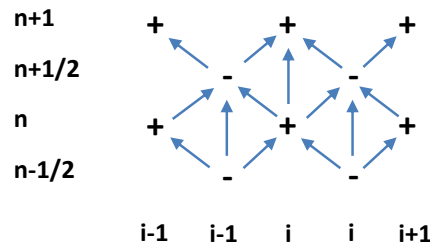

Figure 5.3   Leap-frog time integration scheme

Using this straightforward finite volume approach, complicated transformations of the equations are avoided and the solution scheme remains transparent. It is also completely compatible with the original rectilinear implementation and is even slightly more efficient.

B.3.4 Groundwater flow

In order to solve (B.12), the spatial and temporal domain of the groundwater system is split into the same spatial grid and time steps as the XBeach surface water model it is coupled to. At each time step in the numerical model, the depth average groundwater head is calculated in the center of the groundwater cells, and the fluxes (specific discharge, submarine exchange, infiltration and exfiltration) are calculated on the cell interfaces

At the start of the time step, every cell is evaluated whether the groundwater and surface water are connected:

$$
\kappa_{i,j} = \eta_{gw,i,j} \geq z_{b,i,j} - \varepsilon \wedge \eta_{i,j} \geq z_{b,i,j} + \varepsilon
$$

(B.12)

In (B.12) ε is a numerical smoothing constant used to deal with numerical round off errors near the bed (equal to the keyword *dwetlayer* in the case of hydrostatic groundwater flow, and to the parameter *eps* in the case of non-hydrostatic groundwater flow), and *i* and *j* represent cross-shore and longshore coordinates in the numerical solution grid, respectively. Infiltration

is calculated in cells where the groundwater and surface water are not connected and there exists surface water. As shown in (2.65) the infiltration rate is a function of the thickness of the wetting front, which is zero at the start of infiltration, and increases as a function of the infiltration rate. The equations for the infiltration rate and the thickness of the wetting front are approximated by first-order schemes, in which the wetting front is updated using a backward-Euler scheme, which ensures numerical stability:

$$
S_{inf,i,j}^n = K_{i,j} \left(\frac{1}{\rho g} \frac{p_{lpf,i,j}\big|^{z=z_b}}{\delta_{infill,i,j}^n} - 1 \right)
$$

$$
\delta_{infill,i,j}^n = \delta_{infill,i,j}^{n-1} + S_{inf,i,j}^n \frac{\Delta t}{n_p}
$$

(B.13)

In (B.13) the pressure term p_{lpf} is the surface water pressure at the bed, which in the case of non-hydrostatic surface water flow is high-pass filtered at $4/T_{rep}$, the superscript n corresponds to the time step number and Δt is the size of the time step. The infiltration rate in the coupled relationship can be solved through substitution:

$$
S_{inf,i,j}^n = \frac{-\delta_{infill,i,j}^{n-1} + \dfrac{\Delta t}{n_p K_{i,j}} + \sqrt{\left(\delta_{infill,i,j}^{n-1}\right)^2 + \dfrac{2}{n_p} \dfrac{\Delta t}{\delta_{infill,i,j}^{n-1} K_{i,j}} + \dfrac{4\rho g}{n_p} \dfrac{\Delta t}{p_{i,j}\big|^{z=\xi} K_{i,j}} + \dfrac{\Delta t^2}{K_{i,j}^2}}}{\dfrac{2\Delta t}{n_p}}
$$

(B.14)

At the end of infiltration, i.e. when the groundwater and surface water become connected or there is no surface water left, the wetting front thickness is reset to zero. If the infiltration rate exceeds the Reynolds number for the start of turbulence, the local hydraulic conductivity is updated using the local Reynolds number:

$$
K_{i,j} = K_{lam} \sqrt{\frac{\mathrm{Re}_{crit}}{\max(\mathrm{Re}_{i,j}, \mathrm{Re}_{crit})}}
$$

(B.15)

XBeach iterates until a minimum threshold difference between iterations is found for Equation (B.14) and (B.15). Infiltration in one time step is limited to the amount of surface water available in the cell and to the amount of water required to raise the groundwater level to the level of the bed:

$$
S_{inf,i,j}^n = \min\left(S_{inf,i,j}^n, \frac{\eta_{i,j} - z_{b,i,j}}{\Delta t}, \frac{z_{b,i,j} - \eta_{gw,i,j-}}{n_p \Delta t} \right)
$$

(B.16)

If during infiltration the groundwater level reaches the bed level, the fraction of the time step required to do so is estimated [see (B.17)] and the remaining fraction is used in the submarine exchange.

$$\Lambda_{t,i,j} = \frac{n_p \left(z_{b,i,j} - \eta_{gw,i,j} \right)}{K_{i,j} \left(\dfrac{1}{\rho g} \dfrac{p_{i,j} \big|^{z=\xi}}{z_{b,i,j} - \eta_{gw,i,j}} + 1 \right)} \frac{1}{\Delta t}$$

(B.17)

$$0 \le \Lambda_{t,i,j} \le 1$$

Exfiltration is calculated in cells where the groundwater and surface water are not connected and the groundwater level exceeds the bed level:

$$S_{exf,i,j} = n_p \frac{z_{b,i,j} - \eta_{gw,i,j}}{\Delta t}$$

(B.18)

Horizontal infiltration and exfiltration (keyword: *gwhorinfil = 1*) is computed across the numerical vertical interface between the groundwater domain and the surface water domain in adjoining cells. The direction of exchange is determined by the head gradient, and the bed level slope direction:

$$S_{i,j,hor}^u = \begin{cases} K_{i,j}^u \left(\dfrac{\eta_{i,j} + \dfrac{q_{i,j}}{g} - H_{gw,i+1,j}}{\Delta x} \right) \left(z_{b,i+1,j} - z_{b,i,j} \right) & z_{b,i+1,j} > z_{b,i,j} \wedge \eta_{i,j} > eps \\[4ex] K_{i,j}^u \left(\dfrac{\eta_{i+1,j} + \dfrac{q_{i+1,j}}{g} - H_{gw,i,j}}{\Delta x} \right) \left(z_{b,i,j} - z_{b,i+1,j} \right) & z_{b,i+1,j} < z_{b,i,j} \wedge \eta_{i+1,j} > eps \end{cases}$$

(B.19)

$$S_{i,j,hor}^v = \begin{cases} K_{i,j}^v \left(\dfrac{\eta_{i,j} + \dfrac{q_{i,j}}{g} - H_{gw,i,j+1}}{\Delta y} \right) \left(z_{b,i,j+1} - z_{b,i,j} \right) & z_{b,i,j+1} > z_{b,i,j} \wedge \eta_{i,j} > eps \\[4ex] K_{i,j}^v \left(\dfrac{\eta_{i,j+1} + \dfrac{q_{i,j+1}}{g} - H_{gw,i,j}}{\Delta y} \right) \left(z_{b,i,j} - z_{b,i,j+1} \right) & z_{b,i,j+1} < z_{b,i,j} \wedge \eta_{i,j+1} > eps \end{cases}$$

After infiltration and exfiltration have been calculated, the groundwater level and surface water level are updated:

$$\eta_{gw,i,j}^{n+\frac{1}{2}} = \eta_{gw,i,j}^n + \frac{\Delta t}{n_p} \left(S_{\inf} + S_{exf} + S_{hor} \right)$$

(B.20)

$$\eta_{i,j}^{n+\frac{1}{2}} = \eta_{i,j}^n + \Delta t \left(-S_{\inf} - S_{exf} - S_{hor} \right)$$

Whether the surface water and groundwater are connected or unconnected

The cell height at the center of the groundwater cells ($\Delta z_{H,i,j}$) is calculated from the groundwater level and the bottom of the aquifer in the center of the cell, whereas the cell heights at the horizontal cell interfaces are calculated using an upwind procedure:

$$\Delta z_{H,i,j} = \eta_{gw,\text{i,j}} - z_{aquifer,i,j} = h_{gw,i,j}$$

$$\Delta z_{\text{u},i,j} = \begin{cases} \Delta z_{H,i+1,j} & \text{if } q^x_{qw,i,j} < 0 \\ \Delta z_{H,i,j} & \text{if } q^x_{qw,i,j} \geq 0 \end{cases}$$

$$\Delta z_{\text{v},i,j} = \begin{cases} \Delta z_{H,i+1,j} & \text{if } q^y_{qw,i,j} < 0 \\ \Delta z_{H,i,j} & \text{if } q^y_{qw,i,j} \geq 0 \end{cases}$$

(B.21)

In (B.21) $z_{aquifer}$ is the level of the bottom of the aquifer. As described in Section 3.3.6, the head applied on the top boundary of the groundwater domain (H_{bc}) depends on whether the groundwater and surface water are connected or unconnected:

$$H_{\text{bc,i,j}} = \left(1 - \kappa_{r,i,j}\right)\eta_{gw,i,j} + \kappa_{r,i,j}\left(z_{b,i,j} + \frac{p_{i,j}\big|^{z=z_b}}{\rho g}\right)$$

$$\kappa_{r,i,j} = 1 - \frac{z_{b,i,j} - \eta_{gw,i,j}}{\varepsilon} \quad \text{with} \quad 0 \leq \kappa_{r,i,j} \leq 1$$

(B.22)

In (B.22) the parameter κ_r is the relative numerical 'connectedness' of the groundwater and surface water head, determined by linear interpolation across the numerical smoothing constant ε.

In the case of hydrostatic groundwater flow, the groundwater head in each cell is set equal to the head applied on the top boundary of the groundwater domain (H_{bc}) and the horizontal groundwater flux is computed from the groundwater head gradient:

$$q^x_{gw,i,j} = -K_{u,i,j}\Delta z_{u,i}\frac{H_{i+1,j} - H_{i,j}}{\Delta x_{u,i,j}} = -K_{u,i,j}\Delta z_{u,i}\frac{H_{bc,i+1,j} - H_{bc,i,j}}{\Delta x_{u,i,j}}$$

$$q^y_{gw,i,j} = -K_{v,i,j}\Delta z_{v,i}\frac{H_{i+1,j} - H_{i,j}}{\Delta y_{v,i,j}} = -K_{v,i,j}\Delta z_{v,i}\frac{H_{bc,i+1,j} - H_{bc,i,j}}{\Delta y_{v,i,j}}$$

(B.23)

In (B.23) the superscripts x and y refer to the components of the variable in the cross-shore and longshore direction, respectively, and the subscripts u and v refer to variables approximated at the horizontal cell interfaces in the cross-shore and longshore direction, respectively.

In the case of non-hydrostatic groundwater flow, the horizontal specific discharge on each cell interface can be found through an approximation of the non-hydrostatic groundwater head gradient:

$$q^x_{gw,i,j} = -K_{u,i,j}\Delta z_{u,i}\frac{H_{i+1,j} - H_{i,j}}{\Delta x_{u,i,j}} = -K_{u,i,j}\Delta z_{u,i}\frac{H_{bc,i+1,j} - \frac{2}{3}\beta_{i+1,j}\Delta z^2_{H,i+1,j} - H_{bc,i,j} + \frac{2}{3}\beta_{i,j}\Delta z^2_{H,i,j}}{\Delta x_{u,i,j}}$$

$$q^y_{gw,i,j} = -K_{v,i,j}\Delta z_{v,i}\frac{H_{i+1,j} - H_{i,j}}{\Delta y_{v,i,j}} = -K_{v,i,j}\Delta z_{v,i}\frac{H_{bc,i+1,j} - \frac{2}{3}\beta_{i+1,j}\Delta z^2_{H,i+1,j} - H_{bc,i,j} + \frac{2}{3}\beta_{i,j}\Delta z^2_{H,i,j}}{\Delta y_{v,i,j}}$$

(B.24)

In (B.24) the subscript *H* refers to variables approximated at the cell centers. The hydraulic conductivity may be different at each cell interface and is therefore computed at every interface where every *K* is calculated separately.

Continuity in the groundwater cell is found following:

$$q^x_{gw,i-1,j} - q^x_{gw,i,j} + q^y_{gw,i,j-1} - q^y_{gw,i,j} - q^z_{gw,i,j} = 0 \qquad \text{(B.25)}$$

In (B.25) the variable q^z refers to the vertical groundwater discharge (e.g., submarine exchange if connected to the surface water, or groundwater level fluctuations if the groundwater is not connected to the surface water).

In the case of hydrostatic groundwater flow, the variable q^z can be solved through the known variables q^x and q^y. However, in the case of non-hydrostatic groundwater flow, all variables in Equation (B.25) contain an unknown value for the groundwater pressure head, described in terms of a known head at the surface of the groundwater (H_{bc}) and the unknown curvature of the vertical groundwater head function (β). Since water is incompressible, the groundwater pressure must be solved for all cells simultaneously using matrix algebra:

$$Ax + b = 0 \qquad \text{(B.26)}$$

In (B.26) *A* is a matrix containing coefficients for the horizontal and vertical specific discharge, *x* is a vector containing the unknown groundwater head curvature, and b contains the known forcing terms. For a one dimensional cross-shore case, A is reduced to a tridiagonal matrix. The vector of known forcing consists of the numerical gradients in the contribution of the head applied on the top boundary of the groundwater domain to the horizontal specific discharge.

In the one dimensional case, the solution to the tridiagonal matrix A can be computed using the efficient Thomas algorithm (Thomas 1949). In the two dimensional case, matrix A contains two additional diagonals that are not placed along the main diagonal, and vector b contains additional forcing terms from the alongshore contribution. The solution to the two dimensional case requires a more complex and less computationally efficient matrix solver. In this case the Strongly Implicit Procedure (Stone 1968) is used in a manner similar to Zijlema et al. (2011).

Since in both hydrostatic and non-hydrostatic groundwater flow some local velocities may exceed the critical Reynolds number for the start of turbulence (Re_{crit}), the turbulent hydraulic conductivity (*K*) is updated using the local Reynolds number. The solution to (B.15) and the update of the turbulent hydraulic conductivity are iterated until a minimum threshold difference between iterations is found. Note that this approach is only used is the turbulent groundwater model is selected (keyword: *gwscheme* = *turbulent*).

The (iterated) solution for the specific vertical discharge is used to update the groundwater level and surface water level:

$$\eta_{gw,i,j}^{n+\frac{1}{2}} = \eta_{gw,i,j}^{n} + \frac{\Delta t}{n_p}\left(S_{\text{inf}} + S_{exf} + S_{hor}\right)$$

$$\eta_{i,j}^{n+\frac{1}{2}} = \eta_{i,j}^{n} + \Delta t\left(-S_{\text{inf}} - S_{exf} - S_{hor}\right)$$

(B.27)

If the groundwater and surface water are connected, and the submarine exchange from the surface water to the groundwater estimated in (B.27) is greater than the amount of surface water available in the cell, continuity is enforced by lowering the groundwater level to compensate for the lack of permeating water:

$$\eta_{gw,i,j}^{n+1} = \eta_{gw,i,j}^{n+1} + \frac{1}{n_p}\left(\eta_{i,j}^{n+\frac{1}{2}} - z_{b,i,j} - \Delta t\frac{q_{i,j}^z}{\Delta x_{H,i,j}}\right) \text{ if } \kappa_{i,j} \wedge \eta_{i,j}^{n+\frac{1}{2}} - z_{b,i,j} < \Delta t\frac{q_{i,j}^z}{\Delta x_{H,i,j}}$$

(B.28)

B.4 Sediment transport

The advection-diffusion equation for suspended sediment is the basis for the sediment transport computations in XBeach. The partial differential equation to solve is:

$$\frac{\partial hC}{\partial t} + \nabla\vec{S}_s = \frac{hC_{eq} - hC}{T_s} = -\frac{hC}{T_s} + ERO$$

(B.29)

Here C is the depth-averaged concentration, C_{eq} the equilibrium concentration, T_s a typical timescale proportional to water depth divided by fall velocity. As is often done to increase robustness, we treat the erosion term explicitly but taking an implicit scheme for the sedimentation term:

$$\frac{C_z^{i,j,n+1}h_h^{i,j,n+1} - h_h^{i,j,n}C_z^{i,j,n}}{\Delta t} = -\frac{h_h^{i,j,n+1}C_z^{i,j,n+1}}{T_s^{i,j}} - \left(\nabla\vec{S}_s\right)^{i,j,n} + ERO^{i,j,n}$$

(B.30)

This can be rewritten as:

$$C_z^{i,j,n+1} = \frac{T_s^{i,j}\Delta t}{h_h^{i,j,n+1}\left(T_s^{i,j} + \Delta t\right)}\left(\frac{h_h^{i,j,n}C_z^{i,j,n}}{\Delta t} - \left(\nabla\vec{S}_s\right)^{i,j,n} + ERO^{i,j,n}\right)$$

(B.31)

The sediment transport gradient is discretized in a similar way as the mass balance:

$$\left(\nabla\vec{S}_s\right)^{i,j} = \frac{\left(S_{u,s}^{i,j}\Delta n_u^{i,j} - S_{u,s}^{i-1,j}\Delta n_u^{i-1,j} + S_{v,s}^{i,j}\Delta s_v^{i,j} - S_{v,s}^{i,j-1}\Delta s_v^{i,j-1}\right)}{A_z^{i,j}}$$

(B.32)

The sediment transports in the u- points contain an advective term, a diffusive term and a bed slope term:

$$S_{u,s} = C_u u_{rep,s} h_u - D_c h_u \frac{\partial C}{\partial s} - f_{slope} C_u \left| v \right|_u h_u \frac{\partial z_b}{\partial s})$$ (B.33)

Here $u_{rep,s}$ is a representative velocity for suspended transport, which contains contributions due to return flow, wave skewness and wave asymmetry; D_c is a horizontal diffusion coefficient and f_{slope} a coefficient for the bed slope. In discretized form the expression for the suspended transport in the u-point is:

$$S_{u,s}^{i,j} = C_u^{i,j} u_{rep,srep,s}^{i,j} h_u^{i,j} - D_c^{i,j} h_u^{i,j} \frac{c_c^{i+1,j} - c_c^{i,j}}{\Delta s_u^{i,j}} - f_{slope} C_u^{i,j} \left| v \right|_u^{i,j} h_u^{i,j} \frac{z_b^{i+1,j} - z_b^{i,j}}{\Delta s_u^{i,j}})$$ (B.34)

The concentrations in the u-points are computed with a θ-method, where $\theta = 1$ means a fully upwind approximation, and $\theta = 0.5$ a central scheme. In practice, we mostly use the upwind approximation for its robustness.

$$\begin{aligned}
C_u^{i,j} &= \theta C_z^{i,j} + (1-\theta) C_z^{i+1,j} \quad, u_{rep,s}^{i,j} > 0 \\
C_u^{i,j} &= (1-\theta) C_z^{i,j} + \theta C_z^{i+1,j} \quad, u_{rep,s}^{i,j} < 0
\end{aligned}$$ (B.35)

The erosion and deposition terms, which may also be used in the bed updating, are finally computed from:

$$\begin{aligned}
ERO^{i,j,n} &= h_h^{i,j,n} C_{eq}^{i,j,n} / T_s^{i,j} \\
DEPO^{i,j} &= h_h^{i,j,n+1} C_z^{i,j,n+1} / T_s^{i,j}
\end{aligned}$$ (B.36)

The evaluation of the bed load transport takes place in the same way as in the previous versions of XBeach, except for the fact that the directions are taken in local grid direction, and will not be repeated here.

B.5 Bottom updating schemes

Two alternative formulations are available for the bed updating: one where the bottom changes are computed based on the gradients of suspended and bed load transport, and one where the changes due to suspended transport are accounted for through the erosion and deposition terms [see (B.37)].

$$\begin{aligned}
(1-n_p) \frac{\partial z_b}{\partial t} + MF (\nabla \vec{S}_s + \nabla \vec{S}_b) &= 0a \\
(1-n_p) \frac{\partial z_b}{\partial t} + MF (ERO - DEPO + \nabla \vec{S}_b) &= 0
\end{aligned}$$ (B.37)

In both cases *MF* is the morphological factor used to accelerate morphological changes. In the first case, the sediment in the bottom is conserved in all cases, but changes in the amount of sediment in the water are not considered; one can also say that the sediment in suspension is added to the bottom sediment. In the second case, the storage of sediment in the water is accounted for, but will be distorted in cases of high *MF*. Since under most circumstances the real effect of the storage in the water phase is small we prefer the first

formulation which guarantees mass conservation in the bottom. Both formulations are calculated using an explicit scheme, see also (B.38).

$$
\Delta z_b^{\,i,j,n+1} = \Delta t \frac{MF}{\left(1-n_p\right)} \left(\left(\nabla \vec{S}_s\right)^{i,j,n} + \left(\nabla \vec{S}_b\right)^{i,j,n} \right)
$$

$$
\Delta z_b^{\,i,j,n+1} = \Delta t \frac{MF}{(1-n_p)} \left(ERO^{i,j,n} - DEPO^{i,j,n} + \left(\nabla \vec{S}_b\right)^{i,j,n} \right)
$$

(B.38)

B.5.1 Avalanching
XBeach implements avalanching as described in Section 2.8.2. It first calculates bed level change due to avalanching in the cross-shore dimension. It then calculates the slopes in alongshore direction and bottom change due to avalanching in this direction. To avoid disrupted sediment balance XBeach does not calculate bottom change due to avalanching at the boundary grid cells. Consequently XBeach cannot calculate avalanching at the lateral boundary.

B.5.2 Bed composition
The bed is discretized into layers with mass *M(i,j)* in which *i* refers to the layer number and *j* to the sediment class. The mass fraction per sediment class *p*, layer thickness *Δ* and bed level z_b are defined by:

$$
p(i,j) = \frac{M(i,j)}{\displaystyle\sum_{j=1}^{J} M(i,j)}
$$

$$
\Delta(i) = \frac{1}{\left(1-n_p\right)\rho_s} \sum_{j=1}^{J} M(i,j)
$$

(B.39)

$$
z_b = z_0 + \sum_{i=1}^{I} \Delta(i)
$$

with porosity n_p and sediment density ρ. The level z_0 is the lowest point of the array of bed layers.

Due to bed load transport, sediment is exchanged between the top layer and the four horizontally neighboring top layers. Exchange with the water column and the top layer is due to erosion rate *E* and deposition rate *D*. A mixed Eulerian/Lagrangian framework is proposed. Within the set of layers, one layer is defined as the variable layer. This is the only layer that has a variable total mass. All other layers have a constant total mass, which implies for a constant porosity a constant thickness. Above the variable layer, the layers move with the bed level (Lagrangian): upwards in case of aggradation and downwards in case of degradation. This vertical movement gives an advective flux with advection velocity equal to the bed level change *A=dz/dt*. The variable layer is the transition to the lower layers, which are passive. The number of layers below the variable layer has thus no influence on the computation time. Note that diffusive processes within the bed are not considered yet. These could lead to fluxes between the layers below the variable layer.

The mass balance for the top layer can now be defined by:

$$\frac{\partial M(1,j)}{\partial t} = dy\{p(1,j)S_b(j)\}_W - dy\{p(1,j)S_b(j)\}_E$$
$$dx\{p(1,j)S_b(j)\}_S - dx\{p(1,j)S_b(j)\}_N$$
$$- dxdyp(1,j)E(j) + dxdyD(j) + dxdy\delta Ap_{bot}(1,j) \qquad \text{(B.40)}$$

$$A = \sum_{j=1}^{J} \left\{ \begin{array}{c} dy\{p(1,j)S_b(j)\}_W - dy\{p(1,j)S_b(j)\}_E \\ dx\{p(1,j)S_b(j)\}_S - dx\{p(1,j)S_b(j)\}_N \\ - dxdyp(1,j)E(j) + dxdyD(j) \end{array} \right\}$$

in which S_b is the bed-load transport (e.g. Meyer-Peter-Muller), based on the sediment properties of the specific class. The dimensions of the grid cell are defined by *dx* and *dy*. The subscripts W, E, S and N refer to West, East, South and North indicating the four vertical faces of the bed cell. The horizontal faces are indicated with bot for the bottom of the cell and ceil for the ceiling of the cell. As the fraction p is not defined at the faces but in the cell centers, the upstream fraction is required. For the bed load fluxes, the velocity direction used. For the vertical advection term, the upstream value is based on the bed level variation: in case of aggradation the value in the top layer is used and in case of degradation the value of the second layer is used. If the top layer is the variable layer, there is no advective flux: *δ=0* otherwise *δ=1*.

The mass balance for the layers in between the top layer and the variable layer is:

$$\frac{\partial M(i,j)}{\partial t} = dxdyA\left(p_{bot}(i,j) - p_{ceil}(i,j)\right) \qquad \text{(B.41)}$$

and for the variable layer, it reads:

$$\frac{\partial M(i,j)}{\partial t} = Ap_{ceil}(i,j) \qquad \text{(B.42)}$$

In order to avoid a variable layer which is too thin a or too thick, the variable layer is merged or split. If the thickness is smaller than the critical value Δ_{merge}, the variable layer is merged with the lower layer. To keep the same number of cells, a cell is added at the bottom of the array, implying that $z_0 = z_0 - \Delta$. Similarly, the variable is split into two layers if the critical value Δ_{split} is exceeded. Then, the array is shifted upwards: $z_0 = z_0 + \Delta$.

As the bed level update is explicit, the time step is limited. A conservative estimate can be made by assuming that no more mass can be eroded than available in the top layer:

$$dy\{p(1,j)S_b(j)\}_{W/E} + dx\{p(1,j)S_b(j)\}_{S/N} + dxdyp(1,j)E(j) < \frac{M(1,j)}{dt}$$

$$dt < \frac{dxdy\left(1-n_p\right)\rho_s\Delta(1)}{dyS_{b,W/E}(1) + dyS_{b,N/S}(1) + dxdyE(1)} \qquad \text{(B.43)}$$

The transport rate depends on the direction of the transport. The transport rates and erosion rates should be based on the formulation for the smallest fraction: $j=1$. Note that the fraction p falls out. This time step restriction is less severe than the one for shallow water flow. Only in case of very top layers and/or the use of a morphological factor, this time step restriction might be relevant.

B.6 Boundary conditions

At the start of the XBeach simulation, XBeach checks whether non-stationary varying wave boundary conditions are to be used. If this is the case, it next checks whether the wave spectrum of the wave boundary conditions is to change over time, or remain constant. If the wave spectrum is to remain constant, XBeach will only read from one input file to generate wave boundary conditions. If the wave spectrum is to vary in time, XBeach reads from multiple files.

Whether or not the wave spectrum of the boundary conditions changes over time, the XBeach module requires a record length during which the current wave spectral parameters are applied. For the duration of the record length, boundary conditions are calculated at every boundary condition file time step. These time steps are not required to be the same as the time steps in the XBeach main program; XBeach will interpolate where necessary. The boundary condition time steps should therefore only be small enough to accurately describe the incoming bound long waves. The statistical data for the generation of the wave boundary conditions is read from user-specified files. The XBeach module tapers the beginning and end of the boundary condition file. This is done to ensure smooth transitions from one boundary condition file to the next.

The combination of a large record length and a small time step lead to large demands on the system memory. If the memory requirement is too large XBeach will shut down. The user must choose to either enlarge the boundary condition time step, or to reduce the record length. In case of the latter, several boundary condition files can be generated and read sequentially. It is unwise however to reduce the record length too much, as then the transitions between the boundary condition files may affect the model results.

Every time the XBeach wave boundary condition module is run, it outputs data to the local directory. Metadata about the wave boundary conditions are stored in list files: *ebcflist.bcf* and *qbcflist.bcf*. The main XBeach program uses the list files to know how and when to read and generate boundary condition files. The actual incoming short-wave energy and long-wave mass flux data is stored in other files. These files have $E\_$ and $q\_$ prefixes. The main XBeach program uses these files for the actual forcing along the offshore edge.

B.7 Non-hydrostatic

B.7.1 Global continuity equation
The global continuity equation, which describes the relation between the free surface and the depth averaged discharge, is given by

$$\frac{\partial \eta}{\partial t} + \frac{\partial}{\partial x}(UH) + \frac{\partial}{\partial x}(VH) = 0 \tag{B.44}$$

In which U is the depth averaged velocity vector in x, V in y, H the water depth. A simple semi-discretization of (B.44) using central differences for the space derivative and using the Hansen scheme for the coupling between velocity and free surface results in:

$$\frac{\eta_{i,j}^* - \eta_{i,j}^n}{\Delta t} + \frac{{}^x q_{i+\frac{1}{2},j}^* - {}^x q_{i-\frac{1}{2},j}^*}{\Delta x} + \frac{{}^y q_{i,j+\frac{1}{2}}^* - {}^y q_{i,j-\frac{1}{2}}^*}{\Delta y} = 0 \tag{B.45}$$

With ${}^x q_{i+\frac{1}{2},j}^* = H_{i+\frac{1}{2},j}^n U_{i+\frac{1}{2},j}^{n+\frac{1}{2}}$, ${}^y q_{i,j+\frac{1}{2}}^* = H_{i,j+\frac{1}{2}}^n V_{i,j+\frac{1}{2}}^{n+\frac{1}{2}}$ and the water depth is defined by a first order accurate upwind interpolation:

$$H_{i+\frac{1}{2},j}^n = \begin{cases} \zeta_{i,j}^n + d_{i,j} & if \ U_{i+\frac{1}{2},j}^{n+\frac{1}{2}} > 0 \\ \zeta_{i+1,j}^n + d_{i+1,j} & if \ U_{i+\frac{1}{2},j}^{n+\frac{1}{2}} < 0 \\ \max\left(\zeta_{i,j}^n, \zeta_{i+1,j}^n\right) + \min\left(d_i, d_{i+1,j}\right) & if \ U_{i+\frac{1}{2},j}^{n+\frac{1}{2}} = 0 \end{cases} \tag{B.46}$$

The resulting scheme is only first order accurate by virtue of the upwind interpolations and mass conservative. When first order computations are considered accurate enough $\eta_{i,j}^{n+1}$ is set to $\eta_{i,j}^{n*}$. For higher order accuracy the first order prediction is corrected using a limited version of the McCormack scheme. The corrector step reads:

$$\frac{\eta_{i,j}^{n+1} - \eta_{i,j}^*}{\Delta t} + \frac{{}^x \Delta q_{i+\frac{1}{2},j}^* - {}^x \Delta q_{i-\frac{1}{2},j}^*}{\Delta x} + \frac{{}^y \Delta q_{i,j+\frac{1}{2}}^* - {}^y \Delta q_{i,j-\frac{1}{2}}^*}{\Delta y} = 0 \tag{B.47}$$

With ${}^x \Delta q_{i+\frac{1}{2},j}^{n*} = U_{i+\frac{1}{2},j}^{n+\frac{1}{2}} \Delta H_{i+\frac{1}{2},j}$ and $\Delta H_{i+\frac{1}{2},j}$ is given for positive flow as:

$$\Delta H_{i+\frac{1}{2},j}^{n*} = \tfrac{1}{2} \psi \left({}^\zeta r_{i+\frac{1}{2}}\right)\left(\zeta_{i+1,j}^{n*} - \zeta_{i,j}^n\right)$$

$$\zeta_{r_{i+\frac{1}{2}}} = \frac{\zeta_{i,j}^{n*} - \zeta_{i-1,j}^n}{\zeta_{i+1,j}^{n*} - \zeta_{i,j}^n} \tag{B.48}$$

$$\psi(r) = \max\left(0, \min(r,1)\right)$$

Here $\psi(r)$ denotes the minmod limiter. Similar expression can be constructed for negative flow. The expression for $^{y}\Delta q^{n*}_{i,j+\frac{1}{2}}$ and $\Delta H_{i,j+\frac{1}{2}}$ are obtained in a similar manner. Note that the total flux $^{x}q^{n+\frac{1}{2}}_{i+\frac{1}{2},j}$ at the cell boundaries thus reads

$$
\begin{aligned}
^{x}q^{n+\frac{1}{2}}_{i+\frac{1}{2},j} &= {}^{x}q^{*}_{i+\frac{1}{2},j} + {}^{x}\Delta q^{*}_{i+\frac{1}{2},j} \\
^{y}q^{n+\frac{1}{2}}_{i,j+\frac{1}{2}} &= {}^{y}q^{*}_{i,j+\frac{1}{2}} + {}^{y}\Delta q^{*}_{i,j+\frac{1}{2}}
\end{aligned}
\tag{B.49}
$$

The predictor-corrector set is second order accurate in regions where the solution is smooth, and reduces locally to first order accuracy near discontinuities. Furthermore, the method remains mass conservative. Note that other flux limiters can be used instead of the minmod limiter. However, as the minmod limiter performed adequately, this has not been investigated. (for an overview of flux limiters see Hirsch, 2007)

B.7.2 Local continuity equation

The depth averaged local continuity equation is given by

$$
\frac{\partial HU}{\partial x} + \frac{\partial HV}{\partial y} + w\Big|_{z=\eta} - u\frac{\partial z}{\partial x}\Big|_{z=-\zeta} - v\frac{\partial z}{\partial y}\Big|_{z=-\zeta} = 0
\tag{B.50}
$$

This equation is discretized using central differences

$$
\begin{aligned}
&\frac{H^{n+1}_{i+\frac{1}{2},j}U^{n+1\frac{1}{2}}_{i+\frac{1}{2},j} - H^{n+1}_{i-\frac{1}{2},j}U^{n+1\frac{1}{2}}_{i-\frac{1}{2},j}}{\Delta x} + \frac{H^{n+1}_{i+\frac{1}{2},j}V^{n+1\frac{1}{2}}_{i,j+\frac{1}{2}} - H^{n+1}_{i,j-\frac{1}{2}}V^{n+1\frac{1}{2}}_{i,j-\frac{1}{2}}}{\Delta y} + w^{n+1\frac{1}{2}}_{i,j,s} \\
&-\overline{U}^{n+1\frac{1}{2}}_{i,j}\frac{\eta^{n+1}_{i+\frac{1}{2},j} - \eta^{n+1}_{i-\frac{1}{2},j}}{\Delta x} - \overline{V}^{n+1\frac{1}{2}}_{i,j}\frac{\eta^{n+1}_{i,j+\frac{1}{2}} - \eta^{n+1}_{i,j-\frac{1}{2}}}{\Delta x} = 0
\end{aligned}
\tag{B.51}
$$

Missing grid variables $\eta^{n+1}_{i+\frac{1}{2},j}, \eta^{n+1}_{i,j+\frac{1}{2}}$ are approximated with upwind interpolation. Because there is no separate time evolution equation for the pressure the local continuity equation will be used to setup a discrete set of poison type equations in which the pressures are the only unknown quantities.

B.7.3 Horizontal Momentum

To obtain a conservative discretization of the momentum equation the approach from Stelling and Duinmeijer (2003) is followed. However, to improve the accuracy of the method the combined space-time discretization of the advection is done using a variant of the MacCormack (1969) is used. This scheme consists of a first order predictor step and a flux limited corrector step. The hydrostatic pressure is integrated using the midpoint rule and central differences, while the source terms and the turbulent stresses are integrated using an explicit Euler time integration. Formally the time integration is therefore first order accurate, but in regions where the turbulent stresses are negligible the scheme is of almost second order accuracy.

The depth averaged horizontal momentum equation for HU is given by

$$\frac{\partial}{\partial t}\left(HU\right)+\frac{\partial}{\partial x}\left(HU^2+\tfrac{1}{2}gH^2+H\overline{p}-\tau_{xx}\right)+\frac{\partial}{\partial y}\left(HUV-\tau_{yx}\right)=gH\frac{\partial d}{\partial x}-p\frac{\partial d}{\partial x}+S_x \quad \text{(B.52)}$$

A first order accurate predictor step in time and space is then given as:

$$\frac{\left(HU\right)^{*}_{i+\frac{1}{2},j}-\left(HU\right)^{n+\frac{1}{2}}_{i+\frac{1}{2},j}}{\Delta t}+\frac{{}^{x}\overline{q}^{n+\frac{1}{2}}_{i+1,j}U^{n+\frac{1}{2}}_{i+1,j}-{}^{x}\overline{q}^{n+\frac{1}{2}}_{i,j}U^{n+\frac{1}{2}}_{i,j}}{\Delta x}+\frac{{}^{y}\overline{q}^{n+\frac{1}{2}}_{i+\frac{1}{2},j+\frac{1}{2}}U^{n+\frac{1}{2}}_{i+\frac{1}{2},j+\frac{1}{2}}-{}^{y}\overline{q}^{n+\frac{1}{2}}_{i+\frac{1}{2},j-\frac{1}{2}}U^{n+\frac{1}{2}}_{i+\frac{1}{2},j-\frac{1}{2}}}{\Delta y}$$
$$+g\frac{\left(H^2\right)^{n+1}_{i+1,j}-\left(H^2\right)^{n+1}_{i,j}}{2\Delta x}=g\overline{H}^{n}_{i+\frac{1}{2},j}\frac{d_{i+\frac{1}{2},j}-d_{i-\frac{1}{2},j}}{\Delta x}+{}^{x}\mathrm{Pr}^{n+\frac{1}{2}}_{i+\frac{1}{2},j}+{}^{x}S^{n+\frac{1}{2}}_{i+\frac{1}{2},j}+{}^{x}T^{n+\frac{1}{2}}_{i+\frac{1}{2},j} \quad \text{(B.53)}$$

Here *Pr* represents a discretization of the dynamic pressure; *T* the effect of (turbulent) viscosity and *S* includes all other source terms. The discretization of the (turbulent) viscous terms is given by central differences:

$$
{}^{x}T^{n+\frac{1}{2}}_{i+\frac{1}{2},j}=\frac{2}{\Delta x_{i+\frac{1}{2}}}\left[v^{n}_{i+1,j}H^{n+1}_{i+1,j}\frac{U^{n+\frac{1}{2}}_{i+1\frac{1}{2},j}-U^{n+\frac{1}{2}}_{i+\frac{1}{2},j}}{\Delta x_{i+1}}-v^{n}_{i,j}H^{n+1}_{i,j}\frac{U^{n+\frac{1}{2}}_{i+\frac{1}{2},j}-U^{n+\frac{1}{2}}_{i-\frac{1}{2},j}}{\Delta x_{i}}\right]
$$
$$
+\frac{1}{\Delta y_{i}}\left[\overline{v}^{n+\frac{1}{2}}_{i+\frac{1}{2},j+\frac{1}{2}}\overline{\overline{H}}^{n+\frac{1}{2}}_{i+\frac{1}{2},j+\frac{1}{2}}\frac{U^{n+1}_{i+\frac{1}{2},j+1}-U^{n+\frac{1}{2}}_{i+\frac{1}{2},j}}{\Delta y_{i+\frac{1}{2}}}-\overline{v}^{n+\frac{1}{2}}_{i+\frac{1}{2},j-\frac{1}{2}}\overline{\overline{H}}^{n+1}_{i+\frac{1}{2},j-\frac{1}{2}}\frac{U^{n+\frac{1}{2}}_{i+\frac{1}{2},j}-U^{n+\frac{1}{2}}_{i+\frac{1}{2},j-1}}{\Delta y_{i-\frac{1}{2}}}\right] \quad \text{(B.54)}
$$
$$
+\frac{1}{\Delta y_{i}}\left[\overline{v}^{n+\frac{1}{2}}_{i+\frac{1}{2},j+\frac{1}{2}}\overline{\overline{H}}^{n+\frac{1}{2}}_{i+\frac{1}{2},j+\frac{1}{2}}\frac{V^{n+1}_{i+1,j+\frac{1}{2}}-V^{n+\frac{1}{2}}_{i,j+\frac{1}{2}}}{\Delta x_{i+\frac{1}{2}}}-\overline{v}^{n+\frac{1}{2}}_{i+\frac{1}{2},j-\frac{1}{2}}\overline{\overline{H}}^{n+1}_{i+\frac{1}{2},j-\frac{1}{2}}\frac{V^{n+\frac{1}{2}}_{i+1,j-\frac{1}{2}}-V^{n+\frac{1}{2}}_{i,j-\frac{1}{2}}}{\Delta x_{i+\frac{1}{2}}}\right]
$$

Here $\overline{\overline{v}}^{n+\frac{1}{2}}_{i+\frac{1}{2},j+1}$ and $\overline{\overline{H}}^{n+\frac{1}{2}}_{i+\frac{1}{2},j+1\frac{1}{2}}$ are obtained from the surrounding points by simple linear interpolation.

Due to the incompressible flow assumption the dynamic pressure does not have a separate time evolution equation, but instead it satisfies an elliptical equation in space. As such its effect cannot be calculated explicitly using values at the previous time level. However to improve the accuracy of the predictor step the effect of the dynamic pressure is included explicitly. To do this first the unknown pressure is decomposed as:

$$p^{n+1\frac{1}{2}}_{i,j}=p^{n+\frac{1}{2}}_{i,j}+\Delta p^{n+1\frac{1}{2}}_{i,j} \quad \text{(B.55)}$$

where the difference in pressure $\Delta p^{n+1\frac{1}{2}}_{i,j}$ is generally small. In the predictor step the effect of the pressure is included explicitly using $p^{n+\frac{1}{2}}_{i,j}$. In the corrector step the full Poisson equation is then solved for $\Delta p^{n+1\frac{1}{2}}_{i,j}$. The pressure term in the predictor step is thus given as:

$$
{}^{x}\mathrm{Pr}^{n+\frac{1}{2}}_{i+\frac{1}{2},j}=\frac{H^{n+1}_{i+1,j}\overline{p}^{n+\frac{1}{2}}_{i+1,j}-H^{n+1}_{i,j}\overline{p}^{n+\frac{1}{2}}_{i,j}}{\Delta x}-p^{n+\frac{1}{2}}_{i+\frac{1}{2},j}\frac{d_{i+\frac{1}{2},j}-d_{i-\frac{1}{2},j}}{\Delta x}=\frac{\left(\eta^{n+1}_{i+1,j}+d^{n+1}_{i,j}\right)p^{n+\frac{1}{2}}_{i+1,j}-\left(\eta^{n+1}_{i,j}-d^{n+1}_{i+1,j}\right)p^{n+\frac{1}{2}}_{i,j}}{2\Delta x}
$$
$$\text{(B.56)}$$

Here $\bar{p}_{i+1,j}^{n+\frac{1}{2}}$ represents the average pressure over the vertical which is approximated with $\bar{p}_{i+1,j}^{n+\frac{1}{2}} = \frac{1}{2} p_{i+1,j}^{n+\frac{1}{2}}$, in which $p_{i+1,j}^{n+\frac{1}{2}}$ is the pressure at the bottom. Furthermore $p_{i+\frac{1}{2},j}^{n+\frac{1}{2}}$ is given as $p_{i+\frac{1}{2},j}^{n+\frac{1}{2}} = \frac{1}{2}\left(p_{i+1,j}^{n+\frac{1}{2}} + p_{i,j}^{n+\frac{1}{2}}\right)$.

Currently (B.54) is formulated with the depth integrated momentum as the primitive variable, and not the depth averaged velocity. To reformulate (B.54) in terms of U we use the method by Stelling and Duinmeijer (2003). First note that $\left(HU\right)_{i+\frac{1}{2},j}^{n+\frac{1}{2}}$ and $\left(HU\right)_{i+\frac{1}{2},j}^{*}$ are approximated as $\bar{H}_{i+\frac{1}{2},j}^{n} U_{i+\frac{1}{2},j}^{n+\frac{1}{2}}$ and $\bar{H}_{i+\frac{1}{2},j}^{n+1} U_{i+\frac{1}{2},j}^{*}$. Now using (B.45) $\left(HU\right)_{i+\frac{1}{2},j}^{n+\frac{1}{2}}$ is equivalent to:

$$\left(HU\right)_{i+\frac{1}{2},j}^{n+\frac{1}{2}} = \bar{H}_{i+\frac{1}{2},j}^{n+1} U_{i+\frac{1}{2},j}^{n+\frac{1}{2}} - U_{i+\frac{1}{2},j}^{n+\frac{1}{2}} \Delta t \frac{{}^{x}\bar{q}_{i+1,j}^{n+\frac{1}{2}} - {}^{x}\bar{q}_{i,j}^{n+\frac{1}{2}}}{\Delta x} - U_{i+\frac{1}{2},j}^{n+\frac{1}{2}} \Delta t \frac{{}^{y}\bar{q}_{i+\frac{1}{2},j+\frac{1}{2}}^{n+\frac{1}{2}} - {}^{y}\bar{q}_{i+\frac{1}{2},j-\frac{1}{2}}^{n+\frac{1}{2}}}{\Delta y}$$

$$\bar{H}_{i+\frac{1}{2},j}^{n+1} = \frac{1}{2}\left(H_{i+1,j}^{n+1} + H_{i,j}^{n+1}\right)$$

$${}^{x}\bar{q}_{i,j}^{n+\frac{1}{2}} = \frac{1}{2}\left({}^{x}q_{i+\frac{1}{2},j}^{n+\frac{1}{2}} + {}^{x}q_{i-\frac{1}{2},j}^{n+\frac{1}{2}}\right)$$

(B.57)

$${}^{y}\bar{q}_{i+\frac{1}{2},j+\frac{1}{2}}^{n+\frac{1}{2}} = \frac{1}{2}\left({}^{y}q_{i+\frac{1}{2},j+\frac{1}{2}}^{n+\frac{1}{2}} + {}^{y}q_{i+\frac{1}{2},j-\frac{1}{2}}^{n+\frac{1}{2}}\right)$$

Substituting (B.57) into (B.54) the full expressions (including those for $V_{i,j+\frac{1}{2}}^{*}$) become:

$$\frac{U_{i+\frac{1}{2},j}^{*} - U_{i+\frac{1}{2},j}^{n+\frac{1}{2}}}{\Delta t} + \frac{{}^{x}\bar{q}_{i+1,j}^{n+\frac{1}{2}} U_{i+1,j}^{n+\frac{1}{2}} - {}^{x}\bar{q}_{i,j}^{n+\frac{1}{2}} U_{i,j}^{n+\frac{1}{2}}}{\bar{H}_{i+\frac{1}{2},j}^{n+1}\Delta x} + \frac{{}^{y}\bar{q}_{i,j+1}^{n+\frac{1}{2}} U_{i,j+1}^{n+\frac{1}{2}} - {}^{y}\bar{q}_{i,j}^{n+\frac{1}{2}} U_{i,j}^{n+\frac{1}{2}}}{\bar{H}_{i+\frac{1}{2},j}^{n+1}\Delta y} - \frac{U_{i+\frac{1}{2},j}^{n+\frac{1}{2}}}{\bar{H}_{i+\frac{1}{2},j}^{n+1}} \frac{{}^{x}\bar{q}_{i+1,j}^{n+\frac{1}{2}} - {}^{x}\bar{q}_{i,j}^{n+\frac{1}{2}}}{\Delta x}$$

$$- \frac{U_{i+\frac{1}{2},j}^{n+\frac{1}{2}}}{\bar{H}_{i+\frac{1}{2},j}^{n+1}} \frac{{}^{y}\bar{q}_{i,j+1}^{n+\frac{1}{2}} - {}^{y}\bar{q}_{i,j}^{n+\frac{1}{2}}}{\Delta y} + g\frac{\eta_{i+1,j}^{n+1} - \eta_{i,j}^{n+1}}{\Delta x} = \frac{{}^{x}\mathrm{Pr}_{i+\frac{1}{2},j}^{n+\frac{1}{2}} + {}^{x}\mathrm{S}_{i+\frac{1}{2},j}^{n+\frac{1}{2}} + {}^{x}\mathrm{T}_{i+\frac{1}{2},j}^{n+\frac{1}{2}}}{\bar{H}_{i+\frac{1}{2},j}^{n+1}}$$

(B.58)

$$\frac{V_{i,j+\frac{1}{2}}^{*} - V_{i,j+\frac{1}{2}}^{n+\frac{1}{2}}}{\Delta t} + \frac{{}^{y}\bar{q}_{i,j+1}^{n+\frac{1}{2}} V_{i,j+1}^{n+\frac{1}{2}} - {}^{y}\bar{q}_{i,j}^{n+\frac{1}{2}} V_{i,j}^{n+\frac{1}{2}}}{\bar{H}_{i,j+\frac{1}{2}}^{n+1}\Delta y} + \frac{{}^{x}\bar{q}_{i+1,j}^{n+\frac{1}{2}} V_{i+1,j}^{n+\frac{1}{2}} - {}^{x}\bar{q}_{i,j}^{n+\frac{1}{2}} V_{i,j}^{n+\frac{1}{2}}}{\bar{H}_{i,j+\frac{1}{2}}^{n+1}\Delta x} - \frac{V_{i+\frac{1}{2},j}^{n+\frac{1}{2}}}{\bar{H}_{i,j+\frac{1}{2}}^{n+1}} \frac{{}^{y}\bar{q}_{i,j+1}^{n+\frac{1}{2}} - {}^{y}\bar{q}_{i,j}^{n+\frac{1}{2}}}{\Delta y}$$

$$\frac{V_{i,j+\frac{1}{2}}^{n+\frac{1}{2}}}{\bar{H}_{i,j+\frac{1}{2}}^{n+1}} \frac{{}^{x}\bar{q}_{i+1,j}^{n+\frac{1}{2}} - {}^{x}\bar{q}_{i,j}^{n+\frac{1}{2}}}{\Delta x} + g\frac{\eta_{i,j+1}^{n+1} - \eta_{i,j}^{n+1}}{\Delta x} = \frac{{}^{y}\mathrm{Pr}_{i,j+\frac{1}{2}}^{n+\frac{1}{2}} + {}^{y}\mathrm{S}_{i,j+\frac{1}{2}}^{n+\frac{1}{2}} + {}^{y}\mathrm{T}_{i,j+\frac{1}{2}}^{n+\frac{1}{2}}}{\bar{H}_{i,j+\frac{1}{2}}^{n+1}}$$

Where we again use a first order upwind interpolation for $U_{i+1,j}^{n+\frac{1}{2}}$ and $U_{i,j+1}^{n+\frac{1}{2}}$. This is exactly the approximation used by Stelling and Duinmeijer (2003) and is fully momentum conservative.

The predictor step (B.58) is first order accurate in both space and time due to the use of upwind approximations for and Euler explicit time integration for the advective terms, and first order time integration for the source/viscous terms. This level of accuracy is acceptable near shore, where strong non-linearity (wave breaking, flooding and drying) will force the use of small steps in space and time anyway. However, in the region where waves only slowly change (e.g. shoaling/refraction on mild slopes), the first order approximations suffer from significant numerical damping. To improve the accuracy of the numerical model in these regions a corrector step is implemented after the predictor step.

The corrector step is given by:

$$\frac{\left(HU\right)^{n+1\frac{1}{2}}_{i+\frac{1}{2},j}-\left(HU\right)^{n*}_{i+\frac{1}{2},j}}{\Delta t}+\frac{{}^{x}\overline{q}^{n+\frac{1}{2}}_{i+1,j}\Delta U_{i+1,j}-{}^{x}\overline{q}^{n+\frac{1}{2}}_{i,j}\Delta U_{i,j}}{\Delta x}+\frac{{}^{y}\overline{q}^{n+\frac{1}{2}}_{i,j+1}\Delta U_{i,j+1}-{}^{y}\overline{q}^{n+\frac{1}{2}}_{i,j}\Delta U_{i,j}}{\Delta y}+$$

$$\frac{\left(\eta^{n+1}_{i+1,j}+d^{n+1}_{i,j}\right)\Delta p^{n+1\frac{1}{2}}_{i+1,j}-\left(\eta^{n+1}_{i,j}-d^{n+1}_{i+1,j}\right)\Delta p^{n+1\frac{1}{2}}_{i,j}}{2\Delta x}=0 \tag{B.59}$$

Or, when formulated in terms of the depth averaged velocity

$$\frac{\left(HU\right)^{n+1\frac{1}{2}}_{i+\frac{1}{2},j}-\left(HU\right)^{n*}_{i+\frac{1}{2},j}}{\Delta t}+\frac{{}^{x}\overline{q}^{n+\frac{1}{2}}_{i+1,j}\Delta U_{i+1,j}-{}^{x}\overline{q}^{n+\frac{1}{2}}_{i,j}\Delta U_{i,j}}{\Delta x}+\frac{{}^{y}\overline{q}^{n+\frac{1}{2}}_{i,j+1}\Delta U_{i,j+1}-{}^{y}\overline{q}^{n+\frac{1}{2}}_{i,j}\Delta U_{i,j}}{\Delta y}+$$

$$\frac{\left(\eta^{n+1}_{i+1,j}+d^{n+1}_{i,j}\right)\Delta p^{n+1\frac{1}{2}}_{i+1,j}-\left(\eta^{n+1}_{i,j}-d^{n+1}_{i+1,j}\right)\Delta p^{n+1\frac{1}{2}}_{i,j}}{2\Delta x}=0$$

$$\frac{U^{n+1\frac{1}{2}}_{i+\frac{1}{2},j}-U^{n*}_{i+\frac{1}{2},j}}{\Delta t}+\frac{{}^{x}\overline{q}^{n+\frac{1}{2}}_{i+1,j}\Delta U_{i+1,j}-{}^{x}\overline{q}^{n+\frac{1}{2}}_{i,j}\Delta U^{n*}_{i,j}}{\overline{H}^{n+1}_{i+\frac{1}{2},j}\Delta x}+\frac{{}^{y}\overline{q}^{n+\frac{1}{2}}_{i+\frac{1}{2},j+\frac{1}{2}}\Delta U_{i+\frac{1}{2},j+\frac{1}{2}}-{}^{y}\overline{q}^{n+\frac{1}{2}}_{i+\frac{1}{2},j-\frac{1}{2}}\Delta U_{i+\frac{1}{2},j-\frac{1}{2}}}{\overline{H}^{n+1}_{i+\frac{1}{2},j}\Delta y}+...$$

$$...+\frac{\left(\eta^{n+1}_{i+1,j}+d^{n+1}_{i,j}\right)\Delta p^{n+1\frac{1}{2}}_{i+1,j}-\left(\eta^{n+1}_{i,j}-d^{n+1}_{i+1,j}\right)\Delta p^{n+1\frac{1}{2}}_{i,j}}{2\overline{H}^{n+1}_{i+\frac{1}{2},j}\Delta x}=0 \tag{B.60}$$

$$\frac{V^{n+1\frac{1}{2}}_{i,j+\frac{1}{2}}-V^{n*}_{i,j+\frac{1}{2}}}{\Delta t}+\frac{{}^{y}\overline{q}^{n+\frac{1}{2}}_{i,j+1}\Delta V_{i,j+1}-{}^{y}\overline{q}^{n+\frac{1}{2}}_{i,j}\Delta V_{i,j}}{\overline{H}^{n+1}_{i,j+\frac{1}{2}}\Delta y}+\frac{{}^{x}\overline{q}^{n+\frac{1}{2}}_{i+\frac{1}{2},j+\frac{1}{2}}\Delta V_{i+\frac{1}{2},j+\frac{1}{2}}-{}^{y}\overline{q}^{n+\frac{1}{2}}_{i-\frac{1}{2},j+\frac{1}{2}}\Delta V_{i-\frac{1}{2},j+\frac{1}{2}}}{\overline{H}^{n+1}_{i,j+\frac{1}{2}}\Delta y}+...$$

$$...+\frac{\left(\eta^{n+1}_{i,j+1}+d^{n+1}_{i,j}\right)\Delta p^{n+1\frac{1}{2}}_{i,j+1}-\left(\eta^{n+1}_{i,j}-d^{n+1}_{i,j+1}\right)\Delta p^{n+1\frac{1}{2}}_{i,j}}{2\overline{H}^{n+1}_{i,j+\frac{1}{2}}\Delta x}=0$$

The values of $\Delta U^{n*}_{i+1,j}$ are obtained from slope limited expressions. For positive flow these read:

$$\Delta U^{n*}_{i,j}=\tfrac{1}{2}\psi\left({}^{u}r_{i+\frac{1}{2}}\right)\left(U^{*}_{i+\frac{1}{2},j}-U^{n}_{i-\frac{1}{2},j}\right)$$

$${}^{u}r_{i+\frac{1}{2}}=\frac{U^{*}_{i-\frac{1}{2},j}-U^{n}_{i-1\frac{1}{2},j}}{U^{*}_{i+\frac{1}{2},j}-U^{n}_{i-\frac{1}{2},j}}\qquad\text{if }q^{n+\frac{1}{2}}_{i,j}>0 \tag{B.61}$$

Where ψ again denotes the minmod limiter. Similar expressions can be constructed for $\Delta U_{i+\frac{1}{2},j+\frac{1}{2}}$, $\Delta V_{i,j}$ and $\Delta V_{i+\frac{1}{2},j+\frac{1}{2}}$.

The predictor-corrector set is second order accurate in regions where the solution is smooth, and reduces to first order accuracy near sharp gradients in the solutions to avoid unwanted oscillations. Furthermore, the method remains momentum conservative.

B.7.4 Vertical momentum equations

The depth averaged vertical momentum equation for HW is given by:

$$\frac{\partial}{\partial t}\left(HW\right)+\frac{\partial}{\partial x}\left(HUW\right)+\frac{\partial}{\partial y}\left(HWV\right)=-p_{surface}+p_{bottom}+\frac{1}{p}\frac{\partial}{\partial x}\left(H\overline{\tau_{xz}}\right)+\frac{1}{p}\frac{\partial}{\partial y}\left(H\overline{\tau_{yz}}\right) \quad \text{(B.62)}$$

The vertical momentum equation is discretized in a similar manner to the horizontal momentum equations using the McCormack scheme. In terms of the depth averaged vertical velocity the predictor step is:

$$\frac{\overline{W}_{i,j}^{*}-\overline{W}_{i,j}^{n+\frac{1}{2}}}{\Delta t}+\frac{{}^{x}q_{i+\frac{1}{2},j}^{n+\frac{1}{2}}\overline{W}_{i+\frac{1}{2},j}^{n+\frac{1}{2}}-{}^{x}q_{i-\frac{1}{2},j}^{n+\frac{1}{2}}\overline{W}_{i-\frac{1}{2},j}^{n+\frac{1}{2}}}{H_{i,j}^{n+1}\Delta x}-\frac{\overline{W}_{i,j}^{n+\frac{1}{2}}}{H_{i,j}^{n+1}}\frac{{}^{x}q_{i+\frac{1}{2},j}^{n+\frac{1}{2}}-{}^{x}q_{i-\frac{1}{2},j}^{n+\frac{1}{2}}}{\Delta x}+\frac{{}^{y}q_{i,j+\frac{1}{2}}^{n+\frac{1}{2}}\overline{W}_{i,j+\frac{1}{2}}^{n+\frac{1}{2}}-{}^{y}q_{i,j-\frac{1}{2}}^{n+\frac{1}{2}}\overline{W}_{i,j-\frac{1}{2}}^{n+\frac{1}{2}}}{H_{i,j}^{n+1}\Delta y}$$
$$-\frac{\overline{W}_{i,j}^{n+\frac{1}{2}}}{H_{i,j}^{n+1}}\frac{{}^{y}q_{i,j+\frac{1}{2}}^{n+\frac{1}{2}}-{}^{y}q_{i,j-\frac{1}{2}}^{n+\frac{1}{2}}}{\Delta y}+\frac{p_{i,j,1}^{n+\frac{1}{2}}-p_{i,j,0}^{n+\frac{1}{2}}}{H_{i,j}^{n+1}}=\frac{{}^{w}S_{i,j}^{n+\frac{1}{2}}+{}^{w}T_{i,j}^{n+\frac{1}{2}}}{H_{i,j}^{n+1}} \quad \text{(B.63)}$$

The pressures are defined on the cell faces and therefore do not have to be interpolated. Furthermore, we can exactly set the dynamic pressure at the free surface $p_{i,j,1}^{n+\frac{1}{2}}$ to zero. The vertical velocities are defined on the cell faces and therefore the depth averaged velocity $\overline{W}_{i,j}^{n+\frac{1}{2}}$ needs to be expressed in terms of the bottom and surface velocities. Using a simple central approximation gives

$$\overline{W}_{i,j}^{n+\frac{1}{2}}=\tfrac{1}{2}\left(w_{i,j,1}^{n+\frac{1}{2}}+w_{i,j,0}^{n+\frac{1}{2}}\right)$$
$$\overline{W}_{i,j}^{*}=\tfrac{1}{2}\left(w_{i,j,1}^{*}+w_{i,j,0}^{*}\right) \quad \text{(B.64)}$$

At the bottom the kinematic boundary condition is used for the vertical velocity:

$$w_{i,j,0}^{*}=\tfrac{1}{2}\left(U_{i+\frac{1}{2},j}^{*}+U_{i-\frac{1}{2},j}^{*}\right)\frac{d_{i+\frac{1}{2},j}-d_{i-\frac{1}{2},j}}{\Delta x_{i}}+\tfrac{1}{2}\left(V_{i,j+\frac{1}{2}}^{*}+V_{i,j-\frac{1}{2}}^{*}\right)\frac{d_{i,j+\frac{1}{2}}-d_{i,j-\frac{1}{2}}}{\Delta x_{j}} \quad \text{(B.65)}$$

Horizontal interpolation of $\overline{W}_{i+\frac{1}{2},j}^{n+\frac{1}{2}}$ and $\overline{W}_{i,j+\frac{1}{2}}^{n+\frac{1}{2}}$ is done using first order upwind similar to (B.46). The turbulent stresses are again approximated using a central scheme as:

$${}^{w}T_{i+\frac{1}{2},j}^{n+\frac{1}{2}}=\frac{1}{\Delta x_{i}}\left[{}^{x}\overline{V}_{i+\frac{1}{2},j}^{n}\,{}^{x}\overline{H}_{i+\frac{1}{2},j}^{n+1}\frac{W_{i+1,j}^{n+\frac{1}{2}}-W_{i,j}^{n+\frac{1}{2}}}{\Delta x_{i+\frac{1}{2}}}-{}^{x}\overline{V}_{i-\frac{1}{2},j}^{n}\,{}^{x}\overline{H}_{i-\frac{1}{2},j}^{n+1}\frac{W_{i,j}^{n+\frac{1}{2}}-W_{i-1,j}^{n+\frac{1}{2}}}{\Delta x_{i+\frac{1}{2}}}\right]$$
$$+\frac{1}{\Delta y_{i}}\left[{}^{y}\overline{V}_{i,j+\frac{1}{2}}^{n}\,{}^{y}\overline{H}_{i,j+\frac{1}{2}}^{n+1}\frac{W_{i,j+1}^{n+\frac{1}{2}}-W_{i,j}^{n+\frac{1}{2}}}{\Delta x_{j+\frac{1}{2}}}-{}^{y}\overline{V}_{i,j-\frac{1}{2}}^{n}\,{}^{y}\overline{H}_{i,j-\frac{1}{2}}^{n+1}\frac{W_{i,j}^{n+\frac{1}{2}}-W_{i,j-1}^{n+\frac{1}{2}}}{\Delta y_{j+\frac{1}{2}}}\right] \quad \text{(B.66)}$$

Thus combining (B.64), (B.65) and (B.66) explicit expressions for $w_{i,j,1}^{*}$ and $w_{i,j,0}^{*}$ are obtained. The predicted values are again corrected using a variant of the McCormack scheme and including the pressure difference implicitly gives the corrector step:

Deltares

$$\frac{\overline{W}_{i,j}^{n+1\frac{1}{2}} - \overline{W}_{i,j,1}^{*}}{\Delta t} + \frac{{}^{x}q_{i+\frac{1}{2},j}^{n+\frac{1}{2}}\Delta\overline{W}_{i+\frac{1}{2},j} - {}^{x}q_{i-\frac{1}{2},j}^{n+\frac{1}{2}}\Delta\overline{W}_{i-\frac{1}{2},j}}{H_{i,j}^{n+1}\Delta x} + \frac{{}^{y}q_{i,j+\frac{1}{2}}^{n+\frac{1}{2}}\Delta\overline{W}_{i,j+\frac{1}{2}} - {}^{y}q_{i,j-\frac{1}{2}}^{n+\frac{1}{2}}\Delta\overline{W}_{i,j-\frac{1}{2}}}{H_{i,j}^{n+1}\Delta y} - \frac{\Delta p_{i,j}^{n+1\frac{1}{2}}}{H_{i,j}^{n+1}} = 0 \quad \text{(B.67)}$$

Where $\Delta\overline{W}_{i+\frac{1}{2},j}$ and $\Delta\overline{W}_{i,j+\frac{1}{2}}$ are obtained using relations similar to (B.61). Note that similar to (B.64) $\overline{W}_{i,j}^{n+1\frac{1}{2}} = \frac{1}{2}\left(w_{i,j,1}^{n+1\frac{1}{2}} + w_{i,j,0}^{n+1\frac{1}{2}}\right)$ and again the kinematic boundary conditions is substituted for $w_{i,j,0}^{n+1\frac{1}{2}}$.

The discrete vertical momentum balance of (B.63) and (B.67) looks very different from the relations found in Zijlema and Stelling (2005), Zijlema and Stelling (2008) and Smit (2008). This is mainly due to the application of the McCormack scheme for the advection. The discretization of the pressure term is numerically fully equivalent to either the Keller box scheme as used in Zijlema and Stelling (2005), Zijlema and Stelling (2008) or the Hermetian relation used in Smit (2008).